KANSAS GEOLOGICAL SURVEY
OPEN-FILE REPORT 2001-72

AN EVALUATION OF THE LONG-TERM EFFECT OF
WATER-RESOURCES DEVELOPMENT ON THE DAKOTA AQUIFER
IN THE VICINITY OF THE HAYS WELL FIELD
VOLUME 2: NUMERICAL MODELING
FINAL DRAFT REPORT

by

P. Allen Macfarlane
C.K. McCormick

Kansas Geological Survey
1930 Constant Avenue
University of Kansas
Lawrence, KS 66047-3726

AN EVALUATION OF THE LONG-TERM EFFECT OF WATER-RESOURCES DEVELOPMENT ON THE DAKOTA AQUIFER IN THE VICINITY OF THE HAYS WELL FIELD

Volume 2: Numerical Modeling

FINAL DRAFT REPORT

By
P. Allen Macfarlane
C. K. McCormick
Kansas Geological Survey

Kansas Geological Survey

AN EVALUATION OF THE LONG-TERM EFFECT OF WATER-RESOURCES DEVELOPMENT ON THE DAKOTA AQUIFER IN THE VICINITY OF THE HAYS WELL FIELD

Volume 2: Numerical Modeling

FINAL DRAFT REPORT

By

P. Allen Macfarlane
C.K. McCormick

Kansas Geological Survey

GEOHYDROLOGY

The University of Kansas, Lawrence, KS 66047 Tel.(785) 864-3965

EXECUTIVE SUMMARY

The need for additional water supply prompted the city of Hays, Kansas, to locate a supplemental source in the upper Dakota aquifer to the southwest of the city in Ellis County in 1992. At the time the wellfield was installed, a temporary permit was issued by the Division of Water Resources, Kansas Department of Agriculture (DWR), to allow the city to use the upper Dakota aquifer as a source of water for a 5 yr period. A temporary permit was issued because the local impact of wellfield operation on the aquifer was uncertain. Concerns were expressed about possible impairment of other users of the upper Dakota in the local area outside of the wellfield. Impairment results when one well diminishes the supply of water available to another well either by lowering the static water level unreasonably or causing an unreasonable deterioration of water quality.

The city of Hays, Kansas, contracted with the Kansas Geological Survey (KGS) to conduct an investigation of the Dakota aquifer in the vicinity of their wellfield. The purpose of this work was twofold. First, the data and the results of this project will be used by the city to assemble and submit an application for a permanent water right and an increase in annual appropriation of water from the wellfield. And secondly, this project was originally designed to produce a computer model of the aquifer that could be used by the city to assess consequences of various short-term, wellfield management plans.

In Volume 1 of this report, concerns were raised about the lack of data with which to characterize the hydrogeology of the upper Dakota aquifer in the wellfield vicinity considering the nature of the questions to be addressed by this investigation. The available data are only generally adequate for determining aquifer extent and properties within the well field; however, outside of the well field the hydrogeology is virtually unknown. The pre-pumping water-level data for the upper Dakota are concentrated within the wellfield and the rest of the data base consists of a few poorly documented historic water levels from wells located several miles or more away from the well field. Also, there is a pronounced lack of data on water-level fluctuations in distant monitoring wells located outside of the well field during the 1993-1999 pumping period. This lack of data makes it nearly impossible to determine the effects of pumping stress on the local ground-water flow system outside of the immediate wellfield area and to directly address issues of impairment with any reliability.

Nevertheless, development of computer models began using Visual MODFLOW to provide an overall understanding of the aquifer system, to simulate the effects of pumping on the Dakota aquifer in the wellfield vicinity, and to guide acquisition of additional, critical pieces of information. Because of the lack of data, the models developed for this project are more conceptual than predictive in nature.

Because of our lack of confidence in the simulations of the aquifer outside of the wellfield, three, equally acceptable, steady-state (predevelopment) and two, equally acceptable, transient conceptual models of the upper Dakota were formulated and calibrated. These models are equally acceptable because they are based on the known hydrologic parameters from the pumping tests and are consistent with the hydrogeologic model presented in Chapter 10, Volume 1, of this report. The calibration performed was limited because only the pre-development water-levels and drawdowns from the pumping tests were available to assess the process.

Further evaluation of one of the transient, conceptual models suggests the strong possibility that neither of the transient models may account for all of the more significant sources of ground water available to the production wells. From this we conclude that the objective to assess the potential effects of various management options on the aquifer can not be completed until a revised hydrogeologic model is developed from the additional information that we recommend collecting, as follows.

Recommendations

On the basis of our work to date, we make the following recommendations to the city:

(1) Test drilling is needed to further define the characteristics of the aquifer and the surrounding low-permeability rocks outside of the immediate wellfield vicinity.

(2) A minimum of 5 new monitoring wells should be constructed in and around the wellfield vicinity. One monitoring well should be located near each of the following three locations: N1/2, N1/2, Sec 21, T. 14 S., R. 19 W.; SW corner Sec. 27, T. 14 S., R. 18 W.; and in the center of the south line Sec. 1, T. 14 S., R. 19 W. Each well should be screened through the entire thickness of the sandstone in Subunit 2 of the Dakota Formation. The fourth and fifth monitoring wells should be located in the SE corner SW, SW, SW, Sec. 13, T. 14 S., R. 19 W. and near the center of Sec. 19, T. 14 S., R. 18 W. These wells should be screened through the entire thickness of sandstone in Subunit 3 of the Dakota Formation. The proposed monitoring

wells in Sec 21, T. 14 S., R. 19 W.; Sec. 27, T. 14 S., R. 18 W.; and in Sec. 1, T. 14 S., R. 19 W. are located approximately 2 miles away from the wellfield and will be used to assess the far field response of the aquifer to pumping. The proposed monitoring well in Sec. 13, T. 14 S., R. 19 W. will be used to assess the importance of leakage from fringe deposits in Subunit 3 of the Dakota Formation to the overlying sandstone aquifer in Subunit 2. The proposed monitoring well in Sec 19, T. 14 S., R. 18 W. would provide drawdown data from what appears to be hydraulically connected sandstones in Subunit 3 of the Dakota Formation. The water levels in these new observation wells should be monitored continuously using pressure transducers and data-logging equipment to provide a continuous record of the effects of pumping in the well field over a period of at least one year. In addition, the city will need to purchase a recording barometer to keep track of atmospheric-pressure fluctuations and their influence on water levels during the monitoring period.

(3) City personnel should continue monitoring water levels in the pumping and existing observation wells and collecting water samples for analysis. Weekly water-level measurements from the pumping and observation wells in the field should adequately provide the data needed for further model calibration should the city decide to collect additional data to support an increase in its annual appropriation of water. The water quality sample analyses will provide useful information on mixing of water masses and may signal important changes in the system over time. As a result, it will be important for the city to contract analytical services with a laboratory that can produce results with the appropriate level of accuracy and reproducibility.

(4) This new water-level and water-chemistry data set should be analyzed to reevaluate and reformulate the existing hydrogeologic model of the upper Dakota aquifer presented herein. The revised hydrogeologic model will be used as a basis for evaluating the conceptual models to date and to assemble a new, ground-water flow model to simulate the drawdown history and to evaluate the potential effects of different pumping scenarios in the wellfield on the surrounding aquifer. If future modeling is to be done on this project, a larger region needs to be included to insure that the effects of pumping do not propagate to the edges of the model. This would entail an expansion of the existing model region a few miles to the west at the minimum.

TABLE OF CONTENTS

Chapter 1: Introduction

The need for additional water supply prompted the city of Hays, Kansas, to locate a supplemental source in the upper Dakota aquifer to the southwest of the city in Ellis County in 1992 (Figure 1). Production well siting was guided using minimal subsurface geologic information. The long history of the oil industry in this area afforded a useful data base of geophysical well logs to provide some subsurface geologic information. The geophysical logs of wells drilled for oil production were used to identify potential wellsites. Limited test-hole drilling was done around these potential wellsites to verify lithologic interpretation of the geophysical logs and assess ambient water-quality. At the completion of well installation, short-term pumping tests were conducted for each of the production wells using nearby observation wells to determine the aquifer's local hydrologic properties. However, because of the high cost of developing and incorporating the new wellfield into the existing water distribution system, no funding was available to collect local hydrogeologic information from an expanded test-drilling and monitoring-well-installation program outside of the wellfield.

At the time the wellfield was installed, a temporary permit was issued by the Division of Water Resources, Kansas Department of Agriculture (DWR), to allow the city to use the upper Dakota aquifer as a source of water for a 5 yr period. A temporary permit was issued because the local impact of wellfield operation on the aquifer was uncertain. Concerns were expressed about possible impairment of other users of the upper Dakota in the local area outside of the wellfield. Impairment results when one well diminishes the supply of water available to another well either by lowering the static water level unreasonably or causing an unreasonable deterioration of water quality. The current DWR interpretation of unreasonable lowering of the static water level in other nearby supply wells for confined aquifers is when the static water level drops below the aquifer top (Scott Ross personal communication, 1999). Water-level declines in the confined Dakota aquifer do not represent a dewatering of the aquifer, but a decrease in fluid pressure. When the static water-level drops below the top of the aquifer, this represents a dewatering of the aquifer.

Historically, the DWR has used well spacing as a means to prevent impairment. If two pumping wells in the Dakota aquifer are spaced a few miles apart and are withdrawing water from the same sandstone body, their zones of influence will likely overlap and coalesce, causing an increase in the drawdown in both wells. Continued pumping by both wells for long periods of time may result in local depletion of the aquifer or may induce poorer quality water to move laterally or vertically toward the wells, such as from the lower Dakota aquifer or the Cedar Hills Sandstone aquifer. The DWR well-spacing regulations take into account intended use and the local hydrogeologic setting. At the time of installation, the spacing between production wells in

Figure 1

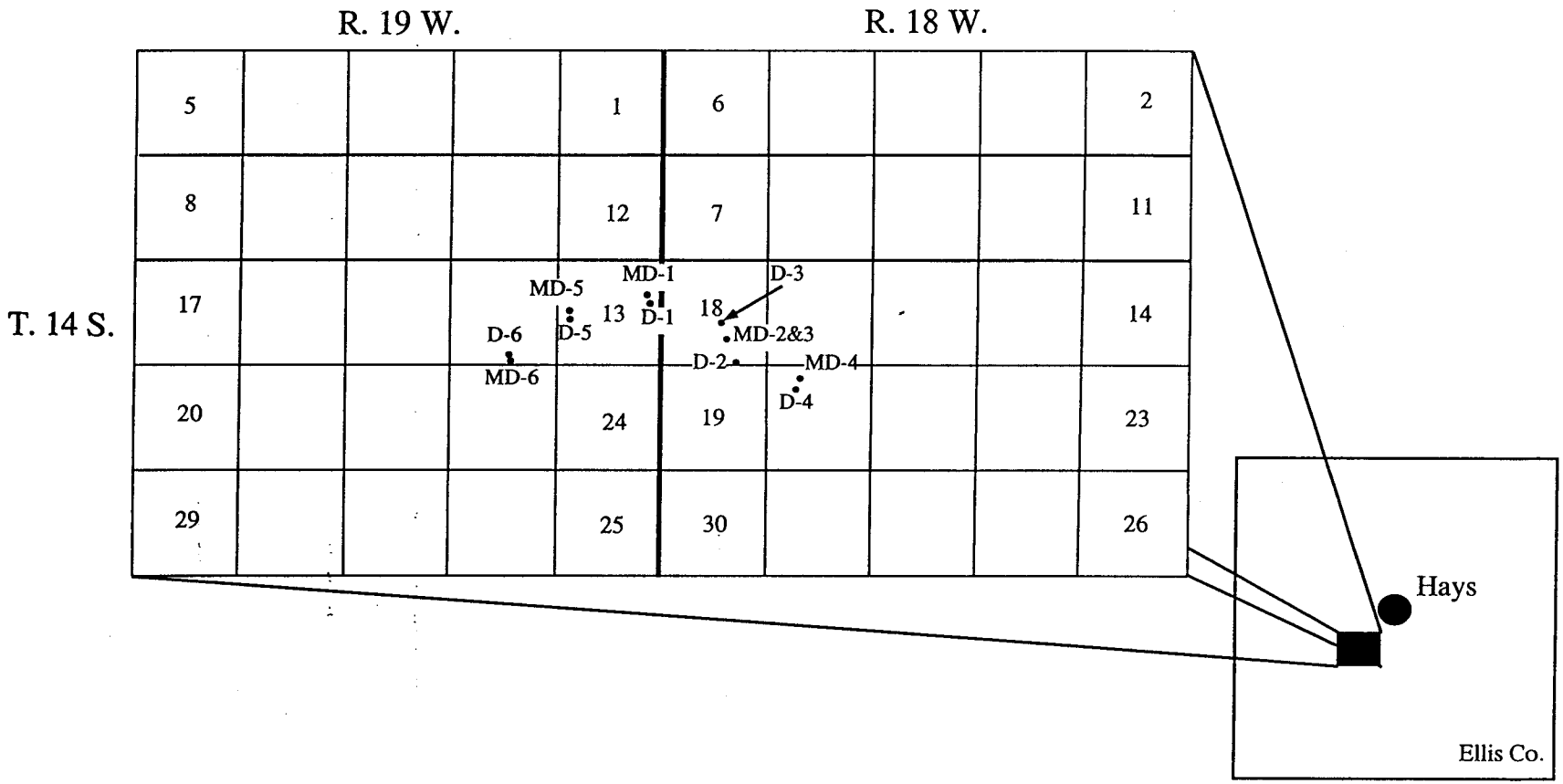

Figure 1. Extent of the study area in central Ellis County, Kansas showing the distribution of pumping wells (labeled D) and monitoring wells (labelled MD) in the confined Dakota aquifer in the Hays wellfield.

the field met the minimum 0.5 mi spacing for producing wells other than domestic in the confined Dakota aquifer. These regulations have since been changed (1994) and the new spacing for wells in the confined Dakota aquifer is now 4 mi. None of the wells in the field meets the newer well-spacing requirement.

Because of these concerns the city has been monitoring water levels periodically in the production and nearby monitoring wells as well as the daily volume of water withdrawn from the aquifer. There has been no attempt by the DWR or the city to monitor water levels or water quality locally outside of the wellfield since pumping from the field began.

Overall goals of the project

The city of Hays, Kansas, contracted with the Kansas Geological Survey (KGS) to conduct an investigation of the Dakota aquifer in the vicinity of their wellfield. The purpose of this work was twofold. First, the data and the results of this project will be used by the city to assemble and submit an application for a permanent water right and an increase in annual appropriation of water from the wellfield. And secondly, this project was originally designed to produce a management tool in the form of a wellfield simulator that could be used by the city to assess consequences of various short-term, wellfield management plans, including rates of withdrawal and the temporary storage of fresh water to recharge the aquifer.

As described in the original proposal, the overall project goals were to: (1) collect and analyze all of the available geologic, hydrologic and water quality information on the Dakota aquifer in the vicinity of the city's wellfield; (2) conduct longer term pumping tests in the city's wellfield to determine aquifer properties and hydrogeologic boundaries; (3) assemble, calibrate, and use numerical models of the Dakota aquifer in the vicinity of the city's wellfield to assess the likely effects of pumpage on aquifer dynamics; and (4) assess viability of various wellfield management options, including the temporary storage of freshwater. The first phase of the project focussed on the first two goals (documented in Volume 1 of this report) and the second phase (documented herein) focussed on the third and fourth project goals.

Changes in project objectives

However, with the completion of the hydrogeologic assessment of the wellfield vicinity (Volume 1: Hydrogeologic Setting), it was evident that the hydrogeologic and hydraulic-head data to assemble and calibrate the required comprehensive numerical ground-water flow model were not available. As a result, the numerical ground-water flow model developed for this project is more conceptual than predictive. A conceptual model is constructed primarily to provide an understanding of aquifer system dynamics (Anderson and Woessner, 1992). This

type of model can also be used to suggest where additional data are needed in order to produce a truly predictive model of the aquifer in the wellfield vicinity.

With these considerations, we revised the original modeling objectives at the outset of this project phase to read as follows: (1) develop, calibrate, and use a conceptual numerical ground-water flow model to provide a better understanding of local aquifer system dynamics prior to wellfield installation and to qualitatively assess how the dynamics have changed as a result of wellfield operation; (2) assess the potential effects of various management options using the numerical model of the aquifer, which is based on what is currently known or what can be reasonably assumed from the findings of this or other investigations of the Dakota aquifer; and (3) identify additional data needed to develop a predictive numerical ground-water flow model of the Dakota aquifer in the wellfield vicinity.

Because of our lack of confidence in the simulations of the aquifer outside of the wellfield, three equally acceptable steady-state (predevelopment) and two equally acceptable transient conceptual models of the upper Dakota were formulated and calibrated. Each model is based on the known hydrologic parameters from the pumping tests and is consistent with the hydrogeologic model presented in Chapter 10, Volume 1, of this report.

Following the limited calibration and further evaluation of one of the transient numerical models in the verification step, we found that there is a strong possibility that neither of the transient models may account for all of the more significant sources of ground water available to the production wells in the wellfield. From this we concluded that the objective to assess the potential effects of various management options on the aquifer can not be completed until a revised hydrogeologic model is developed from the additional information that we recommend collecting (Chapter 7).

Deliverables

This report is the second of two volumes that were prepared as contract deliverables to the city of Hays. From phase 1, the first report volume presented an analysis of what is currently known about the Dakota aquifer in the vicinity of the wellfield from existing data and new information developed from pumping tests conducted by KGS in the wellfield in 1997 (Objectives 1 and 2, cited in the Overall Goals of the Project section of the contract proposal). The second volume summarizes the results of phase 2 of the project and focuses on ground-water flow model development, testing, and application to assess management options for the wellfield.

Objectives of this report

In volume 2 we: (1) describe the process of developing the steady-state (pre-development) and transient, conceptual, three-dimensional, numerical ground-water flow models of the upper Dakota aquifer in the wellfield vicinity; and (2) describe the process used to verify one of the transient numerical models using the historical pumpage and water-level data from within the wellfield; and (3) make recommendations with regard to acquiring additional subsurface geology, aquifer/aquitard properties and hydraulic head data in the aquifer outside of the wellfield to eventually produce an improved numerical model that can be used to assess the city's management/planning options for the wellfield.

Chapter 2: Hydrogeologic Model

Local Subsurface Stratigraphy

The stratigraphy of the shallow subsurface (the upper approximately 1,200 ft) in the wellfield vicinity consists of consolidated geologic units of Cretaceous and Permian age (Zeller, 1968). From youngest to oldest these geologic units are: the Niobrara Chalk, the Carlile Shale, the Greenhorn Limestone, the Graneros Shale, the Dakota Formation, the Kiowa Formation, the Cheyenne Sandstone, and the Cedar Hills Sandstone (Table 1).

At the surface, the trace of the dissected Niobrara Chalk scarp is just to the north of the wellfield and trends in an E-W direction roughly parallel to the line of production and monitoring wells in the Dakota field. Thus, within the wellfield the Carlile Shale is the uppermost bedrock unit. The combined thickness of the Carlile Shale, Greenhorn Limestone, and Graneros Shale ranges from 227 ft at wellsite D-4 to 346 ft at wellsite D-6 (Figure 1).

Beneath the Graneros Shale, the Dakota Formation (Table 1) ranges in thickness from 249–350 ft with an average thickness of 288 ft in the project area (Figure 2). The formation consists of fluvial and deltaic/estuarine sandstone bodies encased in a matrix of alluvial plain to shallow marine mudstone deposits (Hamilton, 1989; 1994). The lower, fluvial channel sandstones are fine to medium, well sorted, and contain large-scale and small-scale cross-beds and are generally oriented in an east-west direction (e.g., Siemers, 1976; Franks et al., 1959). Basal Dakota sandstone bodies thicken appreciably into paleotopographic lows where incised valleys have formed on the underlying Kiowa Formation (Hamilton, 1994). These sandstone beds are abruptly capped by fine-grained deposits or fine upward to interbedded sandstone and mudstone and eventually to mudstone. The upper Dakota Formation fluvial complexes were transgressed and evolved into deltaic and estuarine environments (Siemers, 1976). In the vicinity of the wellfield, approximately the lower two-thirds of the upper Dakota aquifer framework consists of non-marine alluvial sediments, whereas the upper third appears to consist of marine-influenced alluvial and shoreline deposits.

The Kiowa Formation and the Cheyenne Sandstone sequence underlies the Dakota Formation and is 150-200 ft thick in the wellfield vicinity. The upper part of the Kiowa consists primarily of a marine shale that is 50–70 ft thick (Smith, 1995). Below this, the Kiowa contains interbedded thin sandstones, siltstone, and shale deposited in nearshore shallow marine, shoreline and alluvial valley environments. These deposits belong to the Longford Member of the Kiowa Formation. The Longford Member originally was restricted to regressive siltstones, sandstones, and mudstones in the lower Kiowa in north–central Kansas (Franks, 1979). The underlying Cheyenne Sandstone consists predominantly of cross-bedded, fine to medium sandstone with lenses of shale and conglomerate. It was deposited in fluvial to deltaic environments and rests

Table 1

ERA	SYSTEM	ROCK STRATIGRAPHIC UNITS		AQUIFER/AQUITARD UNITS	
Mesozoic	Cretaceous	Colorado Group	Niobrara Chalk Carlile Shale Greenhorn Limestone Graneros Shale	Upper Cretaceous aquitard	
		Dakota Formation		Dakota Aquifer System	Upper Dakota aquifer
		Kiowa Formation			Kiowa shale aquitard
			Longford Member		Lower Dakota aquifer
		Cheyenne Sandstone			
Paleozoic	Permian	Cedar Hills Sandstone		Cedar Hills Sandstone aquifer	

Table 1. Stratigraphy and aquifer/aquitard of the shallow subsurface near the Hays wellfield.

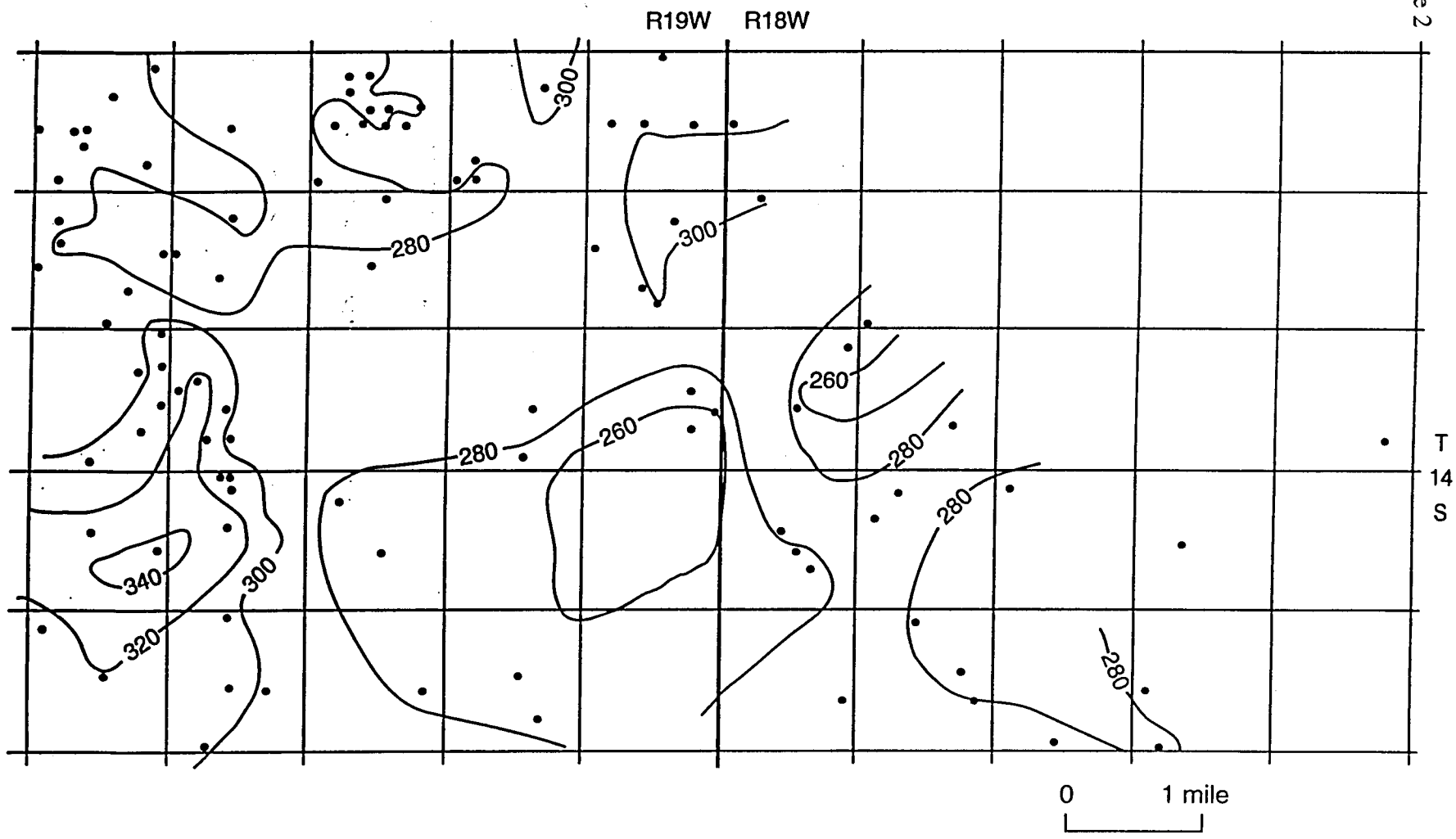

Figure 2. Thickness of the Dakota Formation in the Hays Dakota wellfield vicinty.

unconformably on Permian strata in central Kansas (Hamilton, 1994). The Cheyenne is typically less than 30 ft thick in the wellfield vicinity and tends to thicken into paleotopographic lows (Hamilton, 1994).

The Permian Cedar Hills Sandstone consists of medium to fine sandstone and feldspathic sandstone with interbeds of sandy mudstone (Zeller, 1968; Swineford, 1955; Swineford and Williams, 1945). The total thickness of sandstone ranges up to slightly more than 275 ft in the wellfield vicinity.

Local aquifer/aquitard units

The Upper Cretaceous aquitard

The Upper Cretaceous aquitard consists of the Upper Cretaceous Niobrara Chalk, Carlile Shale, Greenhorn Limestone, and Graneros Shale (Table 1). Due to a lack of data from field or laboratory tests in Kansas, the vertical hydraulic conductivity of the Upper Cretaceous aquitard was estimated from the literature. Belitz and Bredehoeft (1988) reported thickness-dependent vertical hydraulic conductivities for this aquitard ranging approximately from 10^{-6} ft/day for thinner sections to 10^{-10} ft/day for thicker sections from regional model calibration. Also from regional ground-water flow modeling, Macfarlane (1993) reported vertical hydraulic conductivities ranging approximately from 10^{-5} ft/day in central to 10^{-7} ft/day in western Kansas, respectively.

The Dakota aquifer system

At the regional scale, the Dakota aquifer system is subdivided into upper and lower units consisting of interbedded sandstone/mudstone (Table 1) (Macfarlane 1993). In the wellfield vicinity, the upper aquifer unit consists entirely of sandstones belonging to the Dakota Formation and the lower aquifer unit consists of sandstones belonging to the Longford Member of the Kiowa Formation and the Cheyenne Sandstone. The production and monitoring wells in the city's wellfield are screened entirely in the upper Dakota aquifer. Where the Upper Cretaceous aquitard is present and water levels in wells are above the top of the upper Dakota, the aquifer is considered to be a confined system; elsewhere, the Dakota is considered unconfined.

The upper and lower regional Dakota aquifers are separated by marine shale of the Kiowa Formation, referred to as the Kiowa shale aquitard. From gamma-ray logs of boreholes drilled for oil production, the Kiowa shale aquitard is approximately 50-70 ft in thickness in the wellfield vicinity (Smith, 1995). In a regional flow model of the Dakota aquifer Macfarlane (1993) assumed a vertical hydraulic conductivity of 10^{-6} ft/day for the shale in this aquitard unit, based on values used in previous regional models of the ground-water flow in the Dakota aquifer.

Upper Dakota aquifer framework model

Aquifer sedimentology from outcrop studies

With the exception of the uppermost Dakota, most of the sediments that comprise the formation were deposited by bedload and mixed-load streams on the eastern side of the developing Western Interior seaway in response to sea-level rise. Rising base level may have had little initial effect on fluvial depositional style in the upper coastal plain (Shanley and McCabe, 1994). Progressive upward changes in depositional style from upper to lower coastal plain and shoreface environments indicate that marine influence began to dominate the environment near the end of Dakota Formation deposition.

Early on, deposition filled in the drainage that was incised into the underlying Kiowa Formation. Trunk streams in the drainage network were braided, bedload channels of moderate sinuosity flowing across what is believed to have been the upper coastal plain. These streams left behind laterally extensive tabular sandstone bodies near the base of the formation (Karl, 1976), which can be traced in the subsurface for distances up to 20 mi (Macfarlane et al., 1994). Where the Dakota crops out at the surface in Horsethief Canyon, Ellsworth County, thick sandstones near the base of the formation are entirely composed of 3-5 amalgamated channel-fill elements with very high width/depth ratios (Holbrook et al., 1995). In contrast, sandstones higher up in the Dakota occupy much less of the outcrop area, e.g., the Rocktown channel sandstone elements account for only about 30% of the outcrop area in Russell County (Holbrook et al., 1995). Typical fluvial facies successions pass from lateral to vertical accretion and range in thickness from 18 to 74 ft in outcrop (Hamilton, 1989).

In the upper part of the Dakota Formation, the Rocktown channel sandstone was deposited by a low sinuousity stream (Holbrook et al., 1995) in a lower coastal plain setting (Siemers, 1971). Sandstone body width/depth ratios are much lower than those that would be characteristic of braided streams (Miall, 1996). Abandoned channel fills are common and consist of mudstone or interbedded mudstone and fine sandstone. This infers pervasive cut-off channels from active flow and periodic filling by overbank events, features that are more characteristic of meandering streams. The close association of channels with splay deposits and the fine-grained character of the overbank deposits also suggests that individual channels were well confined by levees. Lateral accretion architectural elements are typically narrow and much less abundant than channel architectural elements.

Mappable subdivisions of the Dakota Formation in the wellfield vicinity

Detailed stratigraphic analysis of the subsurface data in the wellfield vicinity reveals that Dakota Formation strata can be subdivided into two locally mappable subdivisions. The upper subdivision (Subunit 1) appears to be dominated by marine-influenced alluvial and shoreline

sediments that range in thickness from 95 to 141 ft. The lower, approximately two-thirds of the Dakota Formation consists of strata that were deposited in upper coastal plain, alluvial environments, including channel and adjacent floodplain (Figure 3). Lacking any locally traceable and continuous stratigraphic markers, this fluvially dominated interval was arbitrarily split into an upper Subunit 2 and a lower Subunit 3, which are of equal thickness. The lower boundary of Subunit 3 is the erosional base of the Dakota Formation on the underlying marine shale of the Kiowa Formation.

These progressive changes in fluvial depositional style are reflected in the upward decrease in the sandstone proportion from Subunit 3 to Subunit 1 of the Dakota Formation described in Volume 1 of this report. The proportion of aquifer-grade sandstone to total formation thickness ranges widely from less than 5% to slightly more than 55% and averages at approximately 29%. Most of the sandstone occurs in the lower two-thirds of the Dakota Formation. The sandstone isolith maps for each subunit (Figures 4-6) reveal NW-SE and E-W trends in each layer where the aggregate thickness of sandstone exceeds 20% of the total layer thickness. Within each of these trends the proportion of sandstone ranges locally up to more than 80% of the total thickness in Subunits 2 and 3 and more than 40% of the Subunit 1 thickness. Thicker accumulations of sandstone consist of stacked sequences of amalgamated, fluvial channel sandstones in all three subunits associated with valley systems incised into the underlying Kiowa Formation.

Aquifer unit hydraulic connection in the wellfield vicinity

Ground-water flow patterns in interbedded sandstone and mudstone sequences are controlled primarily by channel-belt connectivity (Fogg, 1990) and secondarily by the hydraulic conductivity contrast across the sandstone-mudstone boundary (Toth, 1962; Macfarlane et al., 1994). Jones et al. (1995) indicate that the number of discrete channel sandstone fills stacked to form a channel belt exerts a major influence on ground-water flow within sandstone deposits. At the wellfield scale, connectivity can be assessed using the sandstone fraction as a surrogate and from pumping test results (Galloway and Sharp, 1998a,b). Computer-simulation of a synthetic fluvial depositional system (Bridge and Mackey, 1993) suggests that randomly distributed sandstone channel units are relatively isolated where the sandstone fraction is less than 40% and increases with increasing sandstone fraction up to 75%. At higher sandstone fractions, the channels are highly connected. Using computer simulation, Fogg (1986) analyzed a mixed-load fluvial aquifer in the Wilcox of east Texas and found that sand bodies were effectively isolated where the sandstone fraction was less than 20% and effectively amalgamated where the sandstone exceeded 60%.

Figure 3

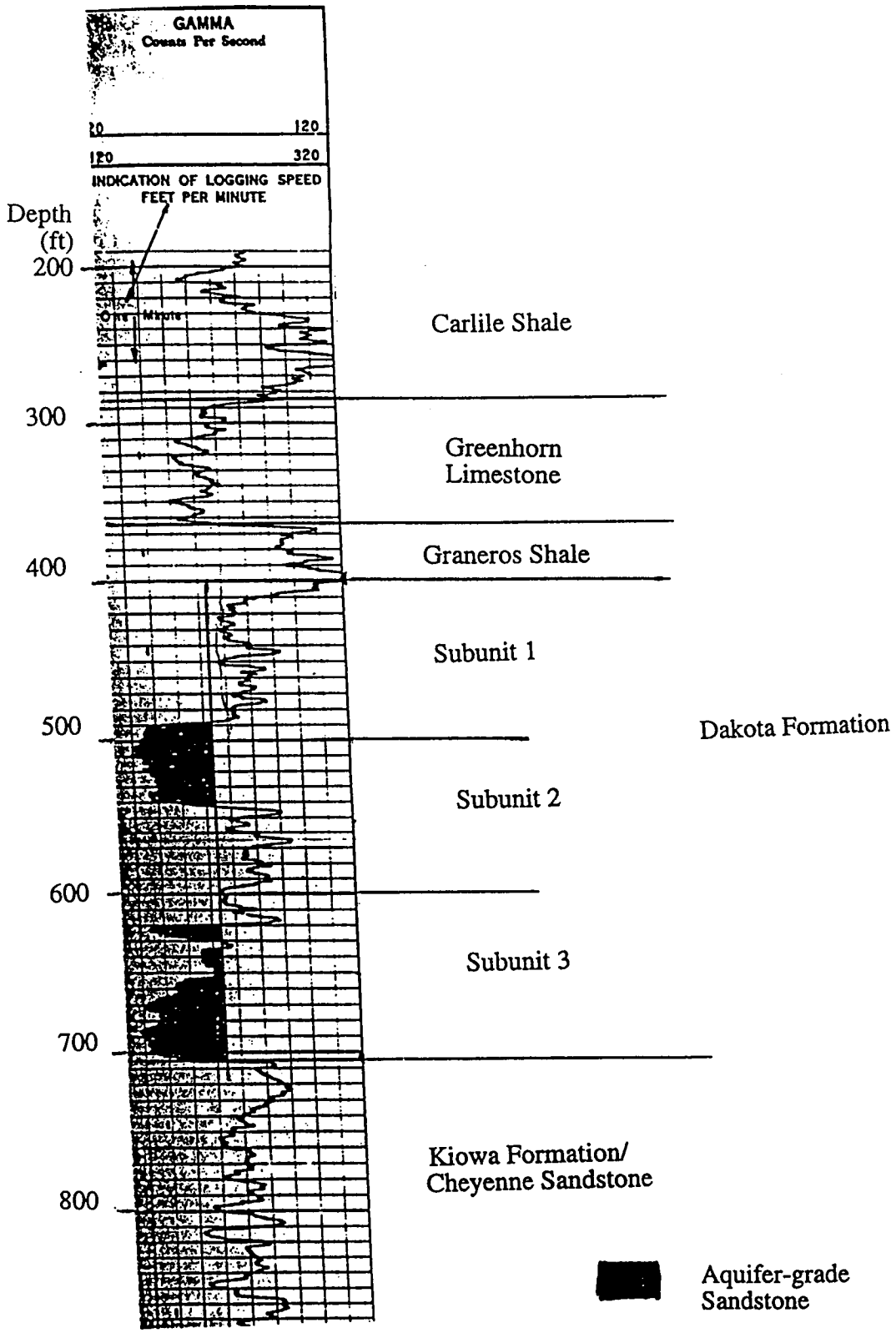

Figure 3. Example gamma-ray log from a borehole drilled for oil production showing the subunits of the Dakota Formation used in this project. The darkened intervals on the log represent significant sandstone aquifers where the gamma ray intensity is less than 60 API units.

Figure 4

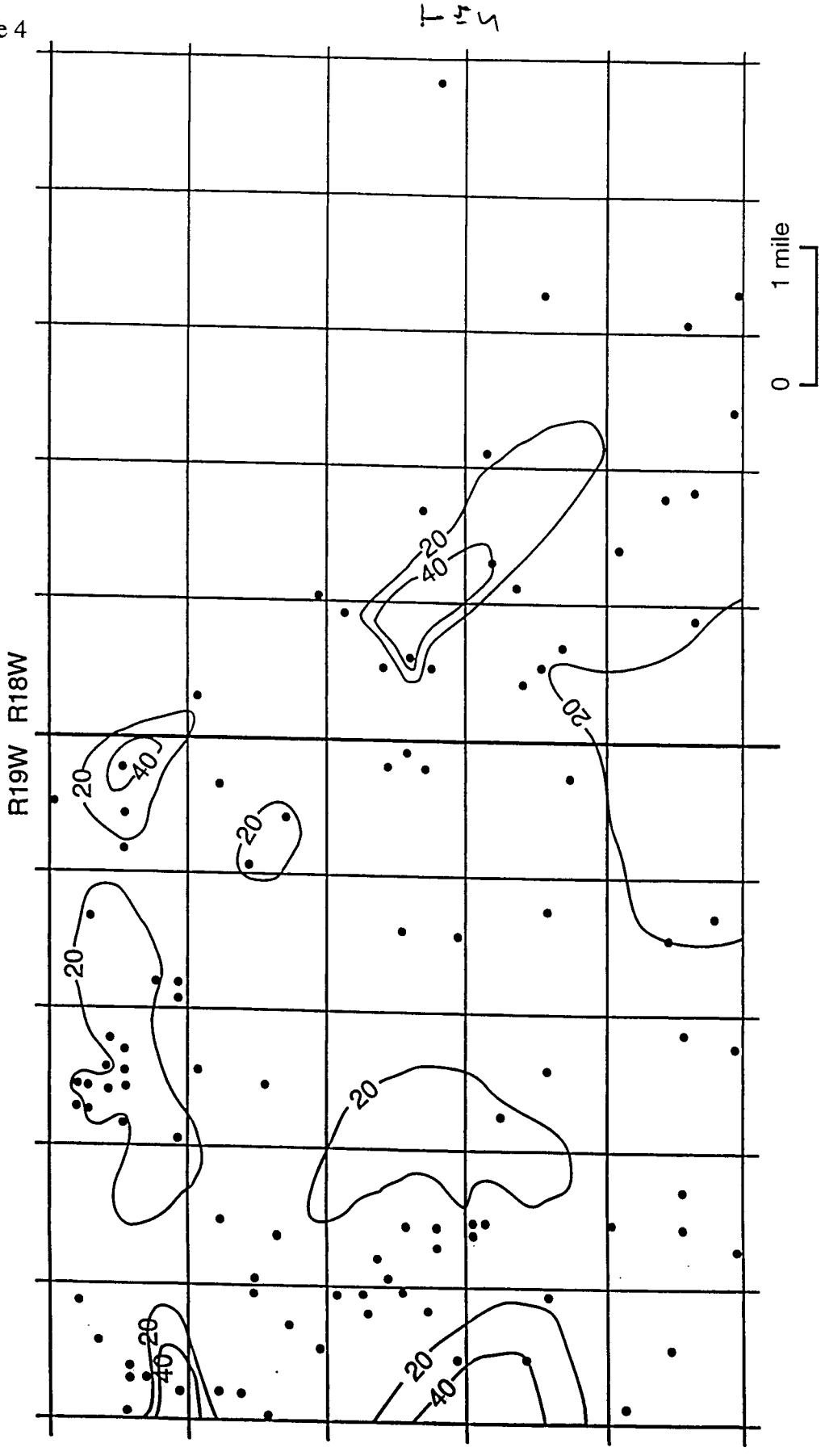

Figure 4. Percent sandstone in Subunit 1 of the Dakota Formation in the study area.

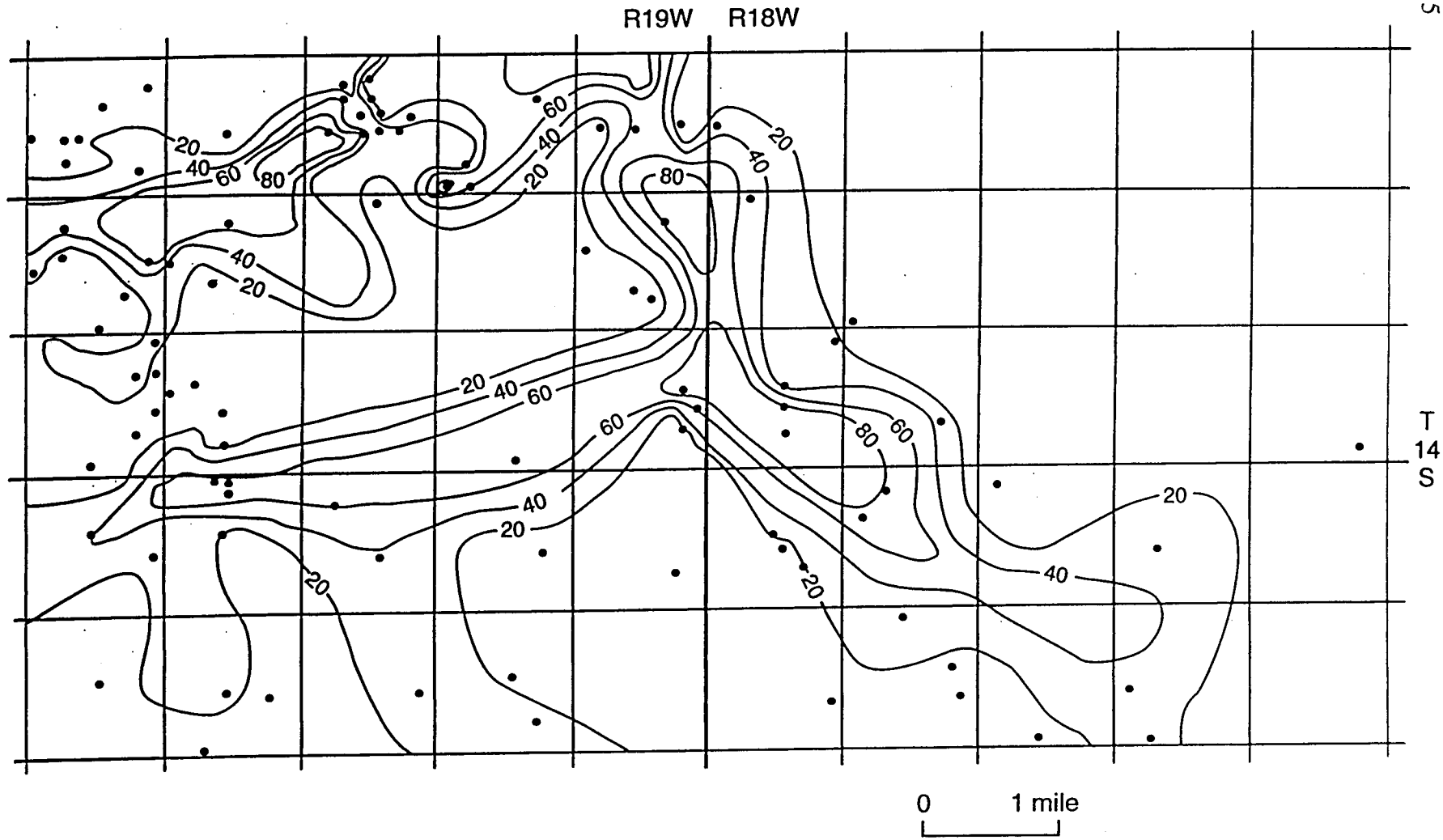

Figure 5. Percent sandstone in Subunit 2 of the Dakota Formation in the study area.

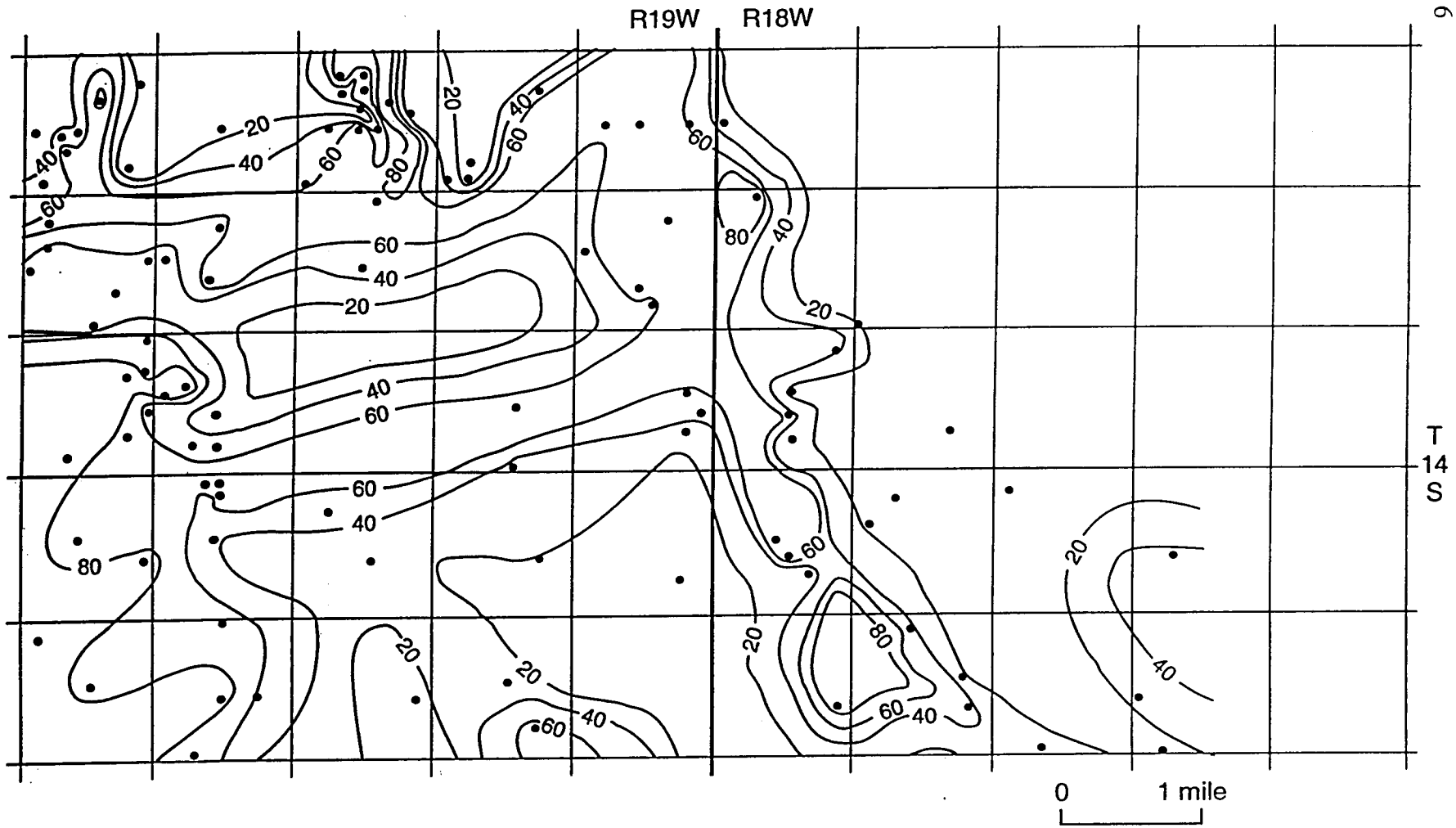

Figure 6. Percent sandstone in Subunit 3 of the Dakota Formation in the study area.

In this project, we assumed that at a minimum sandstone fraction of 50%, connections between sandstones are probable along the main sandstone trends in all Subunits 2 and 3 and in vertically adjacent subunits. Within the wellfield the sandstone fraction exceeds 60% inSubunits 2 and 3 indicating a very high probability of sandstone-body interconnection within each layer. In Subunit 1 sandstone fraction is 40% or less, but the sandstone bodies are sporadically distributed only near the base of and not throughout the subunit thickness, which suggests that where they occur the sandstones form laterally connected bodies.

The sandstones in Subunit 2 are the primary source of ground water for the production wells. The area of probable sandstone-body lateral interconnection for Subunit 2 of the Dakota Formation was modified using the results from the 1992 and 1997 pumping tests (Figure 7). The more hydraulically connected part of the sandstone aquifer in Subunit 2 ranges from approximately 0.5 mi to 1 mi in width within the wellfield. Within this subunit sandstone hydraulic conductivity and specific storage exhibit some systematic variation with generally higher values in the central and eastern parts of the wellfield (Figure 7). Net sandstone thickness in Subunit 2 in this part of the wellfield is the highest, and there is probable vertical connection with sandstones in Subunits 1 and 3 (Figure 5).

Situated in between the more hydraulically connected sandstones and the mudstone (less than 20% sandstone) is a zone where the sandstone is interbedded with mudstone (Figure 8). The sandstone in this zone is assumed to be finer grained, less well sorted, and hence, less permeable than the adjacent channel sandstone. From the low sandstone fraction, these lenses are more likely to be hydraulically isolated from each other than those nearer the axis of the E-W and NW-SE trending amalgamated sandstones.

Sandstone aquifer and mudstone aquitard hydrologic properties

The variation in sandstone hydraulic conductivity appears to be related to texture and sedimentary structures in both the upper and the lower Dakota aquifers in Kansas with an overprinting of the effects of diagenetic and post-diagenetic processes (Macfarlane et al., 1994). Massive, coarser grained, well sorted sandstones typically occur near the base of the Dakota Formation and are more permeable than the cross-laminated, finer grained, less well sorted sandstones higher up in the formation.

In the Hays wellfield the sandstone hydraulic conductivities derived from the pumping tests in the upper Dakota aquifer vary by a factor of two (22.3 ft/day in the D-2 test using MD-2&3 as an observation point to 12.2 ft/day in the 1997 pumping test at D-6 using MD-6 as an observation point) (Figures 1 and 7). Detailed descriptions of the Dakota Formation strata penetrated during the drilling are not available to indicate variations in overall sandstone texture

Figure 7

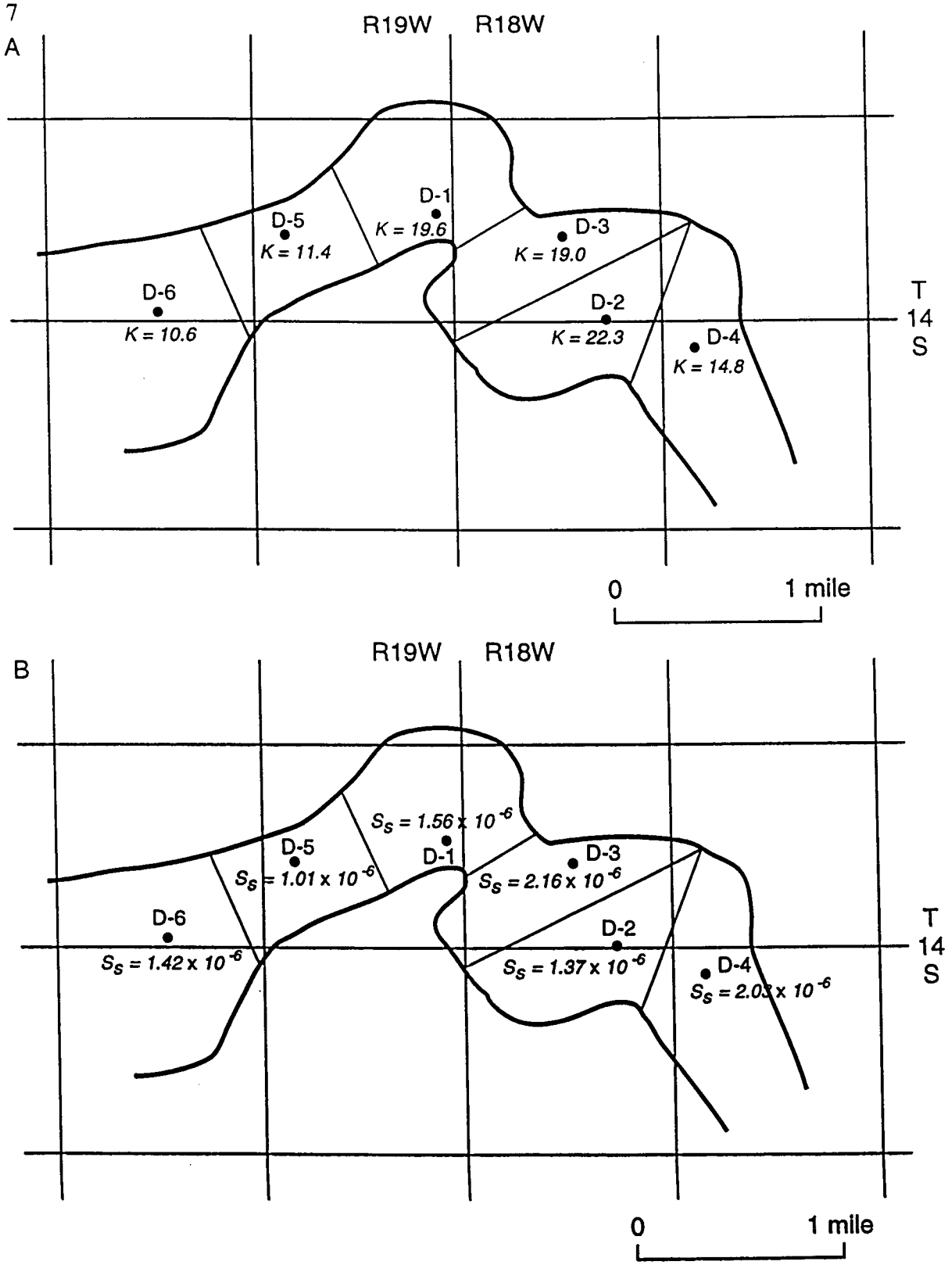

Figure 7. Conceptual hydrogeologic model of the more hydraulically connected sandstone aquifer in the wellfield showing a simplified distribution of aquifer properties (A, hydraulic conductivity and B, speciic storage). Aquifer properties are from the 1997 and 1992 pumping tests.

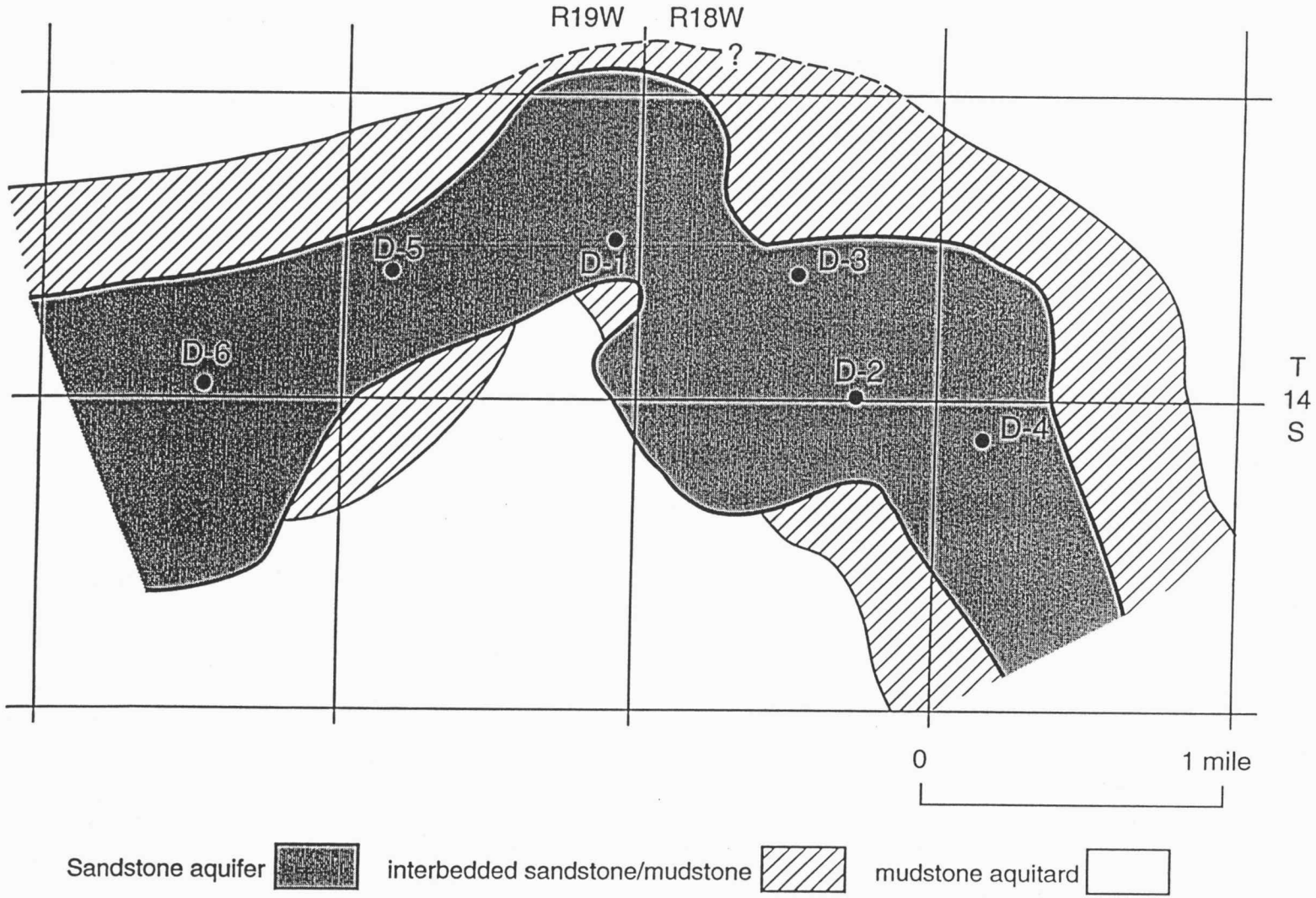

Figure 8. Interpreted extent of the more hydraulically connected sandstones, and fringe (less permeable interbedded sandstone and mudstone) in the Dakota wellfield using subsurface geologic refined by the results of the 1992 and 1997 pumping test results.

from wellsite to wellsite or vertically at a given wellsite. However, the small variation in hydraulic conductivity across the wellfield suggests little overall textural variability.

The sandstone specific storage values calculated from the 1992 and 1997 pumping tests vary from 7.7×10^{-7} ft^{-1} to 2.0×10^{-6} ft^{-1} (Figure 7). These property values are well within the range of specific storage values for Dakota aquifer sandstones calculated from other pumping tests conducted in the Dakota aquifer in Kansas and southeastern Colorado (Macfarlane et al., 1998).

Hydraulic conductivity values for the mudstone could not be derived from the pumping tests because there were no observation wells to observe the flow system response to pumping and recovery in the mudstone. Similarly, earlier tests conducted by the Kansas Geological Survey in the Dakota Aquifer Program were also not configured to provide estimates of these mudstone flow properties. Mudstone hydraulic conductivity values from the literature range from 2.8×10^{-6} to 7.9×10^{-2} ft/day (Freeze and Cherry, 1979; Domenico and Schwartz, 1992; Spitz and Moreno, 1996). In this project we assumed that the mudstone hydraulic conductivity was near the middle of this range at 1×10^{-4} ft/day. This assumed value is consistent with estimates inferred from pumping and slug test results reported in Wade (1992) and Macfarlane et al. (1994).

No specific storage values for mudstone were found from a review of the literature. Consequently, it is assumed that the mudstone specific storage is in the same range of values as the sandstone specific storage.

Ground-water Flow

The potentiometric surface map of the upper Dakota aquifer shows higher hydraulic heads to the west of the wellfield than to the east. This indicates a predominantly eastward ground-water flow direction across the wellfield (Figure 9). The apparent smoothness of the potentiometric surface belies the complex distribution of aquifer and aquitard units within the upper Dakota and is due to the lack of data throughout much of the study area. The slight bending of the contours in the center of the study area is due to the concentration of data within and the lack of data outside of the wellfield. From MD-6 to MD-2&3 the hydraulic gradient is much steeper than it is from MD-2&3 to MD-4 (Figure 9). The change in hydraulic-head gradient appears to be related to a higher transmissivity in the eastern half of the wellfield than in the west. From the pumping tests discussed in Volume 1 of this report, transmissivity values increase from 584 ft^2/day at wellsite 6 at the west end of the field to 1,946 ft^2/day at wellsite 4 at the east end. The increase in transmissivity is due to higher hydraulic conductivity and greater sandstone aquifer thickness.

Figure 9

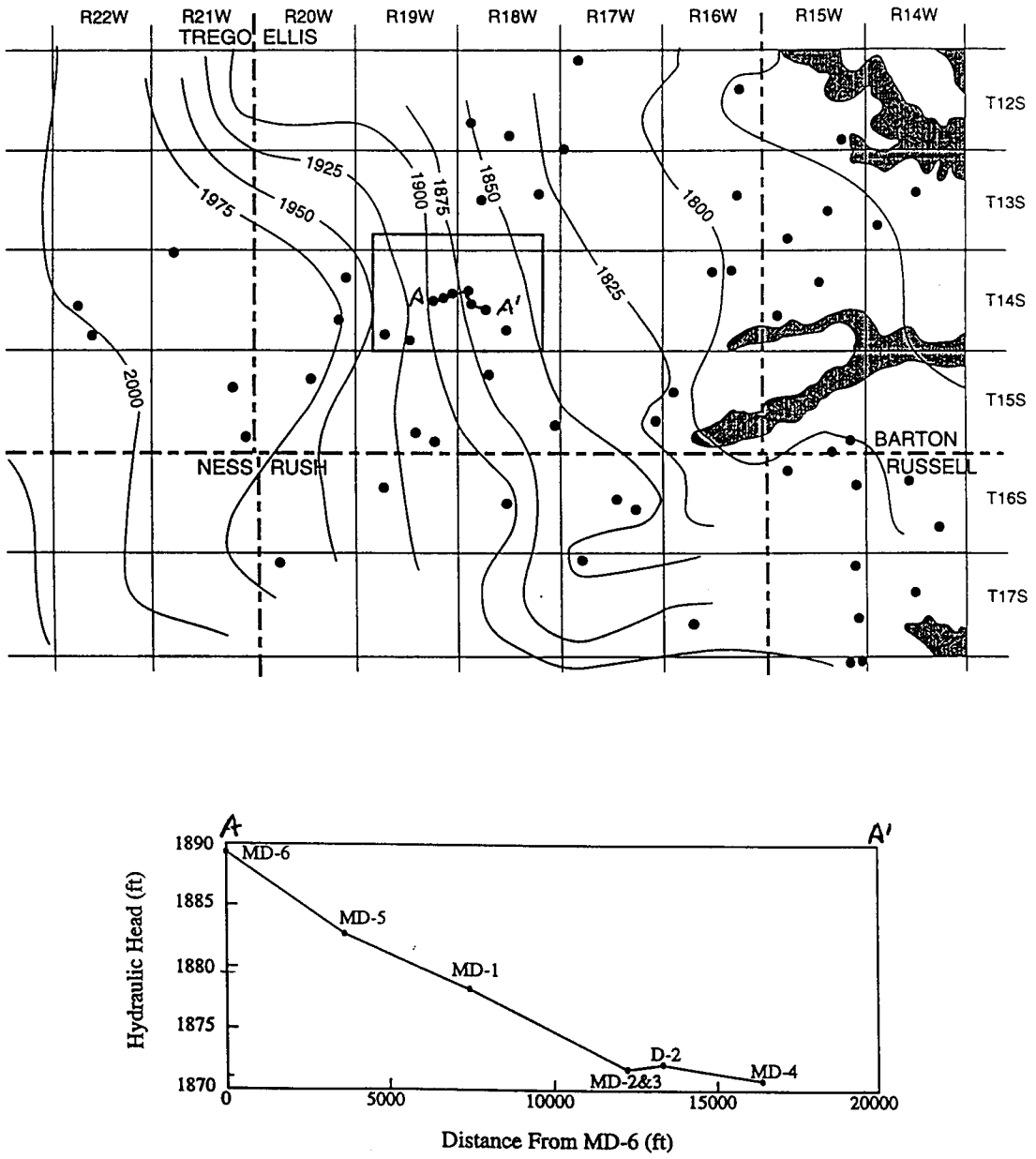

Figure 9. Regional potentiometric surface map of the upper Dakota aquifer and hydraulic head profile (A-A') in the vicinity of the study area.

Local Sources of Recharge

Local recharge from overlying sources enters the upper Dakota aquifer as leakage from the Upper Cretaceous aquitard and is on the order of 0.1% or less of lateral flow in the confined Dakota aquifer to the west of the wellfield (Macfarlane and Smith, 1994; Helgeson et al., 1993; and Belitz and Bredehoeft, 1988). Eastward of the wellfield, the regional aquitard is a thinner, more permeable unit and recharge entering the top of the aquifer may amount to as much as 10% of the lateral flow within the Dakota (Smith and Macfarlane, 1994; Smith, 1995).

An additional source of recharge to the Dakota aquifer system comes from the underlying Permian Cedar Hills Sandstone aquifer where both aquifers are hydraulically connected, including the area around the city's Dakota wellfield. The total recharge from this source is estimated to be less than 1% of the lateral flow in the upper Dakota aquifer. The Cedar Hills Sandstone aquifer is a source of both natural halite-solution and injected oil brines (Macfarlane et al., 1988).

No field studies have been conducted to verify these estimates of recharge in the wellfield vicinity.

Chapter 3: Simulation of Ground-water Flow in the Upper Dakota Aquifer in the Wellfield Vicinity

In hydrogeology, the phenomenon of ground-water flow can only be observed indirectly in boreholes and wells, more often than not. As a result, it is often impossible to fully comprehend or make predictions of the impact of imposed hydrologic stresses on a complex aquifer system like the upper Dakota without a means of synthesizing all of the factors related to its functioning. Simulation of the ground-water flow system with models performs this integrative function and thus is an invaluable tool for developing new insights and for management and planning. For simulation to be useful for these purposes, there must be (1) a correct conceptual hydrogeologic model that includes the salient features of the flow system related to its functioning, (2) an appropriate selection of parameter values and boundary conditions that characterize the hydrogeologic setting, and (3) a selection of spatial and temporal trends in hydrologic stresses and trends in water levels through time projected into the future.

In this project simulations that were developed are based on a rather limited data set: (1) the relatively sparse data base of gamma-ray borehole geophysical logs of oil wells that have been drilled at various times in the past and for the siting of production and monitoring water wells, (2) the pumping test results from the wellfield only and (3) the water-level history from the observation and pumping wells through almost 5 yrs of pumping. Although this represents a large body of information, it is not sufficient to the task of making reliable quantitative assessments considering the extreme complexity of the upper Dakota aquifer.

Overview of ground-water model design

Model design involves translating the hydrogeologic model into a form that is suitable for mathematically simulating ground-water flow using a numerical model (Anderson and Woessner, 1992). The conceptual hydrogeologic model of the upper Dakota aquifer is presented in Chapter 2, of this report volume and is summarized in Figures 7 and 8. The model design part of the process involves model grid design, selection of time step intervals for transient simulation, setting boundary and initial conditions, and preliminary selection of hydrologic properties values and values for hydrologic stresses.

Governing equation

The governing equation that generally describes the transient flow of ground water through a three-dimensional, heterogeneous, anisotropic porous medium is (Anderson and Woessner, 1992):

$$\frac{\partial}{\partial x}\left(K_x \frac{\partial h}{\partial x}\right)+\frac{\partial}{\partial y}\left(K_y \frac{\partial h}{\partial y}\right)+\frac{\partial}{\partial z}\left(K_z \frac{\partial h}{\partial z}\right)+R = S_s \frac{\partial h}{\partial t} \qquad \text{Eqn. 1}$$

Where K_x, K_y, and K_z and are the x, y, and z components of hydraulic conductivity, R is a source or sink (negative when water leaves the system), S_s is specific storage, h is the hydraulic head, and t is time. In this project, R represents the withdrawal of water from the aquifer by pumping wells or the input of water to the aquifer by injection wells. For the steady state case, the time rate of change of fluid mass storage is equal to zero and the hydraulic head is not a function of time (Freeze and Cherry, 1979). Thus, the steady-state ground-water flow equation simplifies to:

$$\frac{\partial}{\partial x}\left(K_x \frac{\partial h}{\partial x}\right)+\frac{\partial}{\partial y}\left(K_y \frac{\partial h}{\partial y}\right)+\frac{\partial}{\partial z}\left(K_z \frac{\partial h}{\partial z}\right)+R = 0 \qquad \text{Eqn. 2}$$

In this project we treat the ground-water flow system prior to installation of the wellfield as the steady-state condition. Macfarlane (1993) concluded that usage of the upper Dakota for water supply prior to wellfield construction was limited to a few scattered domestic wells to the west near the Ellis-Trego county line. As a result, we assume that the regional potentiometric surface has not been significantly affected by these limited withdrawals of water prior to operation of the wellfield. We assume that prior to development a steady-state condition generally existed where the natural ground-water flow pattern was unaffected by significant hydrologic stresses.

Visual MODFLOW and the Zone Budget Utility

MODFLOW (McDonald and Harbaugh, 1988) was selected for this project because it is a commonly used, readily available, off-the-shelf modeling package. Visual MODFLOW (Waterloo Hydrogeologic, 1994) uses a graphical interface, which acts as a pre- and postprocessor for the MODFLOW source code. MODFLOW is used to solve the transient and steady-state, three-dimensional, ground-water flow equations with its attendant boundary and initial conditions. MODFLOW is a block-centered, finite-difference code that can be used to simulate ground-water flow in two or three dimensions. The software has a modular structure and consists of a main program and a series of subroutines referred to as modules. These subroutines are grouped into "packages" that deal with specific features of the hydrologic system to be simulated or with a numerical technique to solve the finite-difference formulation of the flow equation. The packages used for the steady-state (pre-development) model of the wellfield vicinity are the Block Centered Flow, Basic, General Head Boundary, and Strongly Implicit Procedure packages. The Block Centered Flow and Basic packages contain input information on

how the model is constructed and the cell-by-cell hydrogeologic properties and thickness (Waterloo Hydrogeologic, 1994).

Four different solution techniques are available in MODFLOW to solve the finite difference form of the ground-water flow equations. In formulating the Visual MODFLOW software, Waterloo Hydrogeologic developed a proprietary solver package (WHS) in addition to the Strongly Implicit Procedure (SIP), the Slice Successive Overrelaxation (SOR), and the Preconditioned Conjugate-Gradient (PCG2) packages of the original software described by McDonald and Harbaugh (1988). These are described in some detail in the user's manual for Visual MODFLOW.

We tested both the WHS and the SIP solver packages using a simplified, steady-state ground-water flow model of the wellfield and found that the resulting hydraulic-head distributions differed by less than 0.1 ft. We also found that the WHS solver produced a solution to the steady-state problem faster than the SIP solver but noticed that model runs using the WHS solver were more likely to be non-converging. We did not evaluate the SOR or the PCG2 solver packages. We used the SIP solver package in this modeling project.

The utility Zone Budget (Harbaugh, 1990) is an accounting program that uses the cell-by-cell flows from MODFLOW to calculate the ground-water flux from the boundary conditions, pumping wells, and changes in storage during each stress period. Fluxes may be calculated from one cell to another, from one model subregion to another, or for the entire model.

Model grid

The model represents an area 4 mi north-south by 6 mi east-west, within the 5 mi by 10 mi study region, 6 mi southwest of Hays, Kansas (Figure 10). The model is only of the confined upper Dakota aquifer in Secs. 7-9, 16-21, and 28-30, T. 14 S., R. 18 W and Secs. 10-15 and 22-27, T. 14 S., R. 19 W.

The model region is smaller than the study area size because of the complete lack of information over large portions of the study area outside of the immediate wellfield vicinity. Only 116 gamma-ray logs of boreholes were available to map the sandstone distribution in the Dakota Formation in a 50 mi^2 study area, or about 2 logs/mi^2 at best. Because the distribution of these logs is nonuniform, no subsurface information is available locally for significant parts of the study area, even in some areas near the wellfield. Unfortunately, this small size of the model region can pose a problem for transient simulations with pumping wells if the model boundaries are too close to the primary region of interest (Anderson and Woessner, 1992). When the model region is small there is a greater likelihood that the effects of pumping will reach the model boundaries, thus precluding the ability of the model to accurately simulate the effects of pumping throughout the aquifer being simulated.

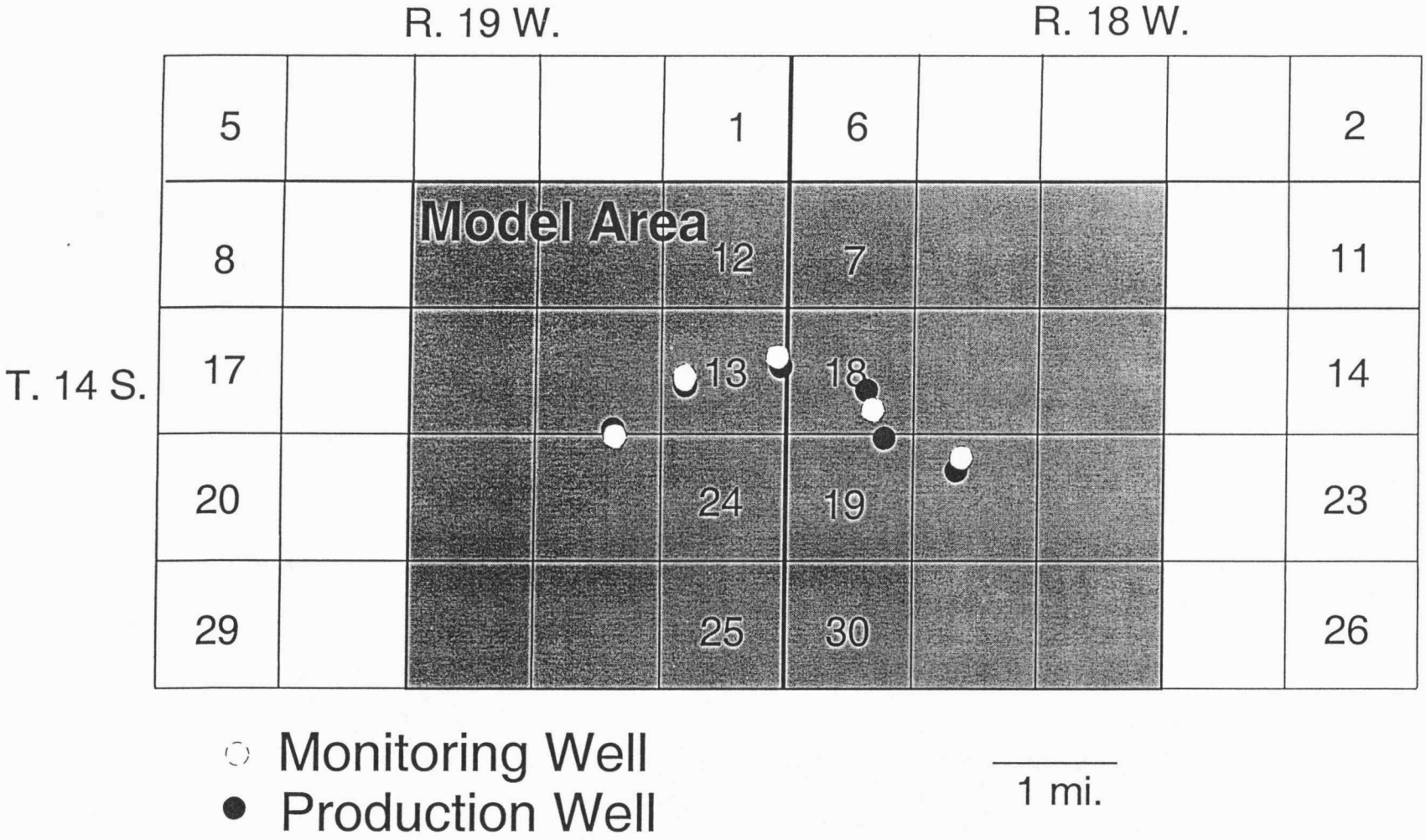

Figure 10. Location of the model area with respect to the study area.

Figure 11

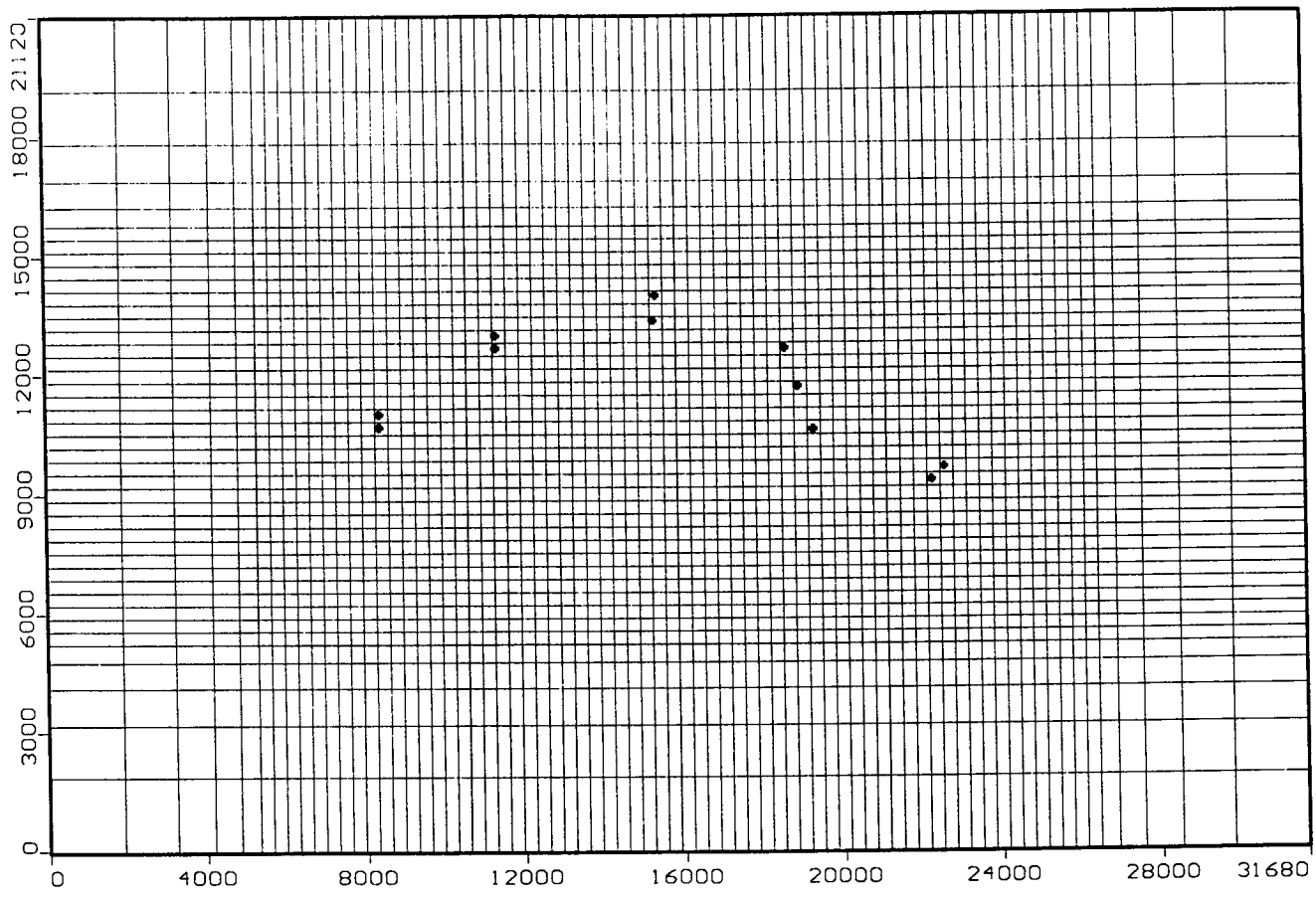

Figure 11. Schematic diagram showing the model grid and the distribution of model cell sizes with respect to the production and monitoring wells (dots). Numbers on the axes the distance in feet away from the southwest edge of the model region.

The three-dimensional model consists of 2 layers with 42 rows and 74 columns in each layer for a total of 3,108 cells, all of which are active (Figure 11). The modeled region can be separated into an inner core region that includes the wellfield vicinity and an outer region nearer the edges of the model. The core region of the model is 2 mi by 4 mi in size and the cells in this part of the model are 330 ft by 330 ft in size. The smaller cell size in the central portion of the model allows for more accurate depiction of (1) the curvature of the potentiometric surface in the wellfield vicinity due to the hydraulic conductivity contrast across the mudstone/sandstone boundary and pumping and (2) the complex shape of the mudstone/sandstone boundary and the nonuniform distribution of aquifer properties in the wellfield as it is represented in the hydrogeologic model (Figures 7 and 8).

This minimum cell size is also a balance between the observation and the production well spacing and the uncertainty in the oil-well borehole locations used to map most of the subsurface geology near the wellfield. In the transient form of the model the x-y dimensions of the cells must be small enough so that the pumping and observation wells are situated in different cells. With this accommodation the pumping test data can be used to assist in model calibration. The actual distance between the pumping and observation wells at wellsites 4, 5, and 6 is less than 300 ft and slightly less than 500 ft at wellsite 1 (Figure 1). On the other hand, most of the borehole locations are recorded only to the nearest 1/64 of a section, a square area 660 ft by 660 ft in size.

Within the 1-mi. wide outer region that surrounds the core region of the model there is very little hydrogeologic data (Figure 11). As a result, the model cells in this part of the model are much larger and the cell dimensions progressively increase in size by a factor of 1.4 toward the boundaries of the model. To maintain model stability, adjacent cells increase in size by more than a factor of 1.5 (Anderson and Woessner, 1992). The cell size at the corners of the grid is 1,883 ft by 1,883 ft.

The upper model layer (model layer 1) corresponds to Subunit 1 of the Dakota Formation. The lower layer (model layer 2) represents Subunit 2 of the Dakota Formation and where there is vertical interconnection between sandstone bodies, Subunits 2 and 3.

The elevation of the model layer tops is based on the subsurface mapping discussed in Volume 1 of this report. Elevations were determined for the center of each cell by interpolation using contoured maps showing the elevation of the tops of the layers in the vicinity of the Dakota wellfield. Figures 12 and 13 are maps showing the elevation of the tops of model layers 1 and 2, respectively, and Figures 14 and 15 show the variation in layer thickness for model layers 1 and 2, respectively. The thickness of model layer 1 ranges from 80 ft in an area 0.75 mi southwest of D-6, to 103 ft at MD-1 and the thickness of model layer 2 ranges from 32 ft at MD-6 to 100 ft at both D-6 and D-4.

Figure 12

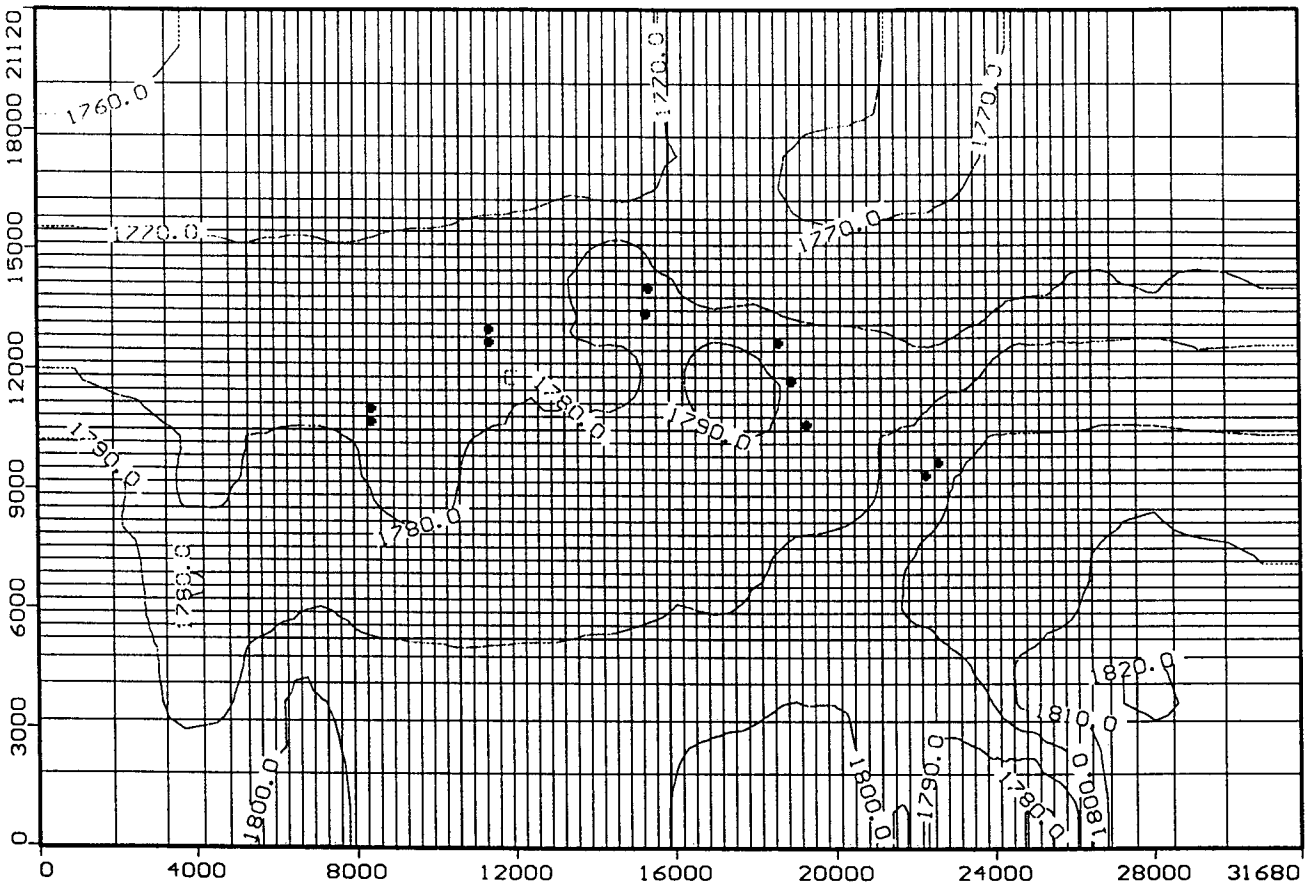

Figure 12. Elevation in feet above mean sea level of the top of model layer 1. Dots represent the pumping and observation wells.

Figure 13

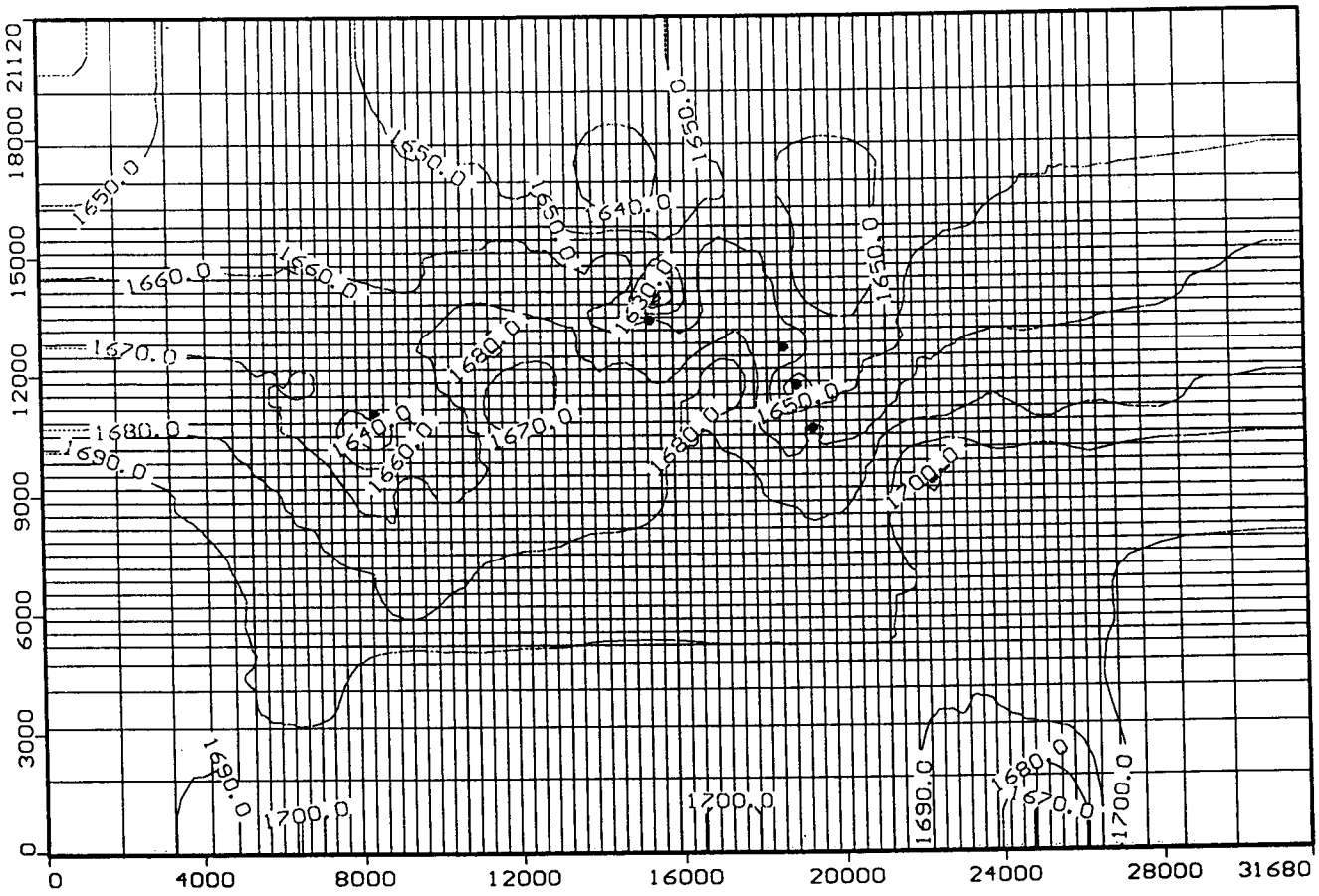

Figure 13. Elevation in feet above mean sea level of the top of model layer 1. Dots represent the pumping and observation wells.

Figure 14

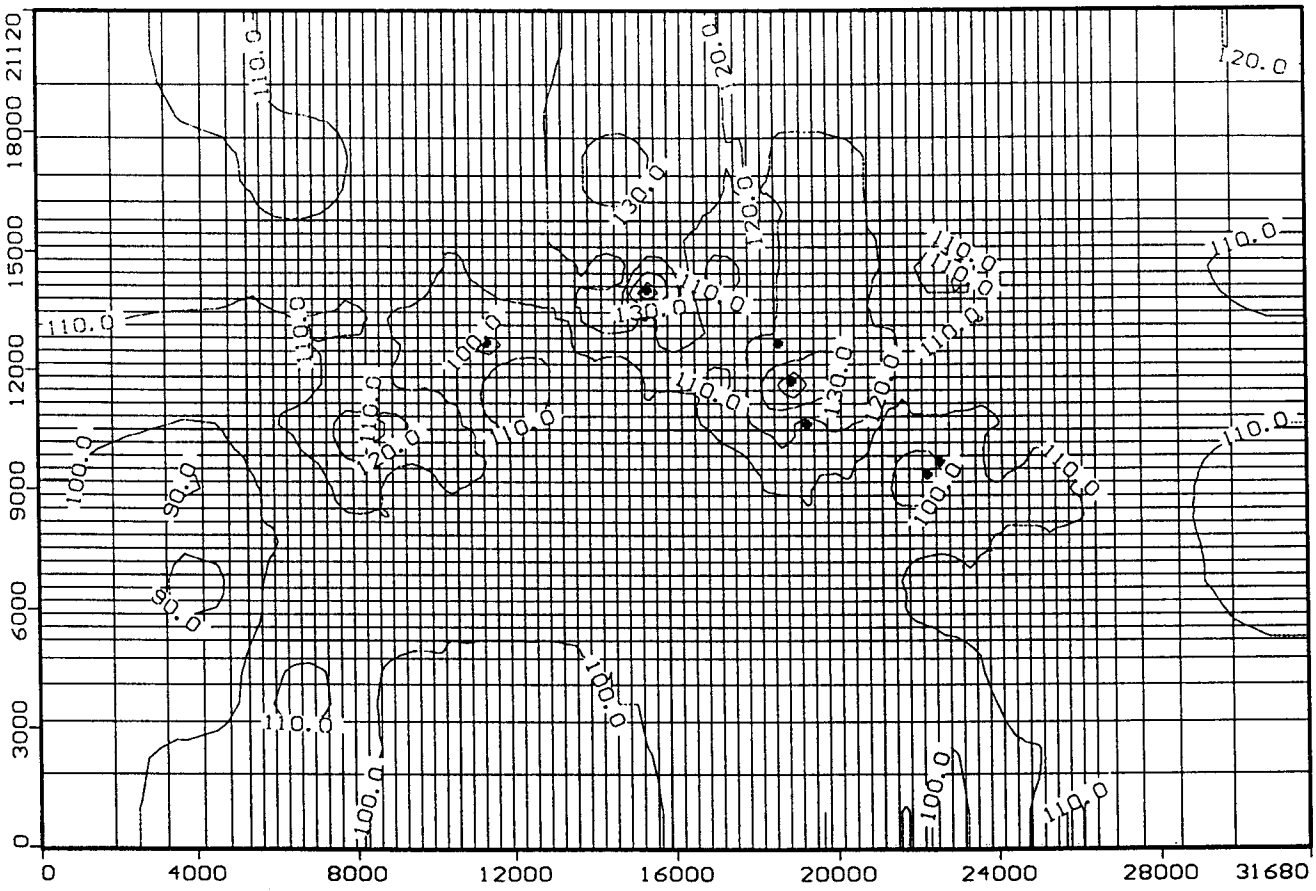

Figure 14. Thickness in feet of model layer 1. Dots represent the pumping and observation wells.

Figure 15

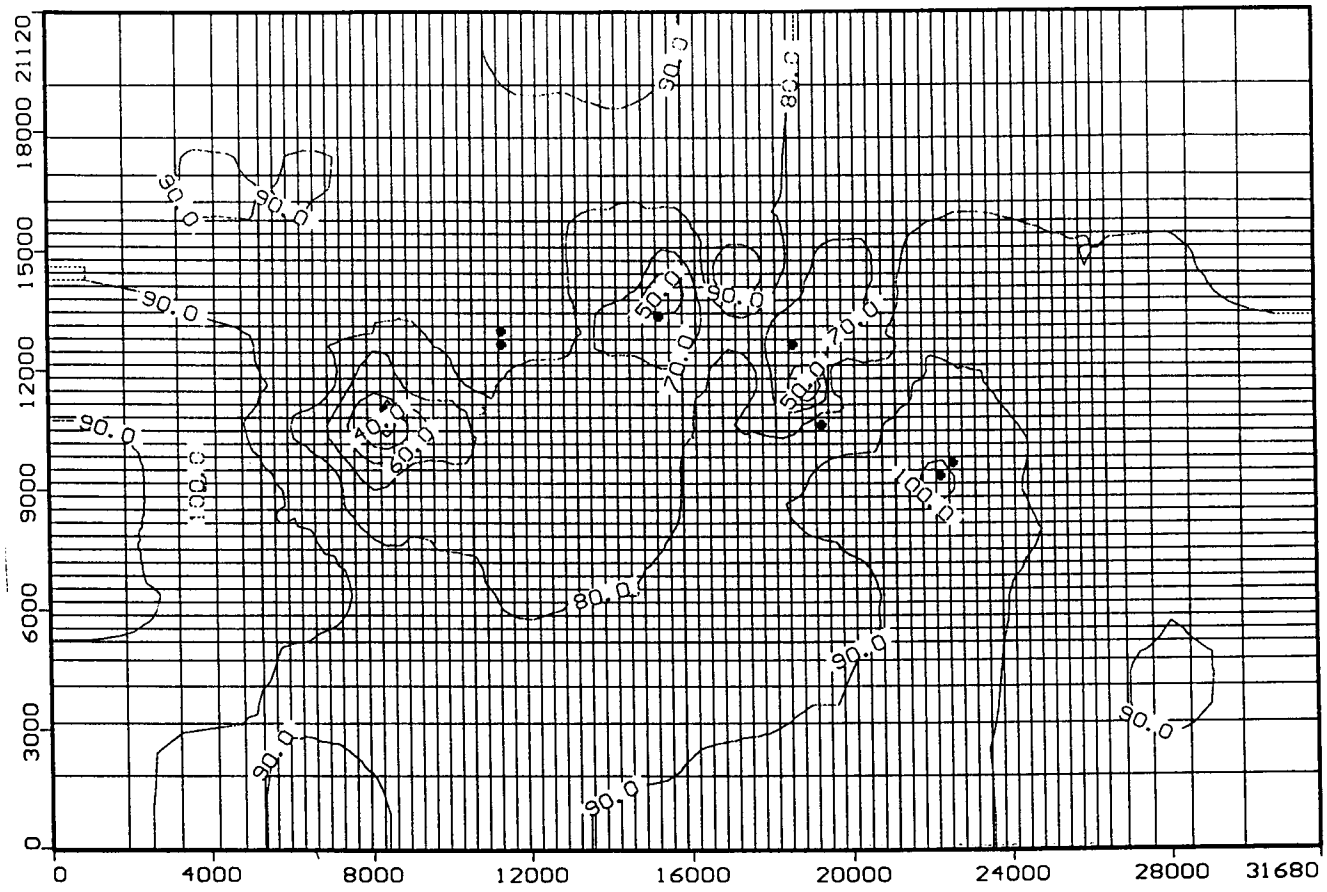

Figure 15. Thickness in feet of model layer 2. Dots represent the pumping and observation wells.

Hydrologic properties

In Visual MODFLOW the aquifer parameters are entered by inputting the horizontal and vertical components of the hydraulic conductivity (K_h, K_v), the within-model-layer anisotropy, the specific storage (S_s), and the layer thickness (b) for each cell in the model (Waterloo Hydrogeologic, 1994). It is assumed that the hydraulic conductivity in the row direction is the same as the hydraulic conductivity in the column. Consistent with what is typically assumed for lithified, sedimentary strata (Domenico and Schwartz, 1992), the vertical component of hydraulic component of hydraulic conductivity, K_v, is assumed to be $0.1K_h$ for each model layer. The transmissivity and storativity are calculated prior to solution of the finite-difference form of the flow equations McDonald and Harbaugh, 1988). Transmissivity (T) and storativity (S) are calculated for each block as:

$$T = K_h b \qquad \text{Eqn. 3}$$

and

$$S = S_s b. \qquad \text{Eqn. 4}$$

In the numerical models that include a sandstone aquifer, wellfield area K_h and S_s values were initially assigned to each cell in the main part of the channel sandstone body according to the hydrogeologic model (Figures 7 and 8). The channel deposits in the wellfield consist of the most permeable, hydraulically connected sandstone. The surrounding mudstones are flood-plain deposits with sporadically distributed, thin, hydraulically isolated lenses of low permeability sandstone amounting to <20% of the total volume of the deposits. These deposits constitute the bulk of the deposits in the model region (Figure 8). Analysis of 1997 D-1 and D-6 pumping test data indicated that mudstone transmissivity is at least 3-4 orders of magnitude lower than the transmissivity of the channel sandstone (Butler, 1998), which is consistent with the range of estimated values from the literature (Freeze and Cherry, 1979; Domenico and Schwartz, 1992; Spitz and Moreno, 1996). Thus, the mudstone K_h was set equal to 1×10^{-4} ft/day. Lacking any information either from this study or the literature, the mudstone S_s was assumed to be the same as for the geometric mean of the sandstone S_s values from pumping tests. Thus, the mudstone S_s was set initially at 1.5×10^{-6} ft^{-1} for all cells in the model representing the mudstone.

Values for other parameters also need to be set prior to running the model. The specific yield of the sandstone was assumed to be 0.05 and the effective and total porosities were assumed to be 0.15. The specific yield of the mudstone was assumed to be 0.01 and the effective and total porosities were assumed to be 0.10 and 0.01, respectively (Spitz and Moreno, 1996).

Starting hydraulic head

Hydraulic head values were estimated for each cell in the model from the pre-development, regional potentiometric surface for the Dakota aquifer in the study area (Figure 9). Additional contours were added by hand to produce a regional potentiometric surface map with a smaller 5-ft contour spacing. Outside of the wellfield, few data points were available to guide placement of these contours. Consequently, an attempt was made to draw the 5-ft in such a way that their spacing on the map was uniform. Hydraulic heads were then determined for each cell center in the model by interpolation. The resulting cell-by-cell hydraulic head distribution was contoured using the Transform module of the NOESYS software package (Fortner Research LLC, 1996) and compared visually with the original, hand-contoured map to spot-check for errors.

Boundary conditions

Determination of which boundary conditions are most appropriate for the model is critical because the boundaries provide a local context that references ground-water flow within the model to the much larger, regional and subregional flow system (Anderson and Woessner 1992). Three boundary condition types were used in the model of the wellfield vicinity: no-flow, constant head, and general head or head-dependent flux boundaries.

Leakage from overlying and underlying units is believed to be a small fraction (1-10%) of lateral flow within the upper Dakota aquifer (Macfarlane, 1993; Smith, 1995). To simplify the conceptual numerical model, it is assumed that recharge from these sources to the upper Dakota aquifer can be ignored given the nature of the problem, the lack of vertical hydraulic conductivity data for the younger Cretaceous rocks above the Dakota, and our uncertainty with respect to recharge rates. In particular, the data of the last 5 yrs do not indicate a diminished water quality in aquifer due to pumping which suggests that hydraulic connection with underlying sources of saline water in the lower Dakota and in the Cedar Hills Sandstone may be very poor. Consequently, the upper and lower boundaries of the model are considered no-flow boundaries. Initially it was assumed that the aquifer would remain confined throughout the simulation period, i.e., transmissivity and storativity, would remain constant during simulation.

From the pre-development regional potentiometric surface, the ground-water flow direction in the study area is believed to be approximately from west to east, perpendicular to the lines of equal hydraulic head for the isotropic porous medium (Figure 9). The north and south model boundaries are sub-parallel to the flow lines in the Upper Dakota aquifer and thus, are considered to be no-flow boundaries (Figure 16). The simulation results indicate that the no-flow boundaries are sufficiently far away from the wellfield to be essentially unaffected by pumping.

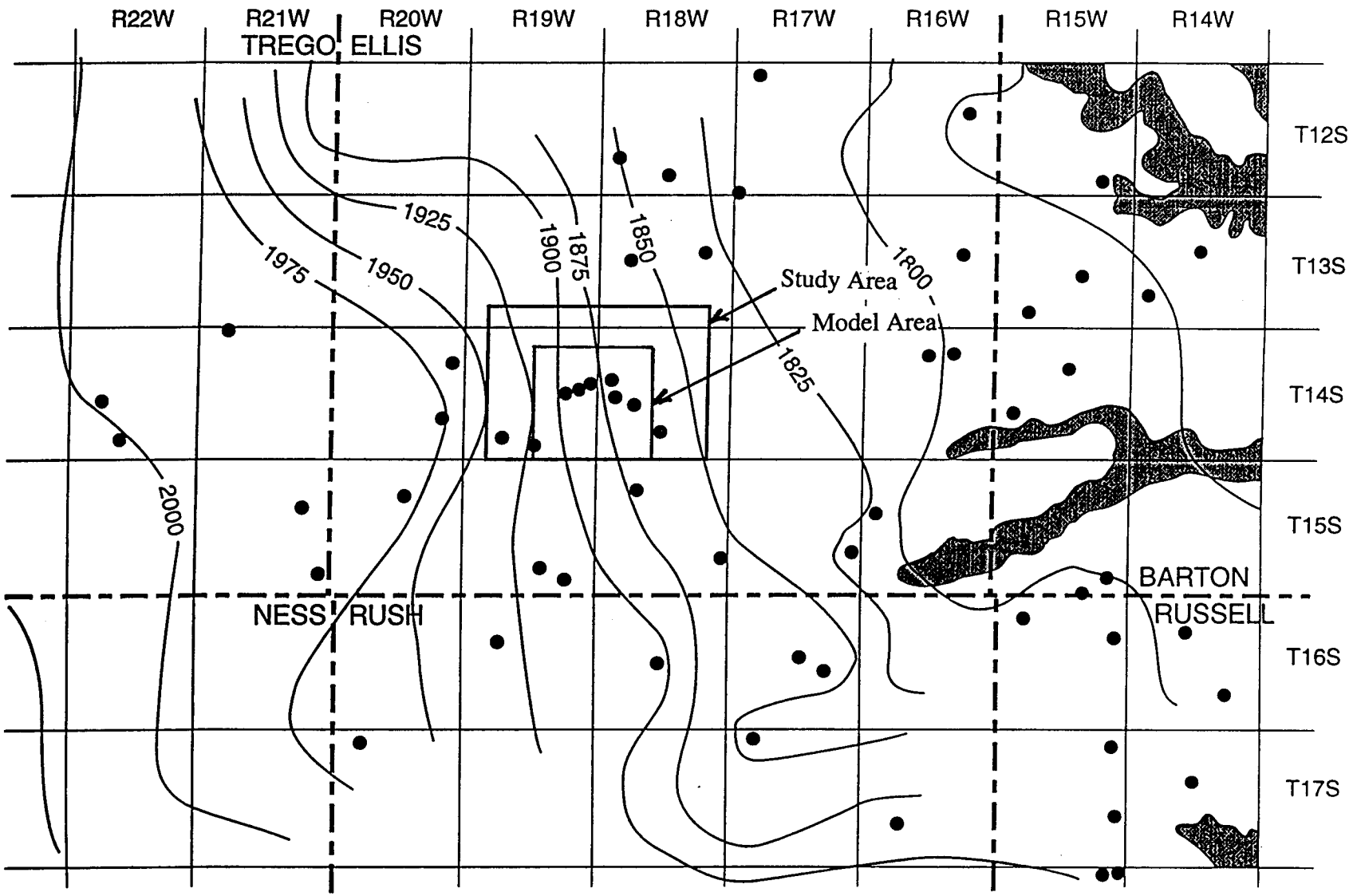

Figure 16. Orientation of the model grid with respect to the potentiometric surface map of the upper Dakota aquifer.

The east model boundary and the cells in the southeast corner of the model form a constant head-boundary which functions as a sink, drawing water into the model from the west to maintain regional hydraulic head gradient (Figure 16). This boundary condition can be used when natural specified-head boundaries are too remote for modeling purposes (Spitz and Moreno, 1996). It is important to insure that hydrologic stresses inside the model do not have a direct effect on the boundary such as might occur if the cone of depression from pumping would encounter the boundary during simulation.

The hydraulic heads in the cells associated with the specified-head boundary decrease from north to south along the east model boundary from 1860.9 ft to 1855.5 ft. In the southeast corner of the model, three cells are included as part of the specified-head boundary. Because of the NW-SE trending very permeable sandstone aquifer, it is assumed that the dominant ground-water flow direction is along the trend of the channel sandstone aquifer near this model boundary. Hence, lines of equal hydraulic head should be perpendicular to the trend of the channel sandstone. The hydraulic head in the cells representing the sandstone aquifer in the southeast corner of the model was assumed to be 1855.5 ft. The Visual MODFLOW graphical display of the flow vectors in the final steady-state model does indicate flow entering the southeast corner specified-head cell from outside of the model area to the south. However, a water-budget analysis shows that water enters the cell only from the model region. This is unexpected, but the inflow is very small (less than 0.1% of the total flow) and is not considered significant.

The hydraulic boundary condition along the west side of the model is simulated by a general head or type III, head-dependent flux boundary (McDonald and Harbaugh, 1988; Spitz and Moreno, 1996). This boundary functions as a water source or sink situated outside of the model. The rate and direction of flow depends on the hydraulic gradient and the conductance between an assumed constant-head reservoir outside of the model and the cells along the west edge of the model region (Anderson and Woessner, 1992). This boundary condition is appropriate because most of the Dakota Formation upgradient of the west model boundary consists of low permeability mudstone (approximately 70%) and sandstones of uncertain hydraulic connection. The combined effect of the head-dependent flux boundary on the west end and the specified-head boundary condition on the east end of the model is to simulate the regional hydraulic gradient through the wellfield vicinity.

The general head boundary condition simulates flow across a permeable model boundary and is dependent on the hydraulic-head difference between a "reservoir of water" outside of the model region and the cell interface with the model boundary (Figure 17). Two terms are required by the general-head boundary package in MODFLOW (McDonald and Harbaugh, 1988). The first is a conductance term, and the second is the elevation of the "reservoir head"

Figure 17

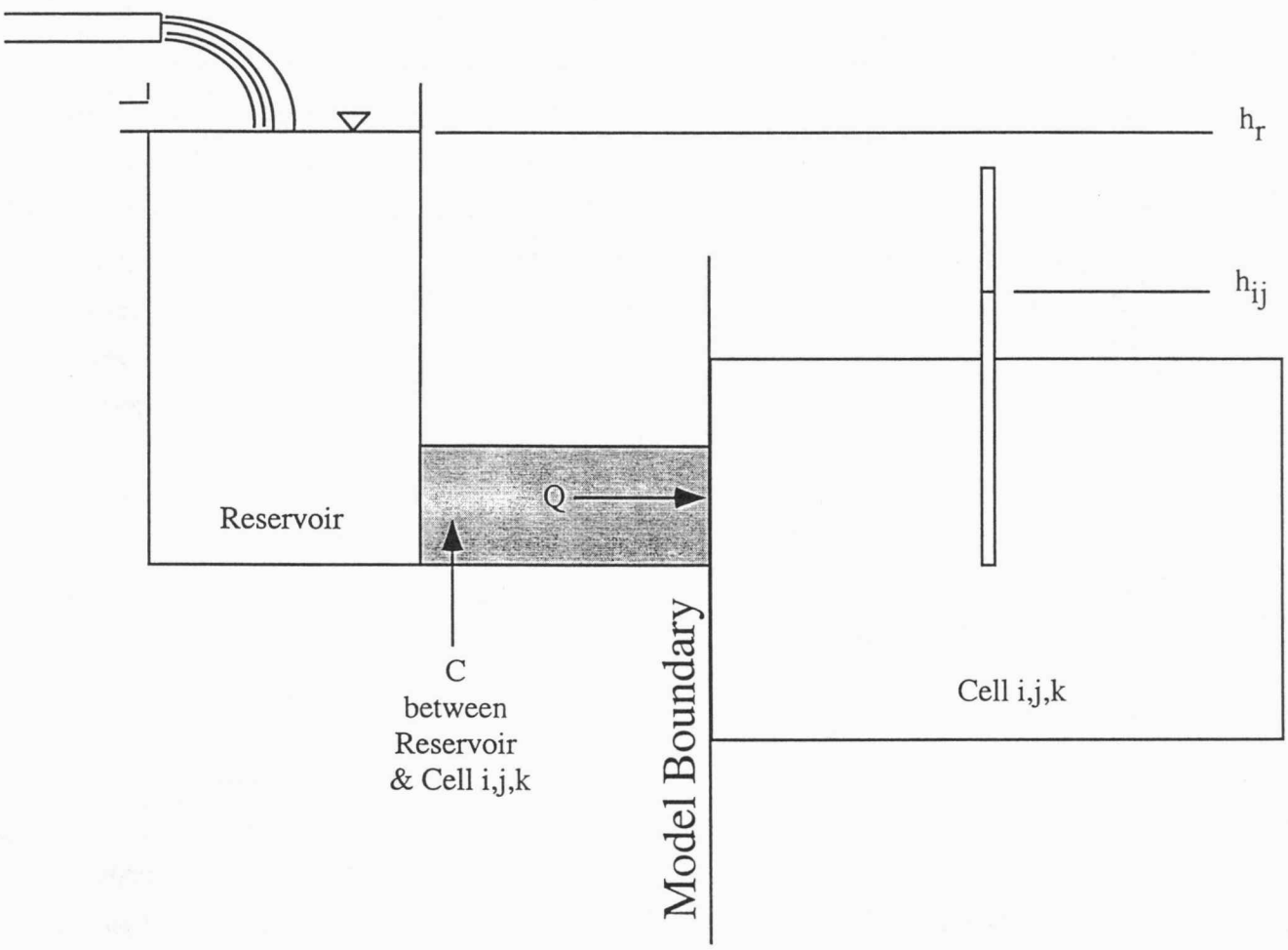

Figure 17. Schematic showing the parameters controlling the flow of water into or out of the model in the general head boundary condition.

located outside of the model. The equation for flow into or out of the model cell on the boundary (Q) is a linear function of the head difference between the reservoir and the model cell:

$$Q = C(h_r - h_{1j}) \qquad \text{Eqn. 5}$$

where C is the conductance, h_r is the reservoir head, and h_{1j} is the head in the cell adjacent to the model boundary in column 1 of the grid. In this model the source of water is regional flow and the "reservoir head" is taken to be the 1,975 ft above mean sea level, which corresponds to a hydraulic head contour on the regional predevelopment potentiometric surface map to the west of the model area (Figure 9). We assume that limited domestic-well pumping to the west of the model region has little effect on the "reservoir head". C is a lumped parameter that is defined by the equation:

$$C = K_h A/L \qquad \text{Eqn. 6}$$

where K_h is the regional equivalent horizontal component of hydraulic conductivity, A is the cross-sectional area of the cell along the boundary through which flow into or out of the model occurs, and L is the distance from the "reservoir head" to the model cell.

Measures of model calibration

Calibration of ground-water flow models usually consists of adjusting the model input parameters until a satisfactory match is achieved between the observed and simulated hydraulic heads, fluxes, or other calibration targets (Wang and Anderson, 1982). In this modeling project, a very limited calibration was performed by trial-and-error adjustment of the model parameters to minimize the head difference at the pumping and observation wells.

The results of each round of calibration were evaluated by computing the root mean square (RMS) error:

$$\text{RMS error} = [(1/n)\Sigma(h_m - h_s)^2]^{0.5}, \qquad \text{Eqn. 7}$$

where h_m and h_s are the measured and simulated hydraulic heads, respectively. Table 2 lists the observed pre-development hydraulic heads used to calculate steady-state model RMS error. This criterion was chosen because the RMS error is thought to be the best measure of uncertainty if the errors are normally distributed (Anderson and Woessner, 1992). The simulated heads from each run were compared visually to the observed potentiometric surface in the model region to assess model fit.

Table 2. Observed steady-state (pre-development) hydraulic heads in the pumping (D) and observation (MD) wells in the Hays Dakota wellfield.

Wellsite	Hydraulic Head Elevation (ft)
D-6	1888.65
D-5	1882.32
D-1	1877.69
D-3	1873.59
D-2	1872.85
D-4	1870.99
MD-6	1888.95
MD-5	1882.10
MD-1	1877.67
MD-2&3	1873.17
MD-4	1870.92

Wells

This package was used to simulate pumpage from the aquifer in the transient numerical model. The model allows the user to place wells at any location within the model, but all calculations assume that wells are located at the center of a cell. Consequently, the actual well location may differ significantly from the location specified in the model.

Assumptions and limitations of Visual MODFLOW

The following assumptions are made in the model: 1) the ground water is of uniform density and viscosity (homogeneous fluids), 2) the geology of the region can be reasonably simulated with a 3-dimensional orthogonal grid, and 3) the only flow into and out of the model is where there are constant head or general head boundary conditions exist.

Chapter 4: Conceptual Steady-state Models of Ground-water Flow in the Upper Dakota Aquifer

This chapter discusses development of steady-state, conceptual ground-water flow models of the Dakota aquifer in the Hays wellfield vicinity. The steady-state model can be used to investigate the flow system and its influences and provides the initial conditions needed for running the transient model to the simulate pumping effects on the aquifer. The chapter begins with a description of the phased modeling approach and includes presentation of model calibration results, descriptions of the alternate steady-state conceptual models, and explanations of the limitations imposed by the data used in formulating the models.

Modeling approach

The effort to effectively simulate the ground-water flow system in the wellfield vicinity is handicapped because of the lack of hydrologic properties for much of the model region and only limited hydraulic information on which to base the model boundary conditions and to perform a rigorous model calibration. Many areas within the model region are also inadequately characterized with respect to the stratigraphic framework within the Dakota Formation. Where only minimal data are available, it is quite possible that alternate, equally statistically valid, model calibrations can be developed from a single data set (Spitz and Moreno, 1996). Thus, the modeling effort in this project was directed towards formulating simulations that are consistent with what is known about (1) the regional hydraulic head gradients, (2) the hydraulic heads in the wellfeld prior to pumping, (3) the hydrologic properties of the aquifer and location of flow boundaries from the pumping test analysis, and (4) the subsurface geologic information.

Starting with simple models of the aquifer and building toward more complex simulations is always prudent, especially where there is little data to directly formulate the more complex steady-state model. In this project, we approach this based on an understanding of the dominant ground-water flow directions and the most important aspects of the aquifer framework as presented in Chapter 2 of this report volume (Spitz and Moreno, 1996). This approach may provide a means of reducing some of the uncertainty in the boundary conditions and hydrologic properties of the geologic framework.

Initially, a simple two-layer model of regional ground-water flow was assembled to simulate the regional potentiometric surface of the Dakota aquifer through the wellfield. The regional potentiometric surface map does not take into account the local heterogeneity of the Dakota aquifer evident at the more local scale. Using the simple two-layer model as a starting point, a more complex model was formulated by incorporating a sandstone aquifer using the hydrologic properties and flow-boundary locations from the pumping tests. It was assumed that the pumping-test derived hydrologic properties carried much less uncertainty than other model

parameters and the respective values are representative of the aquifer in the immediate vicinity of each production and nearby observation well. This is considered as the uncomplicated, base conceptualization of the upper Dakota aquifer in the model region.

A more complex model of the Dakota aquifer in the wellfield vicinity was formulated to take into account the less permeable deposits that may be present adjacent to the sandstone aquifer at certain locations in the model. This took into account the effects of interbedding of less permeable sandstone and mudstone and degrees of sandstone-body hydraulic connection. This is referred to as the fringe model and is presented as the final, steady-state model in this chapter.

However, a later evaluation of the calibrated, transient fringe conceptual model in Chapter 5 of this report suggested that the fit of the simulated to the "observed" drawdowns from pumping could be improved by a slight modification. This modification took into account the likelihood of hydraulic connection between sandstone aquifers in Subunit 2 and Subunit 3 of the Dakota Formation just to the south of D-2. As a result, an additional permeable source of water was made available to nearby pumping wells in the transient simulation. Because this alternative model was developed during transient model calibration it is discussed in Chapter 5 of this report volume. All but the first simple regional models of the upper Dakota aquifer are consistent with what is known about the upper Dakota aquifer in this area.

Regional sandstone-body connectivity and equivalent hydraulic conductivity

Ground-water flow through interbedded sequences of sandstone and mudstone is controlled primarily by the connectivity of the sandstone bodies and secondarily by the hydraulic conductivity contrast between the mudstone and the encased sandstone (Toth, 1962; Fogg, 1990; Macfarlane et al., 1994). The hydraulic conductivity contrast between mudstones and sandstones is on the order of 3-5 orders of magnitude (Domenico and Schwartz, 1992). Thus the regional effective hydraulic conductivity of the Dakota and the hydraulic gradient determines the flux of water into the model as well as the flow patterns within the model area.

Statewide the sandstone fraction in the upper Dakota aquifer is approximately 30%. If it is assumed that this sandstone is distributed randomly through the formation, the likelihood of direct physical, and hence hydraulic, connection is low (Fielding and Crane, 1987). However, examination of gamma-ray logs through the Dakota Formation suggests that the sandstone bodies may occur preferentially at certain levels within the formation and therefore, their distribution is not random. Considering our uncertainty about the degree of sandstone-body hydraulic connection, two alternative end-member regional models can be formulated and used as a basis to calculate effective regional hydraulic conductivity of the upper Dakota aquifer.

One approach to aquifer characterization in these sequences is to use an effective hydraulic conductivity (K_{eff}). In Figure 18A dual porous media consists of interbedded low permeability mudstone of hydraulic conductivity K_1 and randomly-distributed, permeable sandstone bodies of hydraulic conductivity K_2. The sandstone fraction is less than 50% of the total sequence thickness. Ground water is assumed to flow laterally, parallel to the bedding. The hydrogeologic framework in the figure can be reconfigured into separate lumped sandstone and mudstone fractions equal to the proportion of each lithology in the framework (Figure 18B). The total length through the mudstone and sandstone is L and is subdivided into l_1 and l_2 flow path segments for mudstone and sandstone, respectively. l_1/L and l_2/L are equal to the mudstone and sandstone fractions of the aquifer framework (P_1 and P_2), respectively:

$$l_1/L + l_2/L = 1 \qquad \text{Eqn. 8}$$

and

$$P_1 + P_2 = 1 \qquad \text{Eqn. 9}$$

The equivalent horizontal hydraulic conductivity for this one-dimensional aquifer framework is:

$$K_{heff} = L/([l_1/K_1] + [l_2/K_2]) = 1/([P_1/K_1] + [P_2/K_2]) \qquad \text{Eqn. 10}$$

or

$$K_{heff} = K_1K_2/(P_1K_2 + P_2K_1) \qquad \text{Eqn. 11}$$

If we assume that $K_2 >> K_1$, then P_2K_1 is negligible and

$$K_{heff} \approx K_1/P_1 \qquad \text{Eqn. 12}$$

Initially, K_1 and P_1 were set at 1×10^{-4} ft/day and 0.7, respectively, to compute the equivalent hydraulic conductivity of 1.4×10^{-4} ft/day of this interbedded sandstone and mudstone model using Eqn. 7.

Alternatively, the sandstone body distribution may be considered nonrandom and connectivity of the sandstones is higher than expected because the permeable lenses are concentrated at discrete horizons within the mudstone (Figure 19A). The dual porous media can

Figure 18

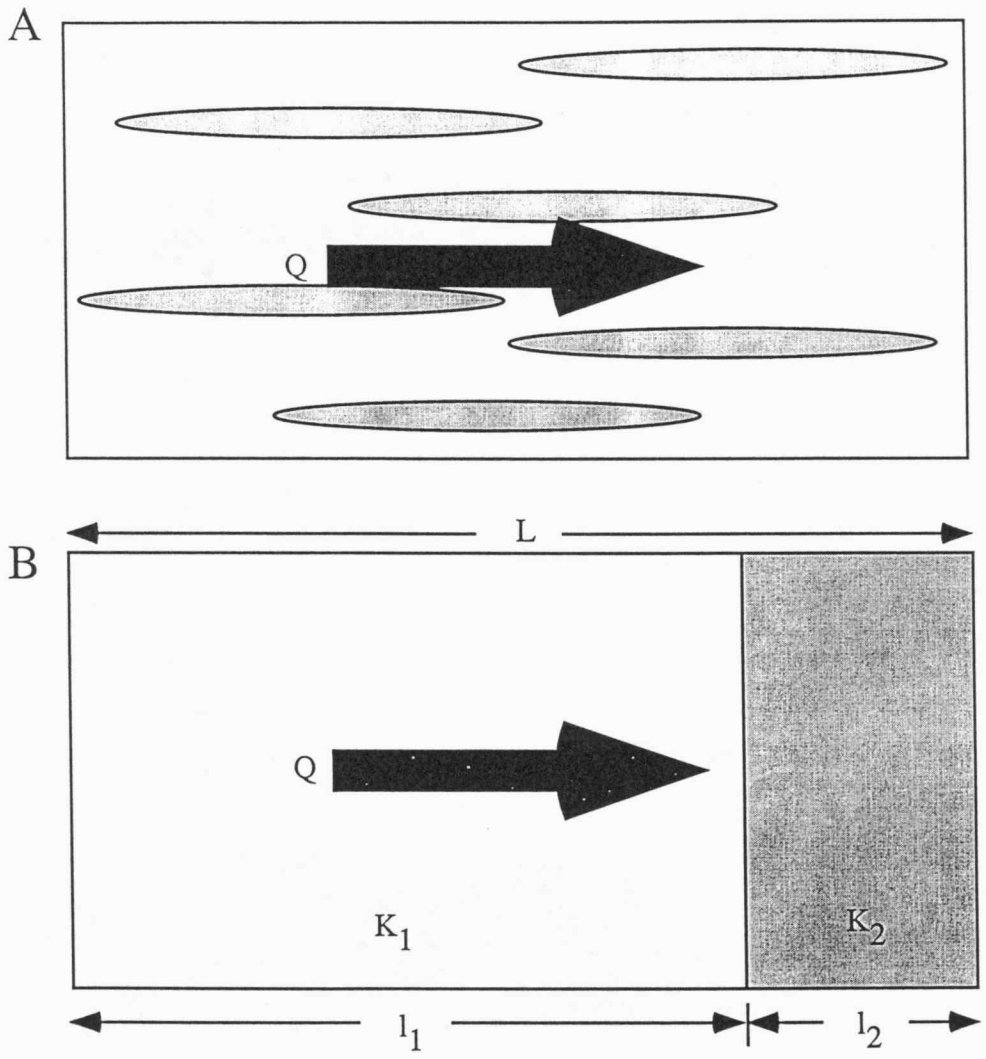

Figure 18. A. Effective hydraulic conductivity in mudstone-dominated mudstone (K_1) and sandstone (K_2) sequences. The sandsone bodies are discontinuous, randomly distributed and hydraulically isolated . The sandstone fraction is assumed to be <50% of the total sequence thickness. B. A one-dimensional model of this sequence as a dual porous media consisting of aggregated sand -stone and mudstone sections.

Figure 19

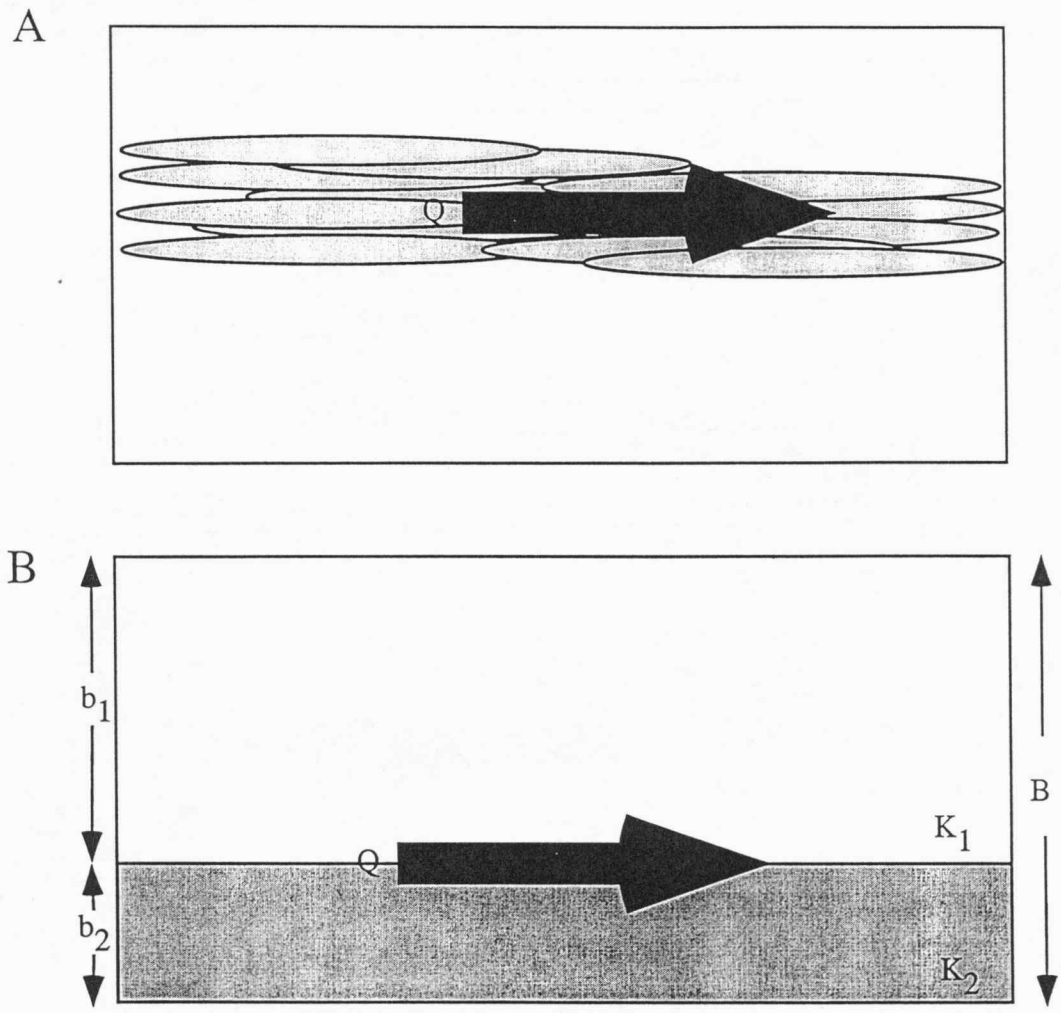

Figure 19. A. Effective hydraulic conductivity in mudstone-dominated mudstone (K_1) and sandstone (K_2) sequences. The sandstone bodies are discontinuous and hydraulically connected . The sandstone fraction is assumed to be <50% of the total sequence thickness. B. A one-dimensional model of this sequence as a dual porous media consisting of aggregated sandstone and mudstone sections.

be subdivided into a mudstone portion of hydraulic conductivity K_1 and a sandstone portion of hydraulic conductivity K_2 (Figure 19B). If the total unit thickness is B and b_1 and b_2 are the total thickness of mudstone and sandstone, respectively, then b_1/B and b_2/B are the mudstone and sandstone fractions, respectively and

$$K_{heff} = K_1(b_1/B) + K_2(b_2/B). \qquad \text{Eqn. 13}$$

If we assume that $K_2 >> K_1$,

$$K_{heff} = K_2(b_2/B). \qquad \text{Eqn. 14}$$

Where several sandstone bodies are hydraulically connected, the equivalent horizontal hydraulic conductivity hydraulic conductivity, K_2 is equivalent to the geometric mean value of the sandstone hydraulic conductivities of the individual sandstone lenses:

$$K_2 = (K_a K_b K_c K_d \ldots K_n)^{1/n} \qquad \text{Eqn. 15}$$

where K_a , K_b, K_c, K_d, ..., and K_n are the hydraulic conductivities of sandstone bodies a, b, c, d,..., n. The geometric mean value of the hydraulic conductivity is chosen as the effective hydraulic conductivity for the hydraulically connected sandstones because the hydraulic conductivity is generally considered to be a log-normally distributed property of granular porous media (Domenico and Schwartz, 1992). Also, the geometric mean value is perhaps more appropriate than the arithmetic or harmonic means because the distribution values from pumping tests of the Dakota aquifer in Kansas and southeastern Colorado appears to be lognormal (Macfarlane, 1998). The geometric mean hydraulic conductivity is 15.7 ft/day from the pumping tests of the sandstones around the Hays wellfield. As a result, the maximum effective hydraulic conductivity of the regional upper Dakota aquifer from Eqn. 14 is 4.71 ft/day.

Hence, the range of the regional effective hydraulic conductivity spans approximately 4 orders of magnitude from 1.4×10^{-4} to 4.71 ft/day depending on which regional scale model of sandstone-body interconnectedness is selected. Desbarats (1987) produced an analytical expression for effective hydraulic conductivity in sand-shale sequences adapted from a relationship developed in Dagan (1979) for a statistically homogeneous porous media:

$$K_{eff} = \frac{1}{3}\left[\frac{V_{ss}}{2K_{eff} + K_{ss}} + \frac{V_{sh}}{2K_{eff} + K_{sh}}\right]^{-1} \qquad \text{Eqn 16}$$

Where V_{ss} and V_{sh} are the volume fractions of the sandstone and shale respectively, and K_{ss} and K_{sh} are the sandstone and shale hydraulic conductivities. If we assume that the regional Dakota Formation is 30% sandstone with an average hydraulic conductivity of 15.7 ft/day and the shale (mudstone, in this case) has an average hydraulic conductivity of 1×10^{-4} ft/day, the effective hydraulic conductivity calculated iteratively using Eqn. 9 is 9.9×10^{-4} ft/day. The calculated value from Eqn. 9 is closer to the lower end of effective hydraulic conductivity range and is more consistent with sandstone lenses that are randomly distributed throughout the mudstone.

Regrettably, there is no basis for narrowing this 4 order of magnitude range of values even on a subregional basis. Pumping tests sample relatively small volumes of the aquifer and are performed primarily in the most permeable sandstone aquifers. Also, these tests are not designed to estimate effective hydraulic conductivities of less permeable interbedded sequences of sandstone and mudstone. At the regional scale numerical simulations indicate a much greater sensitivity of the flow system in the Dakota aquifer to the vertical hydraulic conductivity of the Upper Cretaceous aquitard and land-surface topography than to the Dakota regional effective hydraulic conductivity (Belitz and Bredehoeft, 1988; Macfarlane, 1993, 1995; and Helgeson et al., 1993). Thus, the regional model results cannot be used to constrain this range of regional effective hydraulic conductivity values.

The simple regional aquifer model

The objectives of this part of the modeling effort were to (1) simulate the regional potentiometric surface map and (2) estimate the range of flux values entering the western model boundary. In this first model, a uniform, equivalent hydraulic conductivity aquifer was assumed with an initial K_{heff} of 1.43×10^{-4} ft/day. The purpose of this simulation was to determine if a homogeneous aquifer could be used to simulate the observed regional potentiometric surface within the model region. A second set of model runs was assembled where the aquifer was assumed to be heterogeneous. In this set of slightly more realistic regional scenarios, one simulation was assembled assuming the sandstones to be hydraulically isolated and one assuming the sandstones to be hydraulically connected. As part of the calibration process, the regional effective hydraulic conductivity was varied to achieve the best match to the regional potentiometric surface. The aquifer K_{heff} was assumed initially to be 1.43×10^{-4} ft/day in the first and 4.71 ft/day in the second, more permeable, heterogeneous, equivalent hydraulic conductivity aquifer model. In a similar manner, the conductances for the general-head boundary condition along the west side (upgradient) of the model region were calculated using the appropriate hydraulic conductivity value.

For the uniform, equivalent hydraulic conductivity aquifer case the model was able to simulate the estimated overall hydraulic head drop across the model. However, the fit within the

model was poor because of the inability of the simulation to mimic the change in observed hydraulic gradient near the middle of the model. The RMS error for the entire model was 9.56 ft. The total flux through the model was 1.30 ft^3/day.

For the simple heterogeneous regional aquifer, the best visual match of the simulated to the observed hydraulic heads resulted when the initial hydraulic conductivity was lowered slightly in the western part of the model and increased by a factor of 2 in the eastern half of the model (Figure 20). This is suggested by the spacing of the contours in the observed potentiometric surface (Figure 9). In the low K_{heff} simulation, the final calibrated effective hydraulic conductivity in the western part of the model was 1.07×10^{-4} ft/day and in the eastern part of the model, 2.86×10^{-4} ft/day (Figure 20). In this simulation, the RMS error was 1.73 ft. In the high K_{heff} simulation, the final calibrated effective hydraulic conductivity in the western part of the model was 3.53 ft/day and in the eastern part of the model, 9.4 ft/day. In this simulation, the root mean square error was 1.86 ft. The improvement in model RMS error indicates that the regional potentiometric surface is best simulated as a heterogeneous regional aquifer system where the eastern part of the model is more permeable than the western part.

The apparent increase in effective hydraulic conductivity from the western to the eastern parts of both simple regional heterogeneous models may be due to an eastward increase the proportion of sandstones that are hydraulically connected or an increase in the transmissivity of the mudstone, the sandstone, or both. The increase in the proportion of hydraulically connected sandstones or an increase in mudstone hydraulic conductivity would effectively increase the permeable cross-sectional area through which ground water flows.

To assist in the interpretation of the model results, the average gamma-ray intensity in the mudstones of the Dakota Formation was estimated by visual inspection from the gamma-ray logs of boreholes drilled for oil exploration and production and for the Hays wells in the upper Dakota aquifer. The API gamma-ray intensity provides a measure of clay content and has been used as a proxy to identify significant aquifers in sandstone-mudstone sequences (Macfarlane et al., 1994). Higher clay content and lower permeability are associated with higher API gamma-ray intensities. The average mudstone gamma ray intensity varied from 60 up to 120 API units with a natural break in the data disribution at around 80 API units (Figure 21). The data were classified into one of two groups (boreholes where the mudstones have gamma-ray intensities ≤ 80 API units [less clayey-more silty, slightly more permeable] and those with gamma-ray intensities >80 API units [more clayey-less silty, slightly less permeable]) and plotted on a map of the study area (Figure 22).

From the spatial distribution of API gamma-ray values it appears that the mudstone is more clay-dominated in the eastern and extreme western parts of the study area and more silt-dominated in the central part (Figure 22). The intermingling of average high and low API

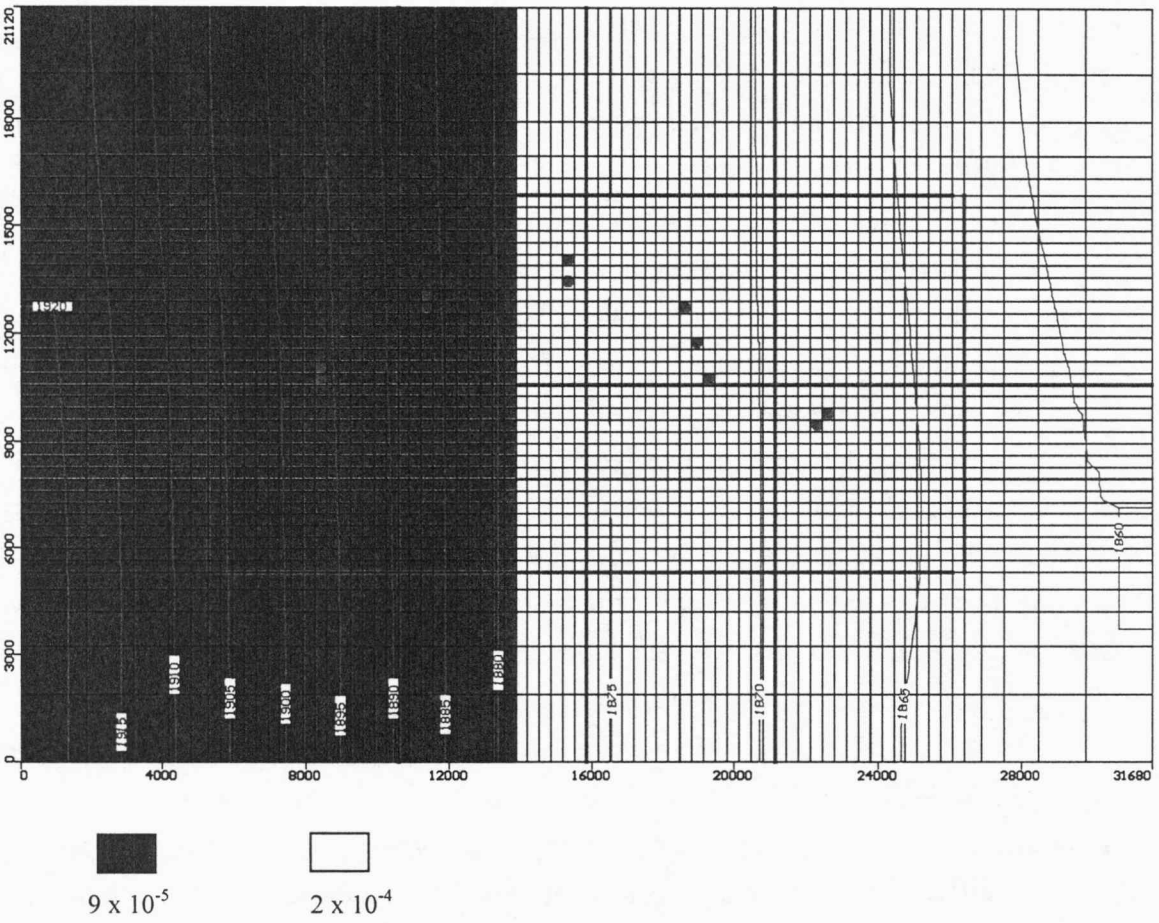

Figure 20. The low flux, heterogeneous, effective hydraulic conductivity model of the upper Dakota aquifer, showing the east and west hydraulic conductivity zones and the simulated potentiometric surface. The boundary between the two conductivity zones applies also to the high flux version of this model.

Figure 21

	API GR Intensity
Minimum	60
Maximum	120
Sum	6237
Points	74
Mean	84.283784
Median	85
RMS	85.567975
Std Deviation	14.869773
Variance	221.11014
Std Error	1.728576
Skewness	0.35506061
Kurtosis	-0.50960527

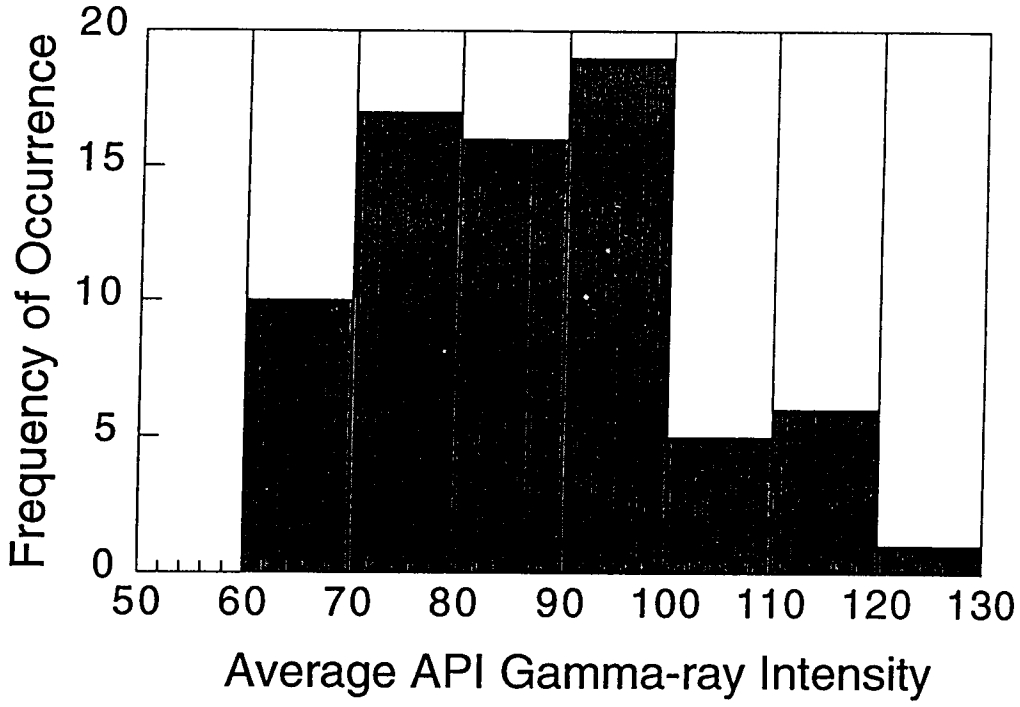

Figure 21. Histogram of average gamma-ray intensities of mudstones in the Dakota Formation from gamma-ray logs of wells in the study area.

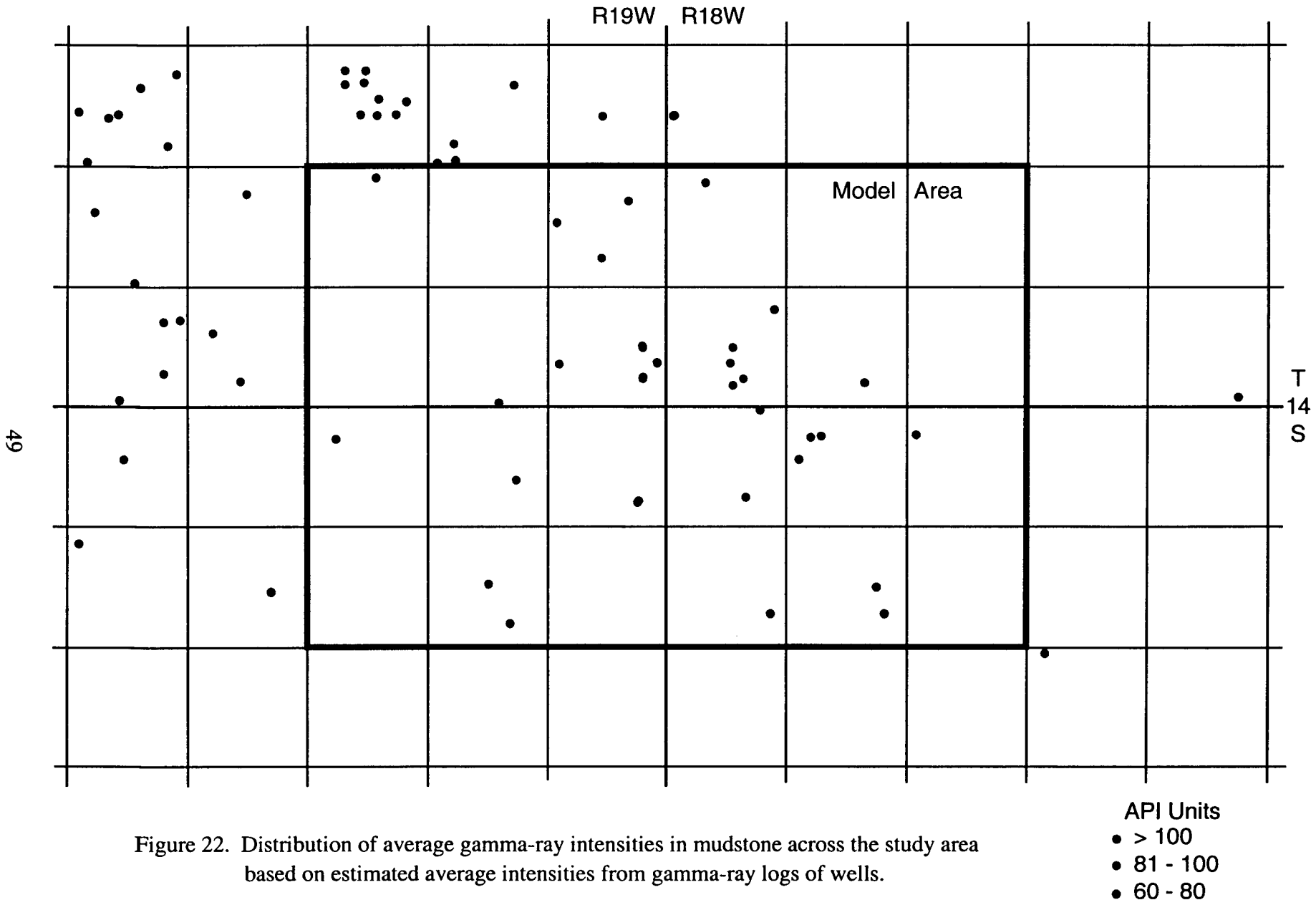

Figure 22. Distribution of average gamma-ray intensities in mudstone across the study area based on estimated average intensities from gamma-ray logs of wells.

gamma-ray values such as near D-1, D-3 and D-4 suggests that the clay-silt boundary is a transition rather than an abrupt boundary. If the average gamma-ray intensity is a reasonable predictor of bulk hydraulic conductivity in these lithologies, then the distribution of intensities does not seem to correspond to the hydraulic conductivities in the calibrated simple heterogeneous regional models. This lack of correspondence may suggest that the higher effective hydraulic conductivities in the eastern part of the model could result from an increase in the hydraulic conductivity of the sandstones or from an increase in the interconnectedness of the sandstones.

The ground-water flux through the simple heterogeneous regional flow models ranges over 4 orders of magnitude from 1.44 ft^3/day for low K_h to 46,075 ft^3/day high K_h. From a steady-state regional vertical profile model, Macfarlane (1993) estimated a flow rate of approximately 1.8 ft^3/day/ft or approximately 38,000 ft^3/day through a 4-mi wide cross-section of the entire upper Dakota aquifer in this part of central Kansas. From a subregional model of the upper Dakota aquifer in southwestern Ellis Co., Smith (1995) estimated flow rates ranging from 11 to 10,900 ft^3/day depending on the assumed degree of hydraulic connection of the sandstones.

The sandstone aquifer model

In the next, more complex, steady-state, conceptual model, a heterogeneous sandstone aquifer was added to layer 2 of the model. The modeling objectives were to (1) simulate the regional potentiometric surface of the upper Dakota aquifer, (2) simulate the local distribution of hydraulic head within the wellfield, and (3) estimate the ground-water flux.

The boundaries of the sandstone aquifer in model layer 2 were initially set to coincide with the aquifer extent in the hydrogeologic model (Figures 7, 8, and 23). Where there is a designated aquifer present in the model, the sandstone fraction in Subunits 2 and 3 is >50%. Where it is believed that there is hydraulic connection between Subunit 2 and Subunit 3, the total sandstone thickness is the sum of the thicknesses in Subunits 2 and 3 (Figures 5 and 6).

The hydrogeologic model of the sandstone aquifer (Figure 7) was used to assign K_h values to the sandstone aquifer model cells in the wellfield vicinity. The aquifer was assumed to be homogeneous locally around each of the pumping-near observation well pairs outward to the boundary with the mudstone aquitard. Model cells to the west and east of the wellfield were initially assigned the effective K_h value of 4.71 ft/day, derived from Eqn. 8.

In Figure 24, the heterogeneous sandstone aquifer extends from the west edge of the model (layer 2) to the southeast corner of the model. For the model cells at the west edge of the model in this bottom layer, the conductances in the general head boundary condition were changed to reflect the continuity of the sandstone aquifer beyond the model region. Thus, the

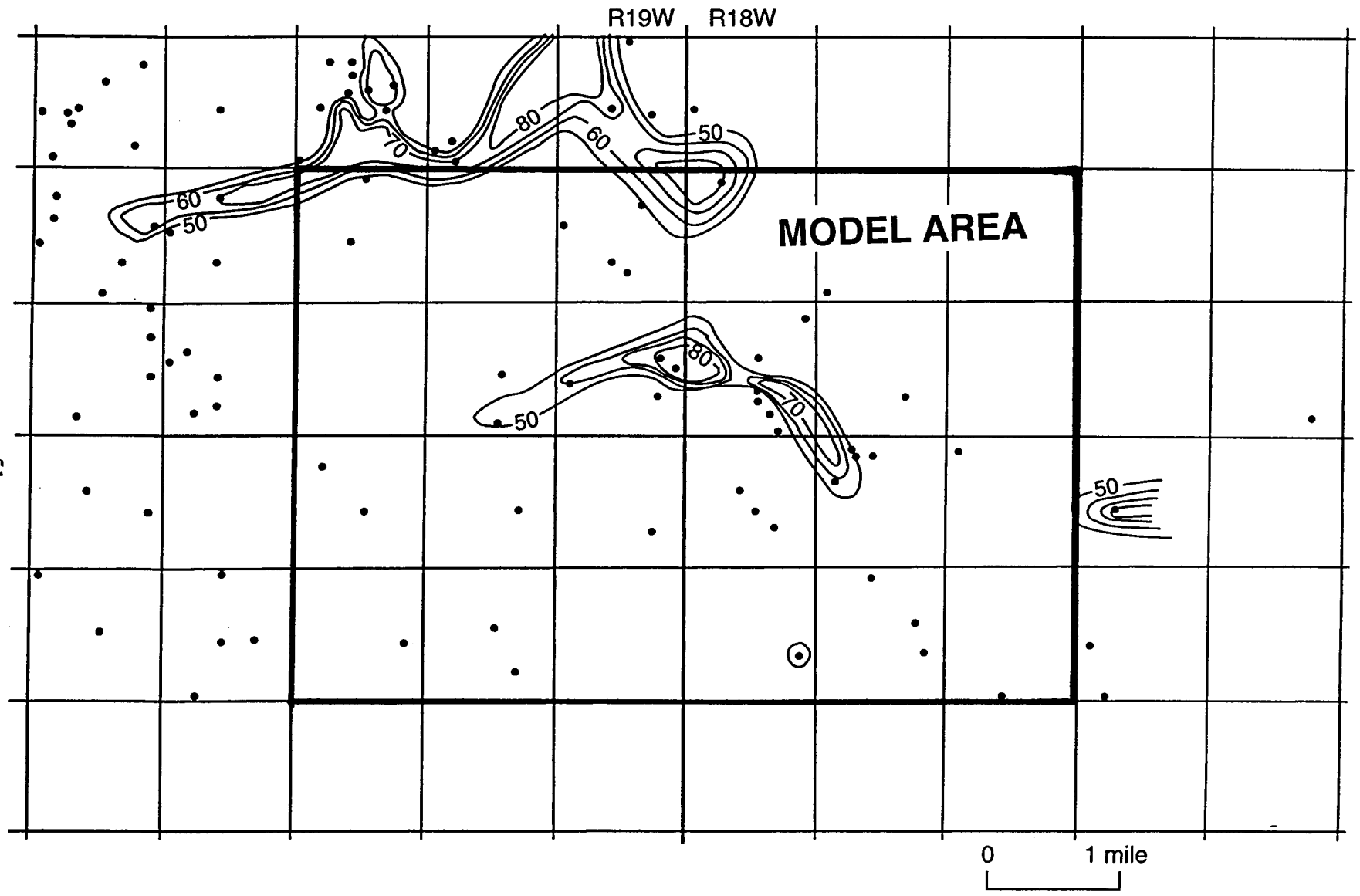

Figure 23. Areas of probable vertical hydraulic connection between sandstones in Subunit 2 and Subunit 3 of the Dakota Formation in the model region.

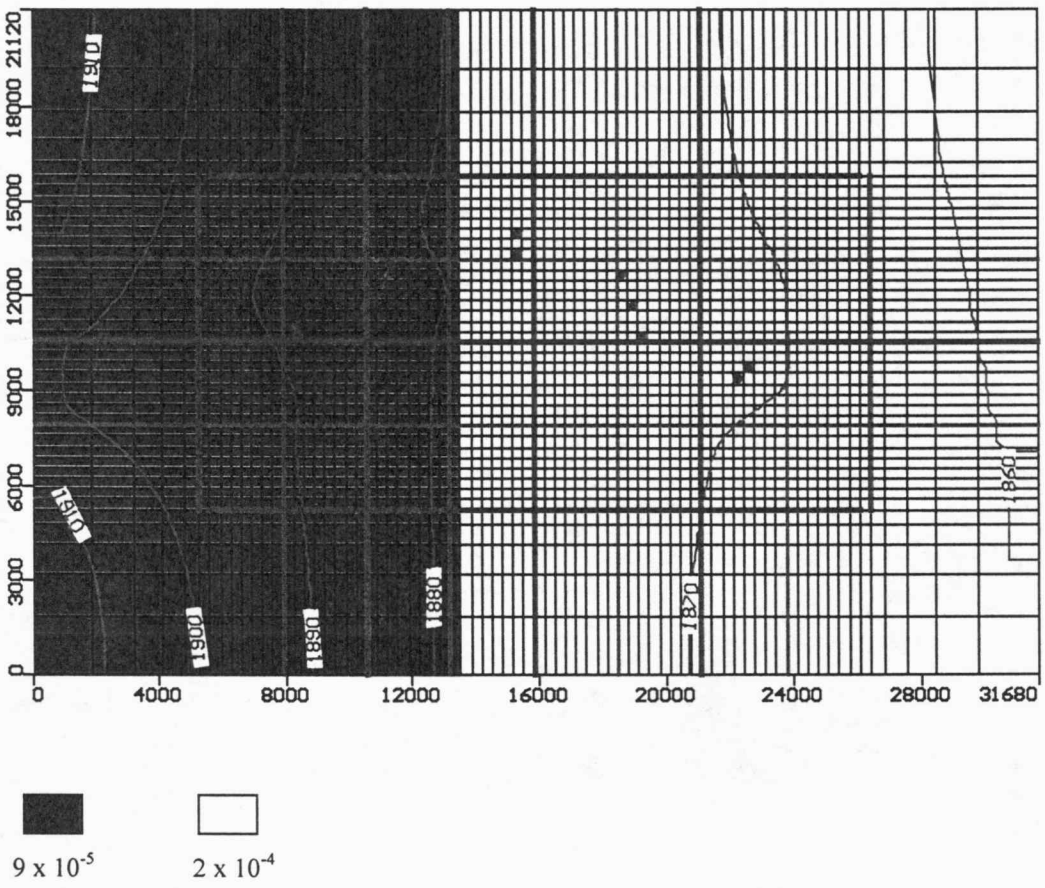

Figure 24. Distribution of hydraulic conductivity in layer 1 of the sandstone aquifer model. Hydraulic conductivity is in units of ft/day. Shown also is the simulated potentiometric surface map with a contour intervel of 5 ft.

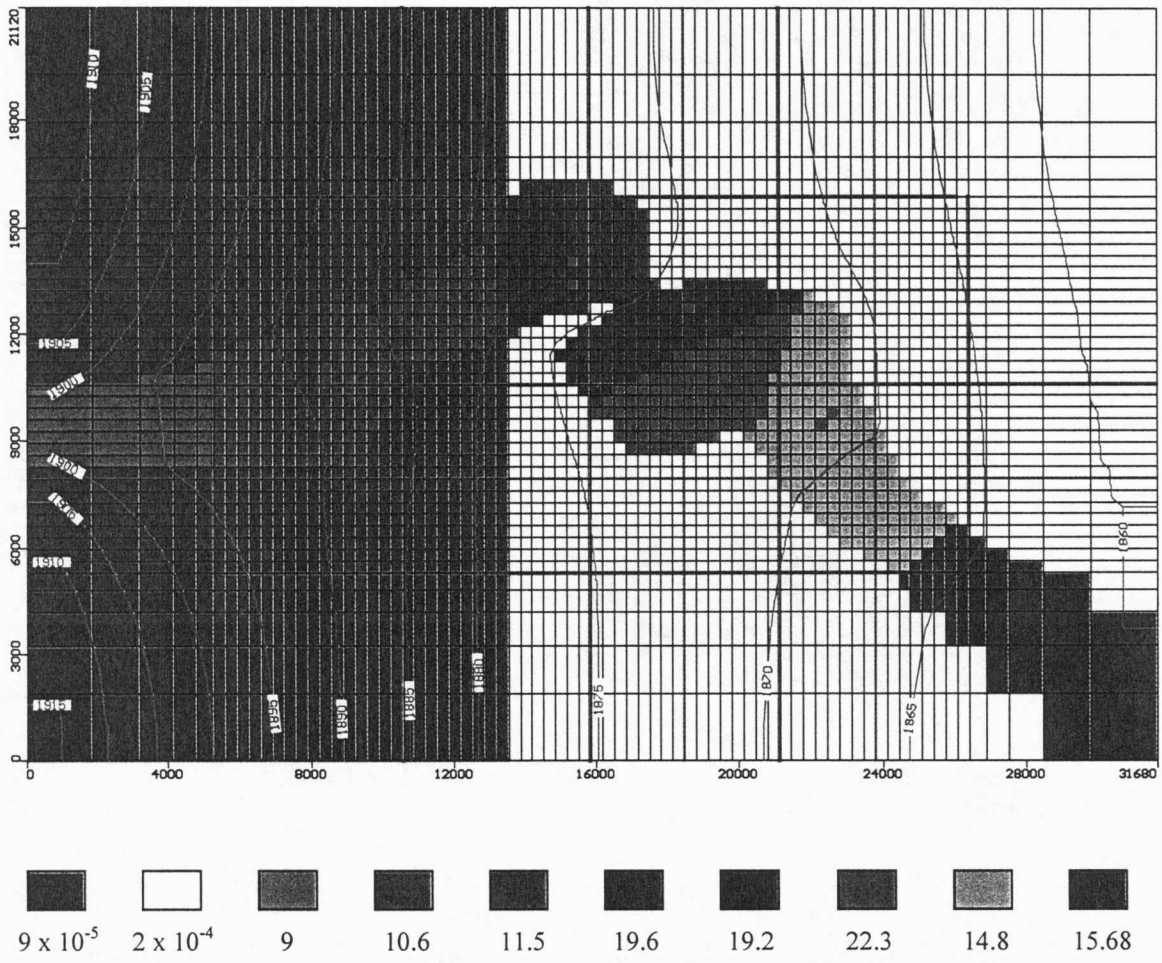

Figure 24 Continued. Distribution of hydraulic conductivity in layer 2 of the sandstone aquifer model. Hydraulic conductivity is in units of ft/day. Shown also is the simulated potentiometric surface map with a contour interval of 5 ft.

initial hydraulic conductivity in the conductance term for this segment of the model boundary was increased from 1.4 x 10^{-4} ft/day to 4.71 ft/day.

In layer 1 the mudstone K_h distribution used in this model was the effective hydraulic conductivity distribution from the final, low flux, heterogeneous, equivalent hydraulic conductivity aquifer model. Mudstone K_h was set at 1.07 x 10^{-4} ft/day and 2.86 x 10^{-4} ft/day in the western and eastern parts of the model, respectively. It is assumed that any sandstone lenses contained within the mudstone (sandstone fraction <50% in Subunit 2 in this case) are hydraulically isolated from one another. The initial hydraulic conductivity used to compute the conductance term in the general head boundary condition where mudstone is present at the west model boundary was 1.4 x 10^{-4} ft/day.

Calibration was carried out by trial-and-error adjustment of (1) the hydraulic conductivities of the sandstone aquifer within the wellfield, (2) the hydraulic conductivities upgradient and downgradient of the wellfield, and (3) the geometry of the sandstone aquifer-mudstone aquitard boundary in the wellfield and elsewhere.

With regard to (1) adjustments made to the hydraulic conductivities used in the model were within the 95% confidence band of the estimated value from the pumping tests. Specifically, the hydraulic conductivity of the sandstone aquifer around D-5 was increased slightly from 11.4 to 11.5 ft/day and around D-3, from 19.0 to 19.3 ft/day to reduce RMS error.

To the west of the wellfield, the hydraulic conductivity was almost doubled from 4.71 ft/day to 9.0 ft/day to allow more water into the model and increase the hydraulic head in the aquifer at wellsite 6. The increase in hydraulic conductivity also helped to bring sandstone aquifer hydraulic heads along the west edge of the model more in line with the expected hydraulic heads from the regional potentiometric surface map. The hydraulic conductivity of the sandstone aquifer near the southeast edge of the model area was increased from the initially assumed 4.71 ft/day to 15.68 ft/day to allow more water to leave the wellfield and decrease the hydraulic head at wellsite 4.

The increase in effective hydraulic conductivity of the aquifer upgradient of the wellfield indicates a sandstone fraction that is approximately twice the regional average of 30%. This increase in thickness is consistent with the estimated sandstone fraction from the subsurface mapping results described in Volume 1 of this report. The more than 3-fold increase in effective hydraulic conductivity to the east of the wellfield is the geometric mean of the hydraulic conductivities from the pumping tests in the wellfield. This suggests that the sandstone aquifer extends farther to the southeast than is suggested by the limited subsurface information.

The hydraulic conductivities of the cells representing the mudstone aquitard were adjusted slightly to maintain the expected regional hydraulic head gradient across the model in the mudstone from the regional potentiometric surface map. The mudstone hydraulic

conductivity in the eastern part model decreased from 2.86 x 10^{-4} ft/day to 2.0 x 10^{-4} ft/day and in the western part from 1.07 x 10^{-4} ft/day to 9.0 x 10^{-5} ft/day.

Only slight differences exist between the extent of the sandstone aquifer between this model and the hydrogeologic model (Figure 24). The sandstone aquifer width was reduced between D-6 and D-5 to increase the hydraulic-head gradient by raising the hydraulic heads at wellsite 6. A further pinching of the sandstone aquifer width was done between wellsite 1 and 3 to restrict flow and reduce the hydraulic heads down gradient at wellsites 3, MD-2&3; 2, and 4.

The RMS error of the calibrated model was 0.65 ft (Figure 25). The solid line in the plot has a slope of 1 indicating perfect simulation of the observed hydraulic heads (the calibration targets) in the model. The dashed line is the best-fit line through the plotted points. The best-fit line has a slope and 95% confidence interval of 0.91 ± 0.04 and the correlation between the simulated and the observed values is 0.998. The best-fit line indicates that the simulated hydraulic heads in this model are slightly less than observed in western part of the wellfield and slightly greater than observed in the eastern part.

Of the total flow into the conceptual model (3,285 ft^3/day), less than 0.02% enters through the low hydraulic conductivity mudstone, as expected (Figure 24). The very small proportion of flow through the mudstones indicates that under natural conditions there is much greater flushing of accumulated salts in the sandstone than in the mudstone by regional flow. In the test-hole drilling program conducted by the city, water quality sampling suggested higher salinities where the sandstones were thinner and more hydraulically isolated. Smith (1995) noted much less flushing of resident salinity by fresher regional flow over geologic time in areas where the sandstone fraction was less and potentially more isolated hydraulically in his subregional study of the Dakota aquifer in southwestern Ellis County.

The potentiometric surface indicates steeper hydraulic head gradient in the sandstone and mudstone through the western part of the conceptual model than in the eastern part (Figure 24). In the western part the sandstone aquifer is oriented sub-parallel to the direction of ground-water flow whereas in the eastern part, it is oriented obliquely to the flow. The hydraulic head contours generally bend toward the sandstone aquifer indicating a small amount of flow from the mudstone to the sandstone under steady-state conditions.

The sandstone aquifer + fringe (the fringe) model

In this next series of steady-state modeling runs, hydraulic conductivity zones were added to simulate areas where the sandstone fraction is ≥ 20% but <50% in model layer 2, and in layer 1, ≥ 20%. These zones of poorly connected to mostly hydraulically isolated sandstone in mudstone are referred to as the fringe zone. These interbedded deposits may represent splay or

Figure 25

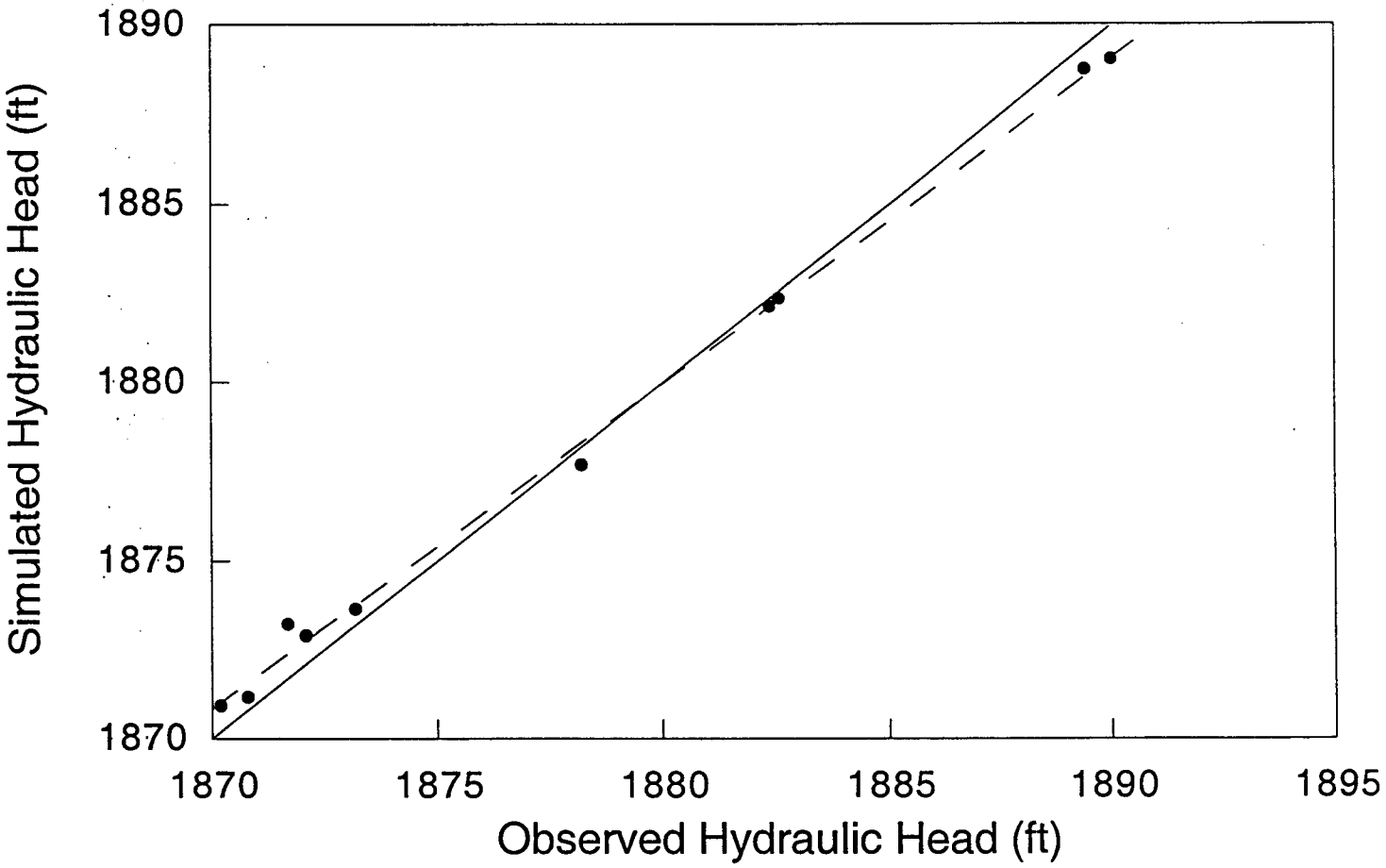

Figure 25. Plot of observed vs. simulated hydraulic heads from the sandstone aquifer model.

levee deposits located near the edge of the meander belt on the flood plain, abandoned channel fills or marine-influenced finer grained, poorly sorted, channel sandstone.

Initially, a fringe zone was added to the calibrated model discussed in the previous section out to the 20% sandstone fraction contour from the isolith maps for subunits 1 and 2 (Figures 4 and 5). Of particular interest was an elongate NNW-SSE trending fringe zone to the south and west of wellsite 6. Here, the fringe zone in Subunit 2 extends southward from the meander belt. Where the main sandstone trend in Subunit 2 intersects with this elongate zone, the meander belt widens appreciably. This suggests that the additional cross-sectional area of permeable, though poorly connected, sandstone could have an impact on the hydraulic head on the upgradient side of the wellfield. An additional fringe zone was also incorporated into the aquifer/aquitard framework in model layer 2 adjacent to the sandstone aquifer south wellsite 5 and in model layer 1, where a thin arcuate interbedded sequence of mudstone and sandstone is present in Subunit 1.

The hydraulic conductivity values assigned initially to the fringe deposits depend on the degree of assumed interconnection of the sandstone bodies. To estimate the edge of the local sandstone aquifer extent in the subunits of the Dakota Formation we have assumed that a high probability of interconnectedness exists where the sandstone fraction is ≥50%. We have also defined the boundary separating the fringe zone from the surrounding mudstone using the 20% sandstone contour on the isolith maps. Consequently, the degree of connectedness of the sandstone bodies varies from marginal near the sandstone aquifer edge to hydraulically isolated near the boundary with the mudstone. As a result, it was difficult to initially assign effective hydraulic conductivity values that reflect the nature of the interbedding. Furthermore, the sandstones further away from the axis of the channel may be finer grained and less well sorted. Macfarlane et al. (1994) reported sandstone hydraulic conductivity values from slug tests in fringe zone-like deposits at other central Kansas locations. These values ranged from 0.0012 ft/day for very poorly sorted carbonaceous silty sandstones to 3.8 ft/day for well sorted, fine grained sandstones, interbedded with mudstone.

The initial effective hydraulic conductivity values assigned to model cells representing the fringe deposits of the meander belt were derived from the degree of hydraulic connection of the sandstones in the sequence. It was assumed that the representative horizontal hydraulic conductivity of a well-sorted sandstone is the geometric mean of the pumping test values from the well field (15.7 ft/day), and that the hydraulic conductivity of the mudstone with less than 20% sandstone is 1×10^{-4} ft/day. The extent of the fringe zone in the meander belt is defined on the basis of the sandstone fraction (50%>sandstone fraction≥20%). Therefore, the effective hydraulic conductivity could vary from 7.85 ft/day at the fringe-aquifer boundary to 1.25×10^{-4} ft/day. The geometric mean value of this effective hydraulic conductiviy range is approximately

0.03 ft/day. This value was assigned initially to the model cells that represent the fringe zone between the channel sandstone aquifer and the mudstone aquitard.

Calibration was carried out by trial-and-error adjustment of (1) the hydraulic conductivities of the fringe zone model cells outside of the wellfield in model layer 2 and the cells representing the fringe in model layer 1, and (2) the extent and geometry of the fringe zone in both model layers. In the early stages of calibration, the extent of fringe zone deposits in the model was pared down to two areas in model layer 2. As the calibration proceeded, successive model runs were made by first decreasing the hydraulic conductivity of the fringe deposits southwest of D-6. This adjustment slightly increased the RMS error of the model. However, the RMS error did decrease slightly by increasing the hydraulic conductivity of the fringe up to 5.5 ft/day. This suggests the possibility that the sandstones in the fringe zone are more hydraulically connected to one another than they are hydraulically isolated. Further improvement in the RMS error resulted by increasing the width of this north-south trending zone from approximately 1 mi to 1.35 mi.

A small patch of fringe was placed to the south of well site 5 along the southern edge of the channel sandstone aquifer and was set at a hydraulic conductivity of 5.5 ft/day. This addition improved the fit of the simulated to the observed hydraulic heads at wellsites 5 and 1 by increasing the effective cross-sectional of the aquifer just down gradient of the restriction between wellsites 6 and 5.

Figure 26 shows the final model configuration and potentiometric surface achieved by the fringe model calibration. The RMS error of the final steady-state sandstone aquifer model with fringe is 0.35 ft. The addition of the fringe zone southwest of wellsite 6 has had some effect on the hydraulic head distribution upgradient of the wellfield. From the west edge of the model to wellsite 6, the hydraulic head gradient is slightly increased but the hydraulic heads are reduced along the west edge of the model. The net effect is a slight improvement in the model fit to the observed data at wellsite 6. Most of the reduction in RMS error is due to a reduction in the error at wellsites 6 and 5 (Figure 27). The flow of water through this model from the upstream reservoir remains unchanged from the earlier simulation.

Summary interpretation of the conceptual steady-state model results

All of the steady-state models presented in this chapter demonstrate that sandstone body interconnection very strongly influences ground-water flow patterns and the flux of water at the local scale. Where interconnection occurs, ground-water flow is channelized (Moreno and Tsang, 1994) and controlled by the orientation of the sandstone aquifers and the geometry of the boundaries between the sandstone aquifer and the contrast in hydraulic conductivity between the

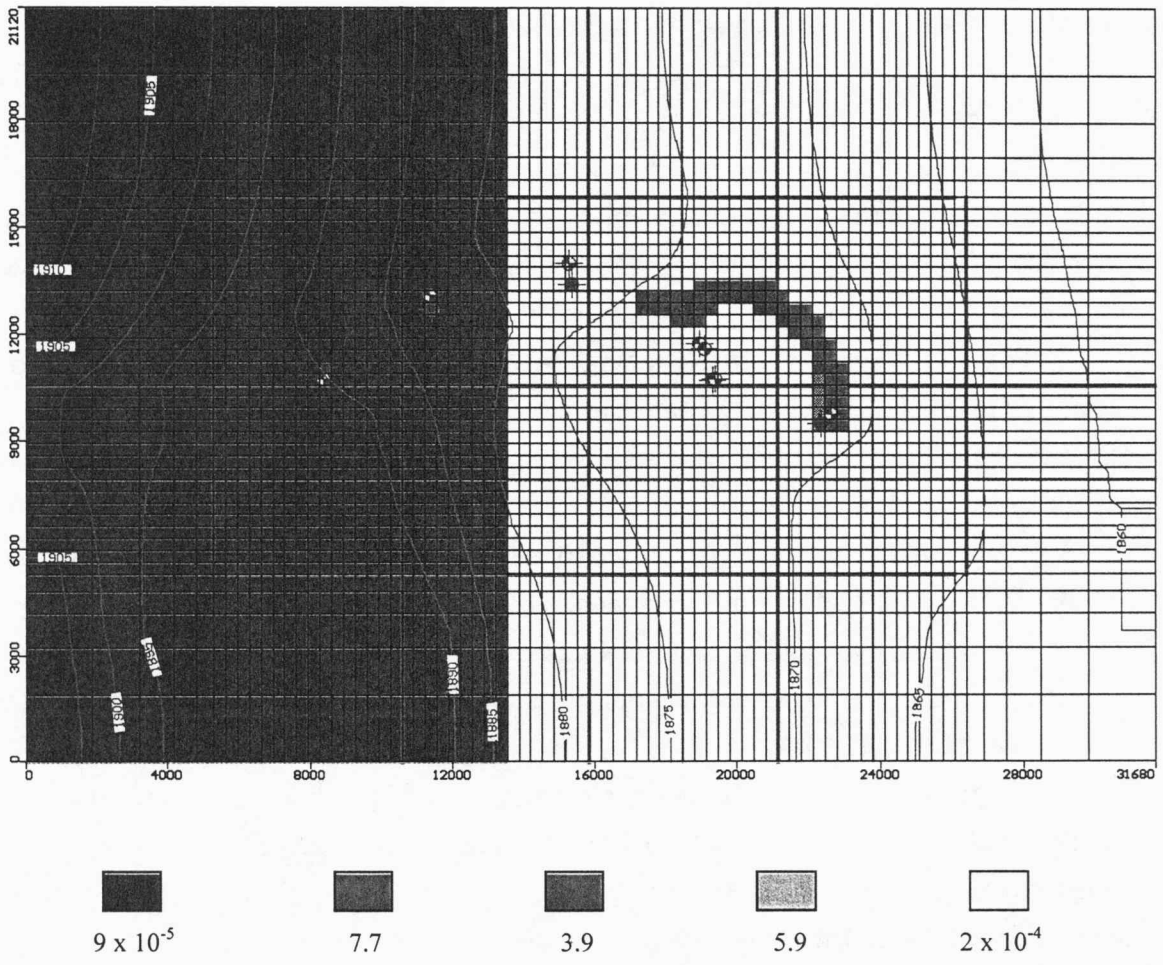

Figure 26. Hydraulic conductivity and hydraulic head distribution of layer 1 in the fringe model. Hydraulic conductivity is in ft/day. The hydraulic head contour interval on the potentiometric surface map is 5 ft.

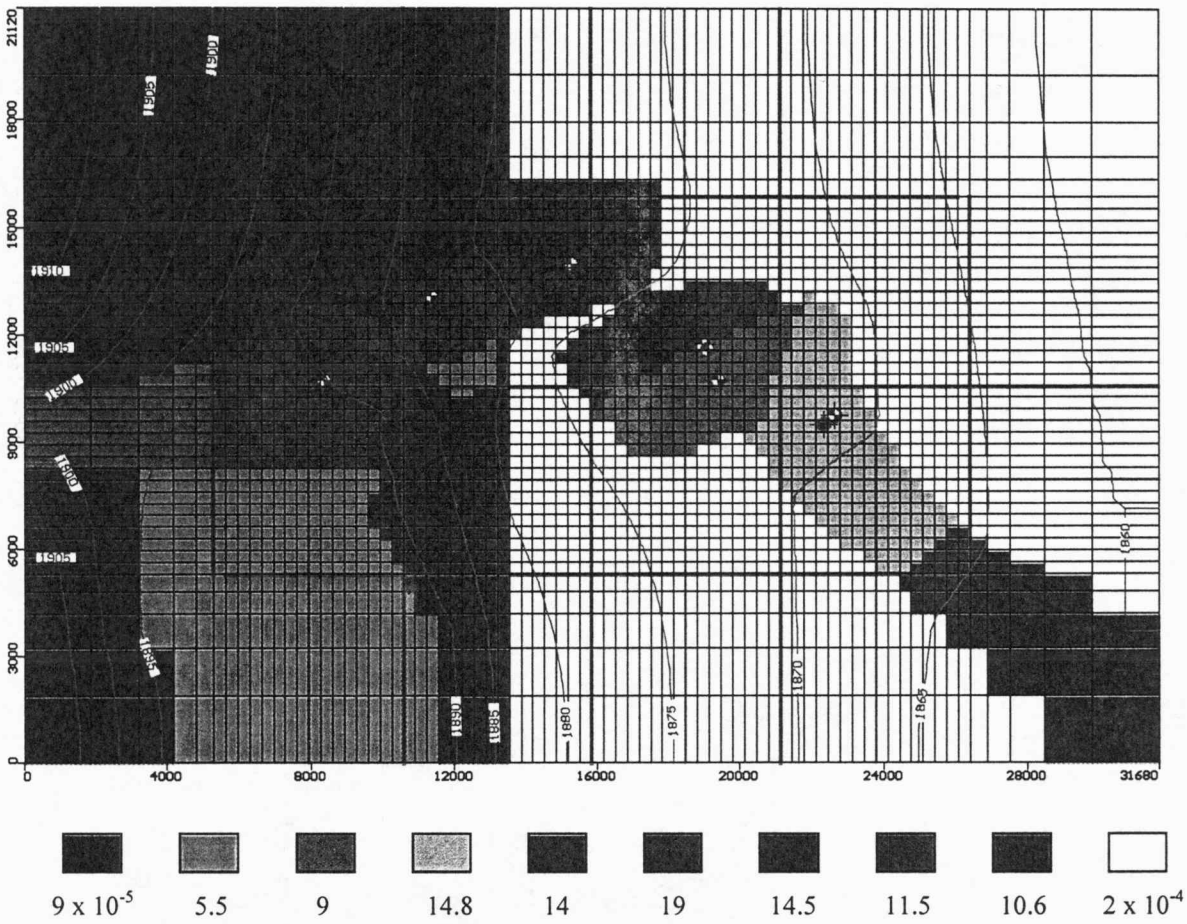

Figure 26 Continued. Hydraulic conductivity and hydraulic head distribution of layer 2 in the fringe model. Hydraulic conductivity is in ft/day. The hydraulic head contour interval on the potentiometric surface map is 5 ft.

Figure 27

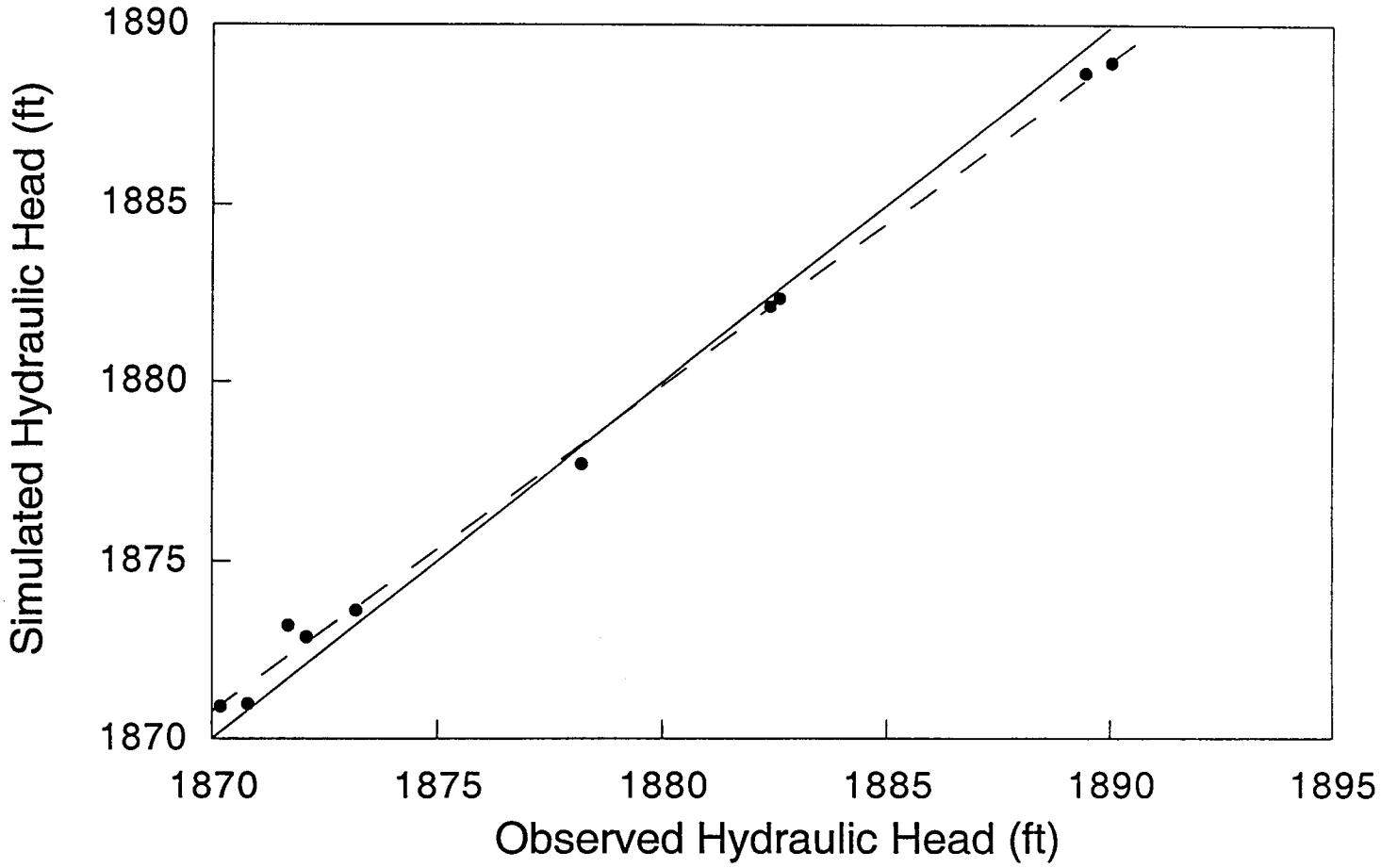

Figure 27. Plot of observed and simulated hydraulic heads from the steady-state, fringe conceptual model. The dashed line is the best-fit from linear regression and the solid line represents a perfect fit of the simulated to the observed.

mudstone and the sandstone. It was stated in Volume 1 of this report that the hydraulic conductivities derived from the pumping tests suggested a west to east increase in hydraulic conductivity. The steady-state models suggest this trend could possibly extend to the western and southeastern edges of the model.

Chapter 5: Transient Conceptual Ground-water Flow Models of the Upper Dakota Aquifer

Transient models of ground-water flow are used to assess the effects of pumping or artificial recharge on the flow system. These models allow the hydraulic head to change in the aquifer with time in response to stresses, such as pumping or injecting water into the aquifer. This part of the project involved development of equally acceptable transient conceptual models of ground-water flow in the upper Dakota aquifer in the vicinity of the Hays wellfield from the steady-state models formulated in Chapter 4. In this chapter we compare two, equally acceptable, transient, conceptual models to the transient, sandstone aquifer conceptual model, which we consider the simple base model in this report.

Transient conceptual model development

The transient conceptual models were developed starting with three equally acceptable, steady-state, conceptual models: the sandstone aquifer and the fringe models from Chapter 4 and the lobe model, which developed following an evaluation of the simulation results from the fringe model. The main features of the sandstone aquifer model are the heterogeneous sandstone aquifer and the surrounding mudstone aquitard. The fringe model includes the heterogeneous sandstone aquifer and the fringe. The fringe is defined as interbedded sandstone and mudstone deposits in the outer part of the meander belt. The lobe model was developed to improve the fit between the "observed" and simulated drawdowns in the 1992 D-3 and D-2 pumping tests. The lobe refers to a sandstone aquifer in Subunit 3 of the Dakota Formation that may be hydraulically connected to the main sandstone aquifer in the overlying Subunit 2. This hydraulically connected Subunit 3 sandstone body is pod-shaped or lobate in map view and is located south of D-2 (Figure 28).

Transformation of the conceptual ground-water flow models from the steady state to the transient condition

In order to transform the steady state, conceptual ground-water flow models to the transient condition, the model input was revised to include (1) information on the number and duration of time steps used to simulate the time rate of change of head due to pumping (drawdown), (2) information on pumping rates and duration from each of the 1992 and 1997 pumping tests used in calibration, (3) time vs. drawdown data for calibration at the observation wells nearest each pumping well, and (4) the assignment of specific storage, specific yield, and porosity values to the cells in the model.

In transient numerical models, the space and time dimensions are discretized into small increments to solve the flow equations in finite-difference form. The discretization of spatial

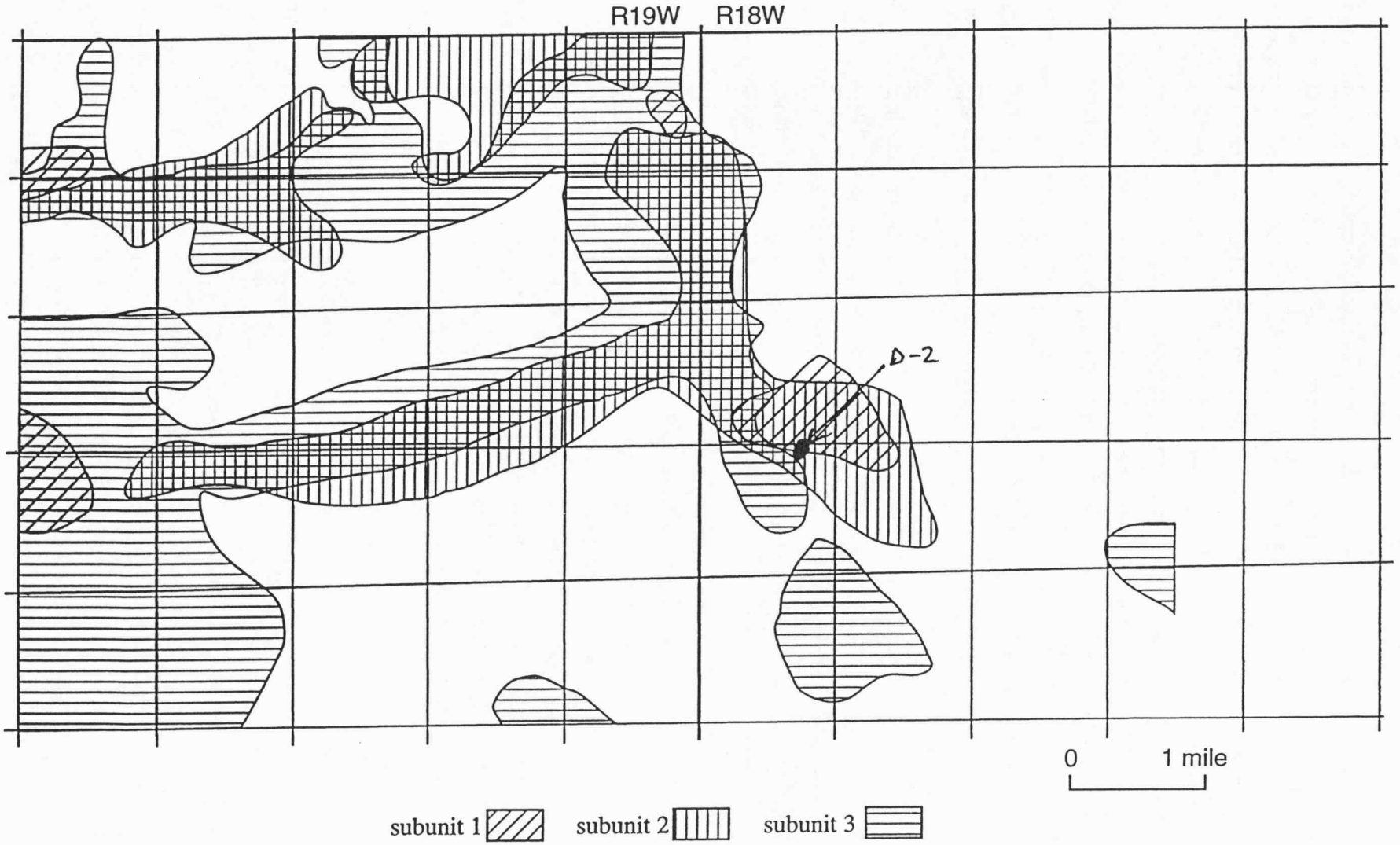

Figure 28. Probable sandstone body intraconnection in Subunits 1, 2, and 3 of the Dakota Formation based on a sandstone fraction of 50% or greater.

dimensions necessitates the time vs. drawdown data from the pumping tests to be adjusted to account for the new spacing between the cell that includes the pumping well and the cell that includes the observation well for each test. This is because the model treats both the pumping and observation wells as though they were each located at the center of their respective cell rather than where they are actually located on the ground. Likewise, because the transient model computes drawdowns for each time step in the model, the time of the observations does not necessarily coincide with the times when the depth to water was measured during the test. As a result the input "observed" time vs. drawdown data for the transient model simulation differs significantly from what was actually measured and recorded in the field. These "observed" data were generated using the SUPRPUMP (Bohling et al., 1990) well simulator from the estimated aquifer hydrologic properties and location of the hydrogeologic boundaries with respect to the pumping well.

Specific storage values were assigned to each cell in the model. In the vicinity of the Hays wellfield, specific storage values were assigned according to the hydrogeologic model of the upper Dakota aquifer (Figures 7 and 8). The specific storage zone boundaries were modified by any prior hydraulic conductivity zone boundary changes that were made in the wellfield vicinity to produce the steady-state model. This made the specific storage zone boundaries consistent with the hydraulic conductivity zone boundaries at the outset of calibration. This made the transient model formulations consistent with the hydrogeologic model. Specific storage data are not available for the sandstone aquifer outside of the wellfield or for the mudstone aquitard. From the available data on the sandstones in the Dakota aquifer of Kansas, specific storage appears to be log-normally distributed (Macfarlane et al., 1998). Thus, the model cells representing the sandstone outside of the immediate wellfield vicinity, the fringe, the sandstone lobe in Subunit 3, and the mudstone were assumed to have a specific storage of 1.5 x 10^{-6} ft^{-1}, the geometric mean of the values from the pumping tests in the wellfield.

Model calibration

The following general procedure was used to calibrate the transient, conceptual models. The goal of the calibration process was to use the model to reproduce the "observed" time vs. drawdown data derived from the field measurements collected from the observation wells during each pumping test. These tests included the 1992 pumping tests for wellsites 5, 1, 3, 2, and 4 and the 1997 pumping test of wellsite 6 (Figure 1). These calibration milestones were selected because the short-term pumping tests provide information on the aquifer characteristics in the vicinity of the test site and in adjacent areas of the wellfield.

The process of calibrating a model in its transient form may also provide additional information that could not be gleaned from the steady-state model. During calibration it was

noted that depending on the duration of pumping all of the wells are located so close together within an aquifer of limited extent that the cone of depression produced from pumping any of them includes at least two to three of the pumping well sites. Thus, the hydraulic information about the aquifer within the wellfield from all of the tests combined provides redundant information on the aquifer hydrologic properties because of the influence of these properties on the propagation of drawdown through the aquifer.

Calibration was accomplished by trial-and-error adjustment of the model parameters. The early time part of the simulated drawdown curve was matched to the "observed" data by adjusting the specific storage and the hydraulic conductivity zone boundaries, or the sandstone aquifer thickness in the cells near the well. For the later part of the test, the position and geometry of the sandstone aquifer boundaries at greater distances from the pumping well were adjusted consistent with the geologic interpretation. Rarely, the hydraulic conductivity, specific storage, and thickness of the sandstone needed adjustment. These more distant adjustments away from the pumping well were then evaluated against the match between the simulated and "observed" drawdowns from the other pumping tests near where those changes were made and against the RMS error of the steady-state model. In this way the trial-and-error calibration proceeded iteratively until a satisfactory match was obtained.

Taking into consideration that these are conceptual and not predictive models, the progress of the calibration process was evaluated on the basis of a visual best fit of the simulated to the "observed" drawdowns. Every attempt was made to match the simulated to the "observed" drawdowns using these conceptual models. However, in some instances only the early part of the simulated drawdown curve could be matched closely to the "observed" drawdown data, whereas the simulated curve only generally follows the "observed" drawdown from the pumping tests in other cases. Overall, the model predicts higher rates of drawdown increase later in the pumping tests than was observed during each pumping test.

Comparison of the calibrated sandstone aquifer and fringe transient conceptual models

The cell-by-cell hydraulic conductivity and specific storage properties are shown for each model layer in the sandstone aquifer and fringe transient models in Figures 29-32. In the sandstone aquifer model the sandstone specific storage near wellsite 6 is 1.4×10^{-6} ft^{-1}; near wellsite 5, 1.0×10^{-6} ft^{-1}; near wellsite 1, 1.6×10^{-6} ft^{-1}; near wellsite 3, 2.2×10^{-6} ft^{-1}; near wellsite 2, 1.4×10^{-6} ft^{-1}; and near wellsite 4, 2×10^{-6} ft^{-1}.

In the fringe model, layer 1 has a thin, arcuate fringe deposit with a hydraulic conductivity ranging from 3.9 to 7.7 ft/day. The highest hydraulic conductivities are in the northwest segment of the arcuate fringe deposit and the lowest are near wellsite 4 at the southern

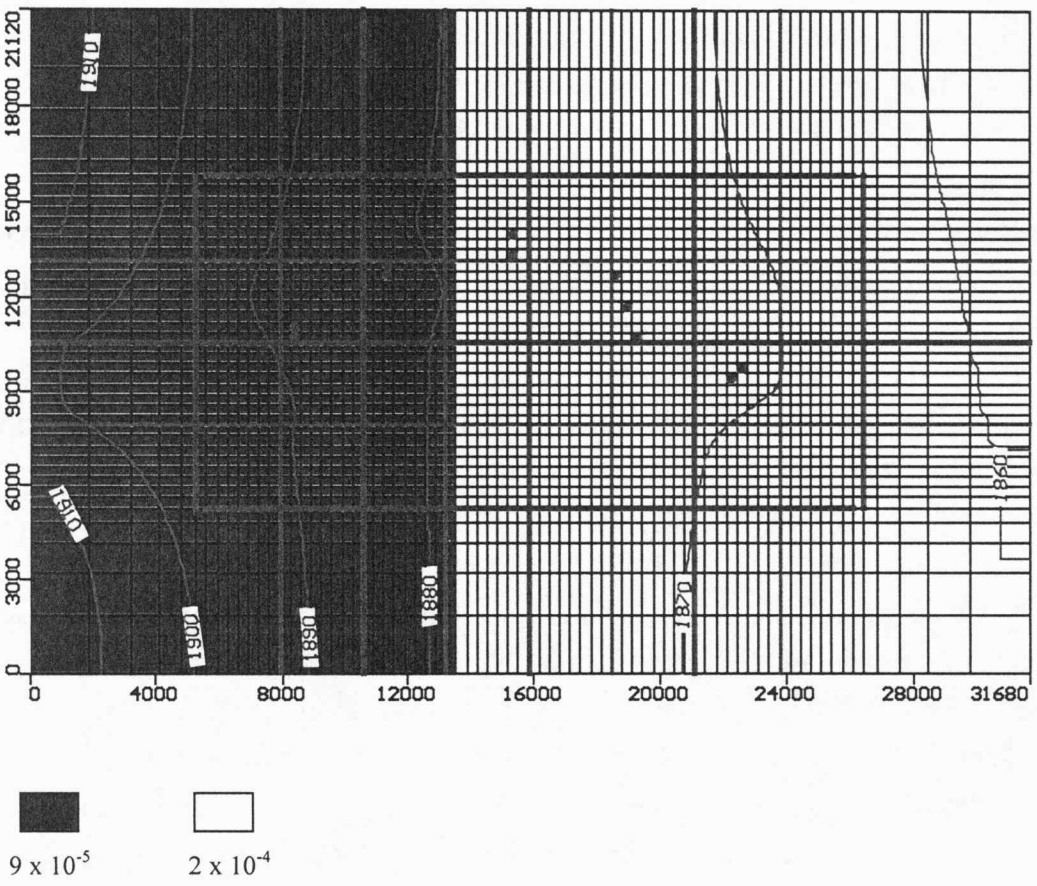

Figure 29 ~~Continued~~. Distribution of hydraulic conductivity in layer 1 of the sandstone aquifer model. Hydraulic conductivity is in units of ft/day. Shown also is the simulated potentiometric surface map with a contour intervel of 5 ft.

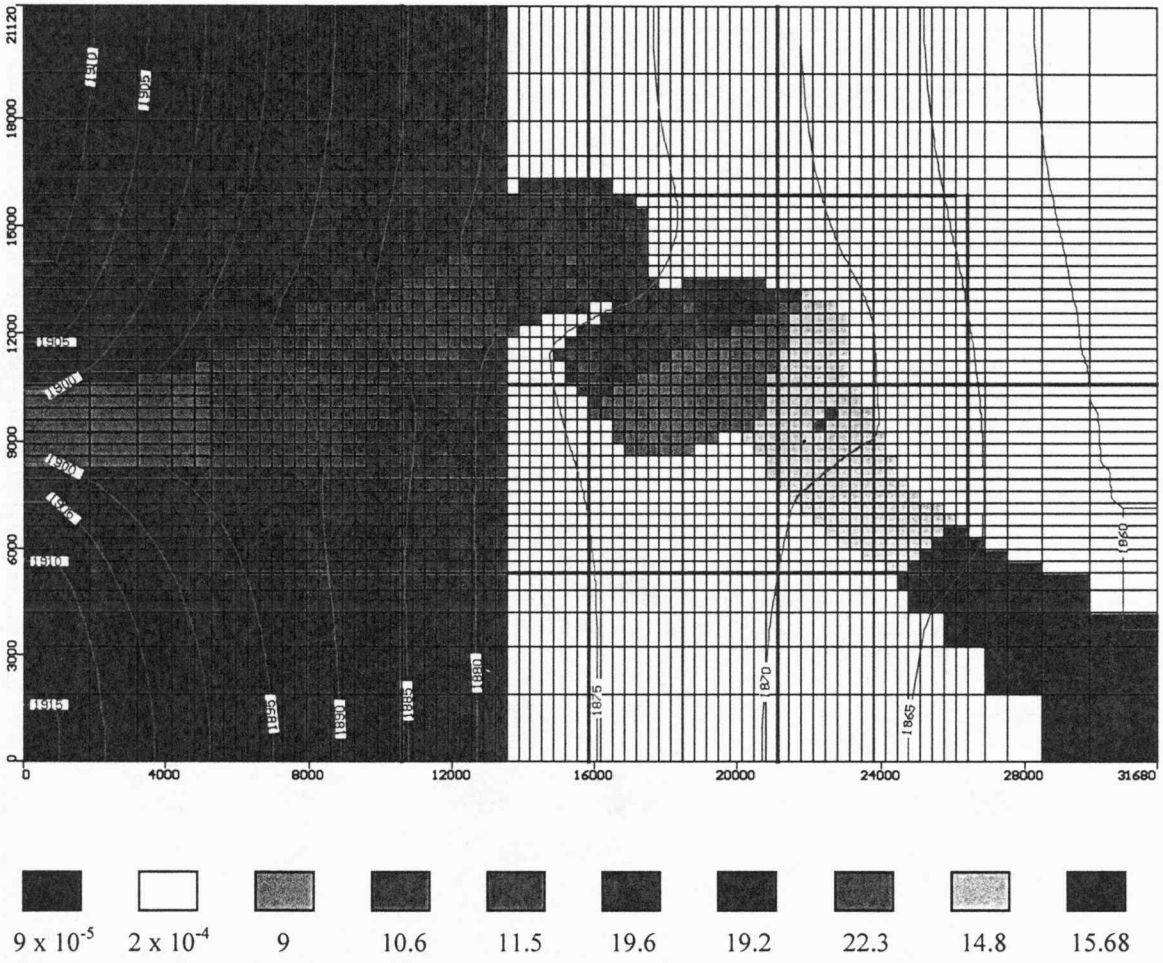

Figure 29 Continued. Distribution of hydraulic conductivity in layer 2 of the transient sandstone aquifer model. Hydraulic conductivity is in units of ft/day. Shown also is the simulated potentiometric surface map with a contour interval of 5 ft.

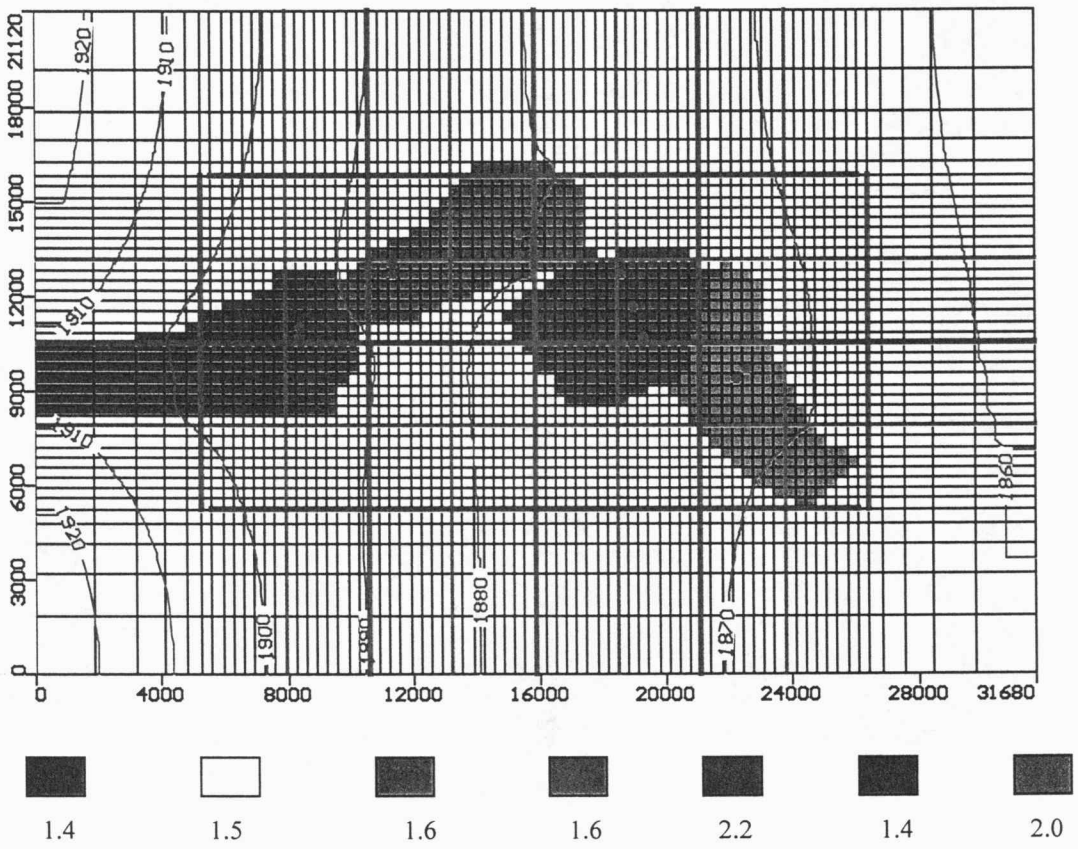

Figure 30. Distribution of specific storage in layer 2 of the transient sandstone aquifer conceptual model. Layer 1 specific storage is a uniform 1.5 x 10^{-6} ft^{-1}. Shown also is the potentiometric surface of the upper Dakota aquifer with a contour interval of 5 ft.

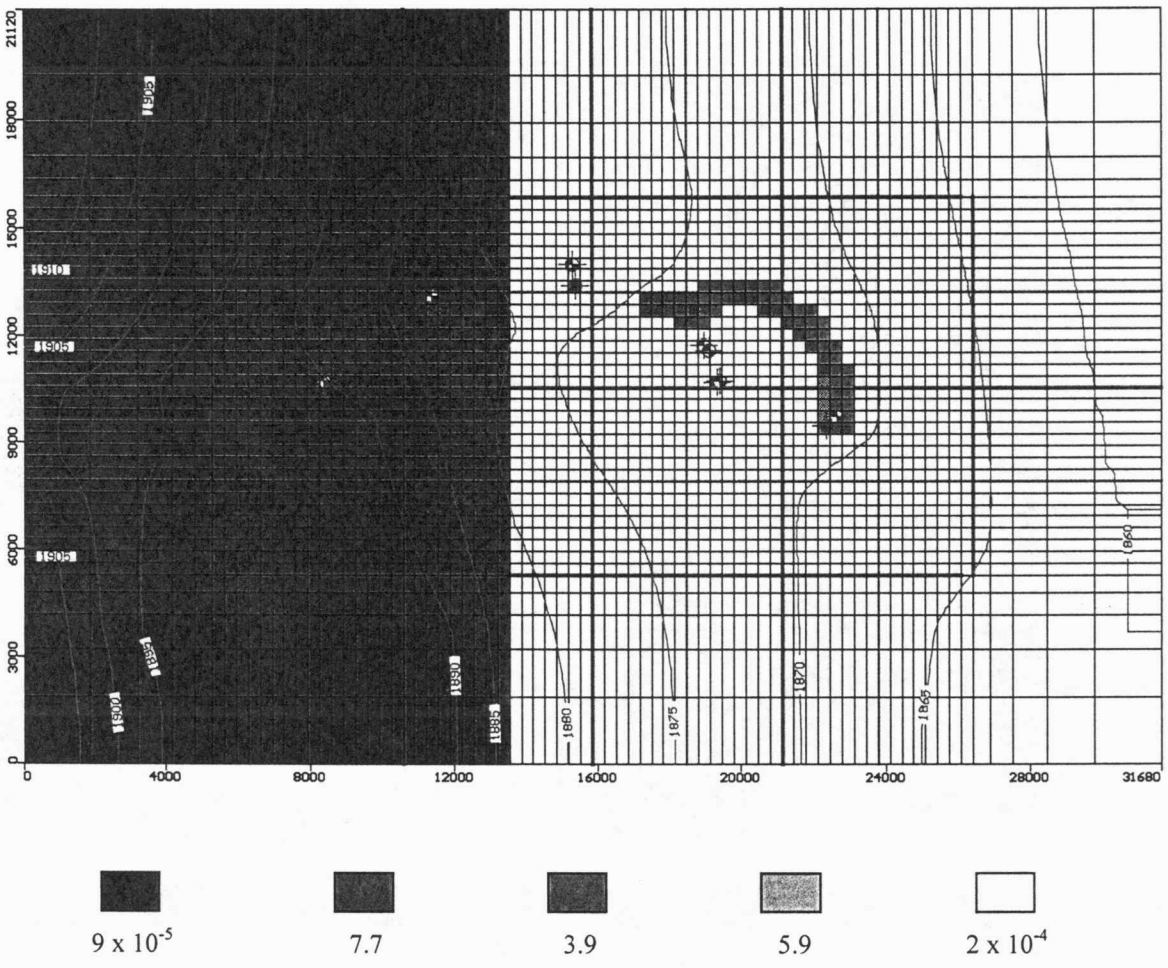

Figure 31. Hydraulic conductivity and hydraulic head distribution of layer 1 in the fringe model. Hydraulic conductivity is in ft/day. The hydraulic head contour interval on the potentiometric surface map is 5 ft.

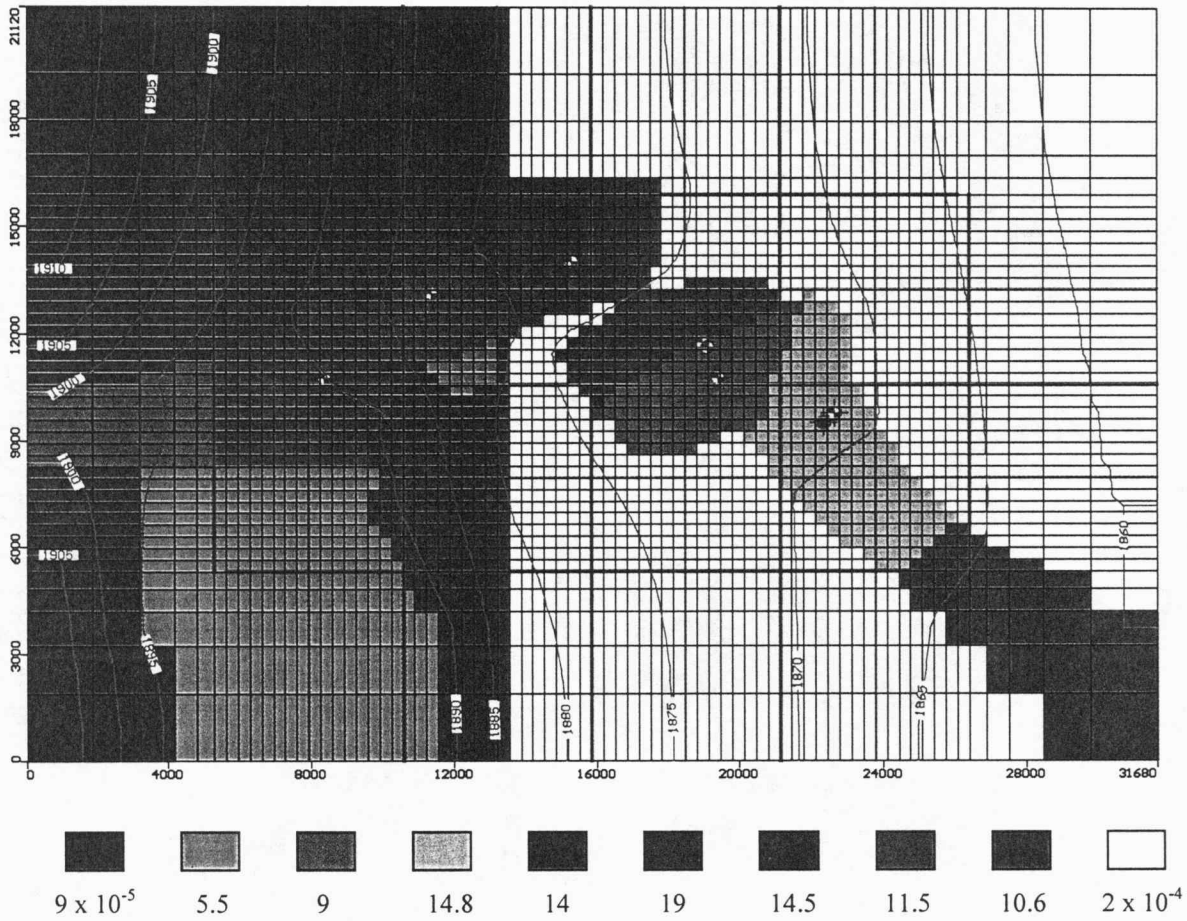

Figure 31 Continued. Hydraulic conductivity and hydraulic head distribution of layer 2 in the fringe model. Hydraulic conductivity is in ft/day. The hydraulic head contour interval on the potentiometric surface map is 5 ft.

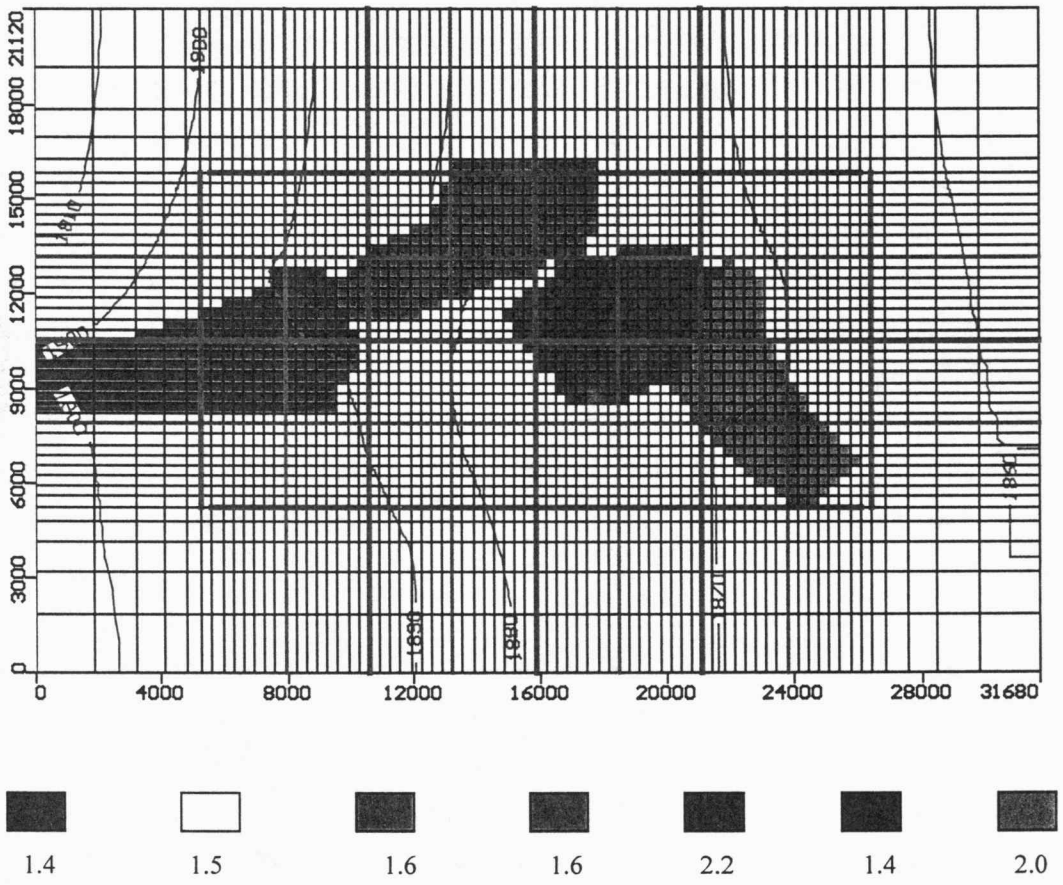

Figure 32. Distribution of specific storage in layer 2 of the transient fringe conceptual model. Layer 1 specific storage is a uniform 1.5×10^{-6} ft^{-1}. Shown also is the potentiometric surface of the upper Dakota aquifer with a contour interval of 5 ft.

edge of the deposit. In layer 2 an extensive fringe zone is located south and west of wellsite 6 and a smaller patch south of wellsite 5.

The following is a comparison of the simulation results for the 1992 and 1997 pumping tests from the sandstone aquifer and fringe models after calibration. Simulation of the 1997 D-6 and 1992 D-1 pumping tests in the sandstone aquifer model results in a significant underestimation of drawdown for the entire test (Figure 33). In comparison the simulation of the same pumping test in the fringe model nearly matches the "observed" drawdown up to about 0.4 days after the start of the test. Beyond this point the "observed" drawdown increase is much less than the rate predicted by the simulation to the end of the test.

Simulations of the 1992 D-5 pumping test using the sandstone aquifer and fringe models yield almost identical results (Figure 33). The results from both models nearly match the early-time "observed" drawdowns from pumping and eventually overestimate drawdown at later times. In the D-5 pumping test simulation this occurs at between 0.1 and 1.0 days after the test. The slight improvement of fit in the fringe model is attributed to the fringe deposits south of D-5. Nevertheless, the improved early time fit does not extend to the later part of the test.

Two "observed" drawdown data sets were available from MD-2&3 and D-2 for model calibration from the 1992 D-3 pumping test (Figure 34A and B). The simulation results from the sandstone aquifer model are a better match to the "observed" drawdowns than are the results from the fringe model. However, drawdown is seriously over predicted after the first day of pumping in the results from the sandstone aquifer model. Comparison of the "observed" and simulated pumping test results using D-2 as an observation point shows that drawdown is overpredicted for the early part of the test and underpredicted for the later part. In contrast, the fringe model simulation results underpredict drawdown for most of the test and near the end overpredict the rate of drawdown increase with time. Comparisons between the "observed" and simulated results from the fringe and sandstone aquifer models for the 1992 D-2 pumping test are similar to the comparisons made between the "observed" and simulated results from the D-3 pumping test (Figures 34C and D).

Comparison of the "observed" and simulated drawdowns at MD-4 during the 1992 D-4 pumping test show that the fringe model does a much better job of simulating the test results than does the channel model (Figure 35). This great improvement may have resulted from the addition of fringe zones to model layer 1 (Figure 31). The fringe deposits may provide a better hydraulic connection to ground water in the sandstone aquifer in model layer 2 upgradient of the constriction in the aquifer between wellsites 1 and 3. Thus the rate of drawdown increase is lower at MD-4 because of the improved accessibility of D-4 to additional ground water upgradient of the well.

Figure 33

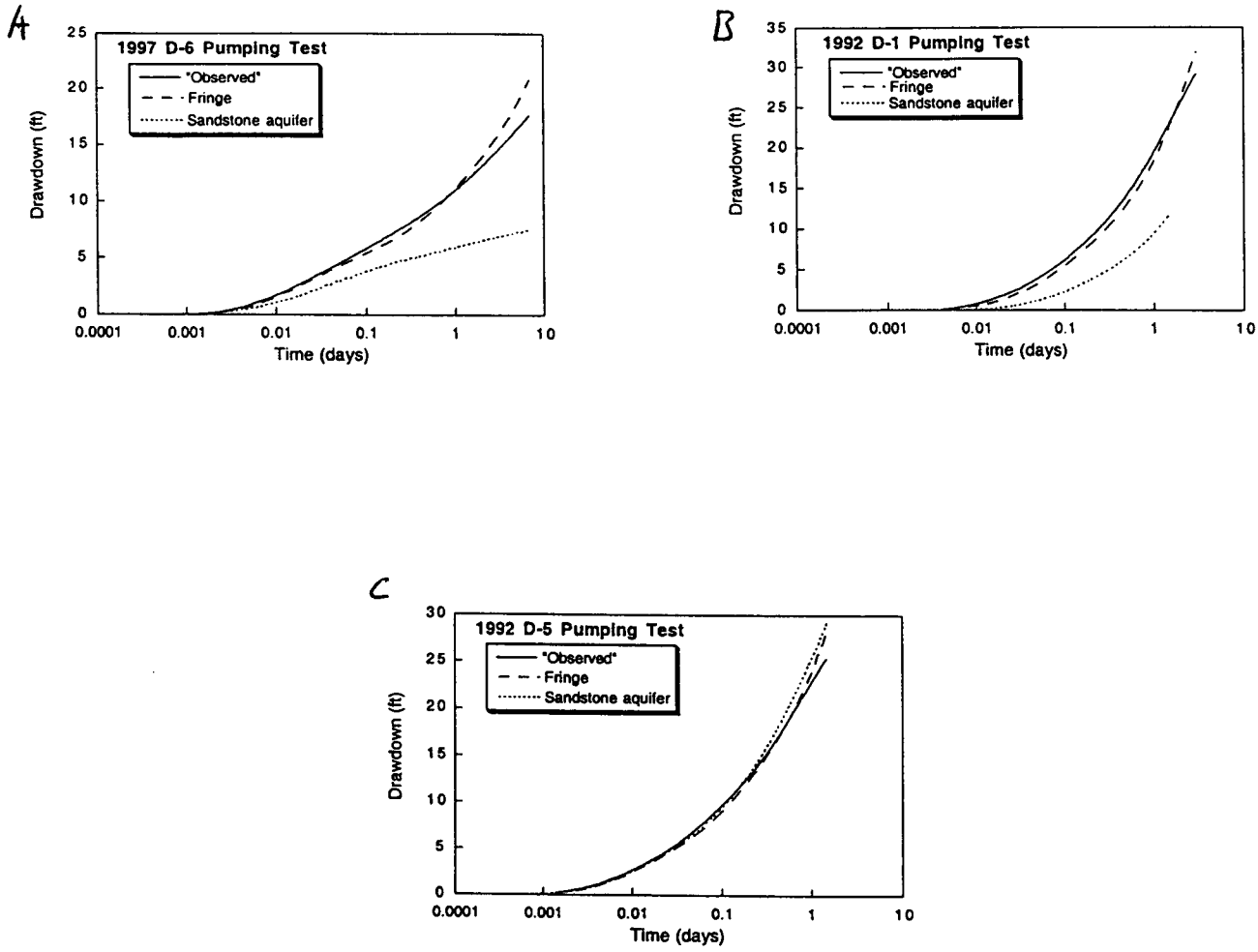

Figure 33. Simulated and "observed" drawdowns from the sandstone aquifer and fringe models at the at the near observation wells in the D-6 (A), D-1 (B), and D-5 (C) pumping tests.

Figure 34

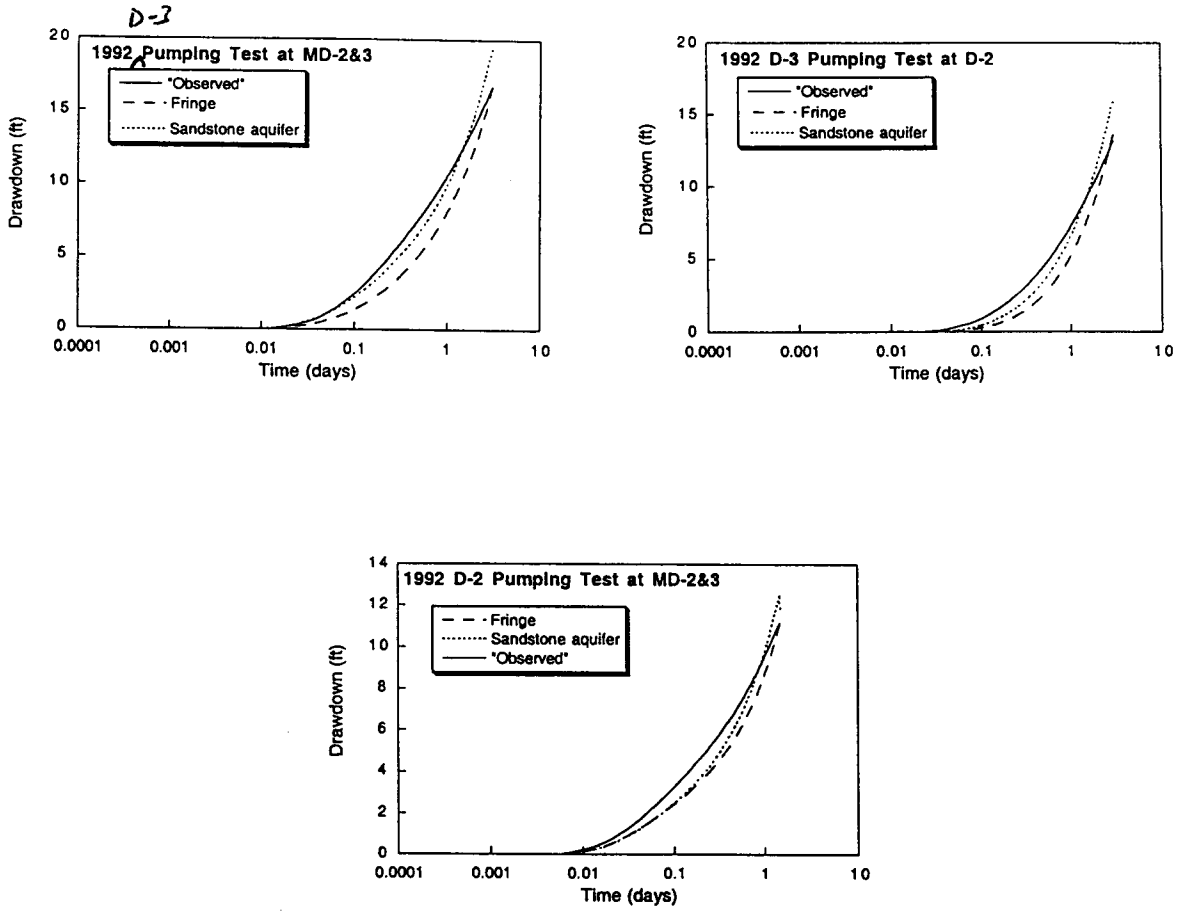

Figure 34. Simulated and "observed" drawdowns from the sandstone aquifer and fringe models at MD-2&3 (A) and D-2 (B) from the D-3 pumping test and MD-2&3 (C) from the D-2 pumping test.

Figure 35

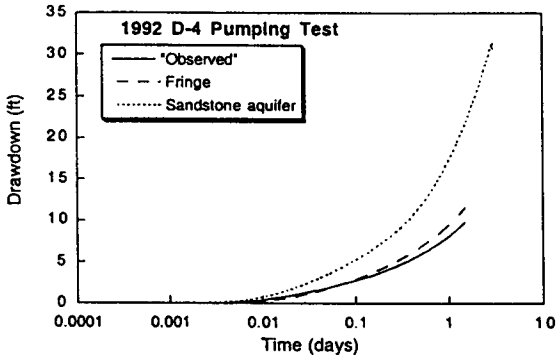

Figure 35. Simulated and "observed" drawdowns from the sandstone aquifer and fringe models at MD-4 from the D-4 pumping test.

Comparison of the calibrated fringe and lobe transient conceptual models

A third model, referred to as the transient, lobe, conceptual model, was developed and calibrated in an attempt to better simulate the 1992 D-2 and D-3 pumping test results. In this model, the sandstone aquifer was expanded to take into account a potentially significant hydraulic connection between the main sandstone aquifer in Subunit 2 and the underlying sandstone aquifer in Subunit 3 of the Dakota Formation. Analysis of the geophysical log cross sections portrayed in Volume 1 of this report suggest that this interconnection of sandstone bodies might exist. The subsurface data are insufficient to show the extent of this interconnection in detail and the aquifer properties of the Subunit 3 sandstone are unknown. Lacking this information, it was assumed that the sandstone hydraulic conductivity was 9 ft/day on the basis of the gamma-ray log appearance in the Subunit 3 sandstone interval. It was also assumed that the extent of the Subunit 3 sandstone closely followed the 50% sandstone fraction contour line portrayed in Figures 6 and 28.

To calibrate this model and produce an improved match to the D-2 and D-3 pumping test results, adjustments were made in the (1) geometry of (a) the hydraulic connection between the Subunit 2 and Subunit 3 sandstones south of D-2, and (b) the Subunit 2 sandstone aquifer extent between D-1 and D-3 and the north aquifer boundary east of D-3, (2) aquifer properties in the section of the Subunit 2 sandstone containing D-2 and D-3, and (3) extent of the fringe in model layer 1.

In the final model, the constriction in the aquifer between D-1 and D-3 was lessened and the north aquifer boundary was moved one row closer to D-3 than it was in the fringe model (Figure 36). These adjustments allow more water to move into the eastern part of the wellfield and increased the drawdown sooner in the simulation of the 1992 D-3 pumping test. Eastward of D-3 and north of D-4, the Subunit 2 north aquifer boundary was adjusted slightly to make it less irregular. This had no discernable impact on the calibration. In the upper model layer, the expanded fringe deposit was nearly doubled in its extent. Apparently, this increase in extent allowed D-4 access to more water during pumping.

Changes were also made to the hydraulic conductivity and specific storage in the sandstone aquifer to arrive at the transient, lobe conceptual model. The hydraulic conductivity in the section of the aquifer containing D-3, MD-2&3, and D-2 after calibration is 19 ft/day. This is an increase in hydraulic conductivity from the previous fringe conceptual model where this section of the aquifer was split into two hydraulic conductivity zones (Figure 31A). In the upper model layer, the high and low hydraulic conductivity zones were expanded, but the intermediate hydraulic conductivity zone around D-4 and MD-4 remained the same in size (Figure 36A). No changes were made to the specific storage distribution in the upper model layer (Figure 37B). In the lower layer, the sandstone specific storage around D-3, MD-2&3, and D-2 was reduced to 1.0

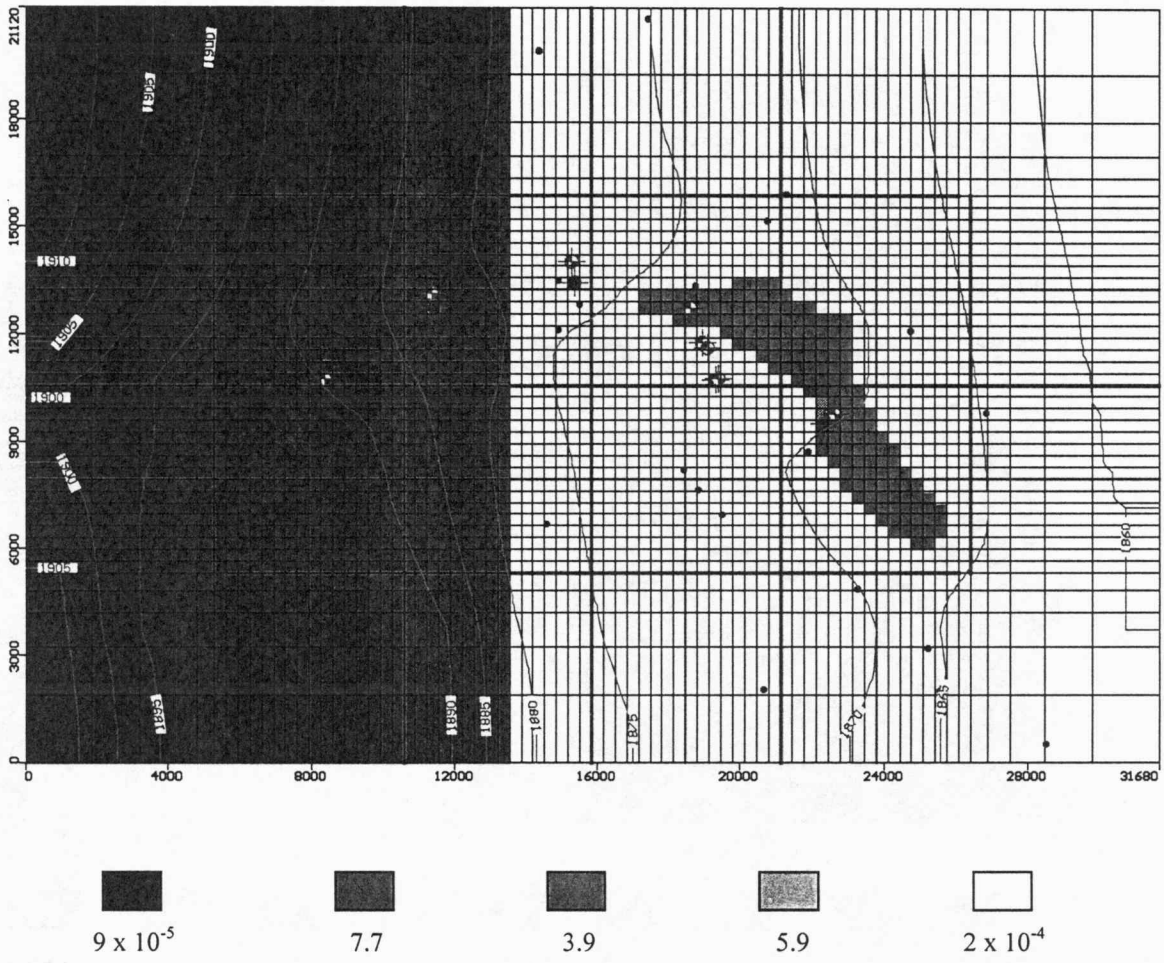

Figure 36. Hydraulic conductivity and hydraulic head distribution of layer 1 in the lobe model. Hydraulic conductivity is in ft/day. The hydraulic head contour interval on the potentiometric surface map is 5 ft.

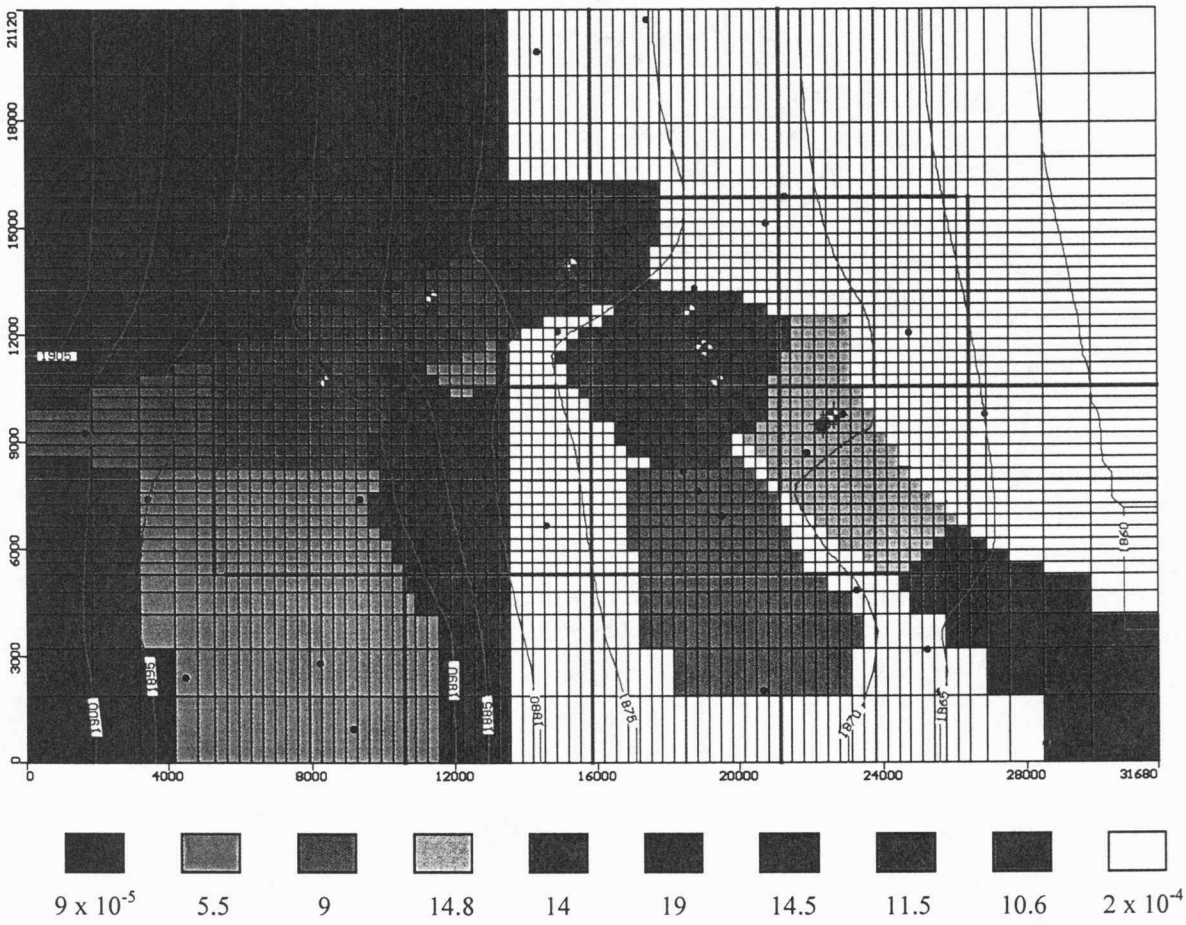

Figure 36 Continued. Hydraulic conductivity and hydraulic head distribution of layer 2 in the lobe model. Hydraulic conductivity is in ft/day. The hydraulic head contour interval on the potentiometric surface map is 5 ft.

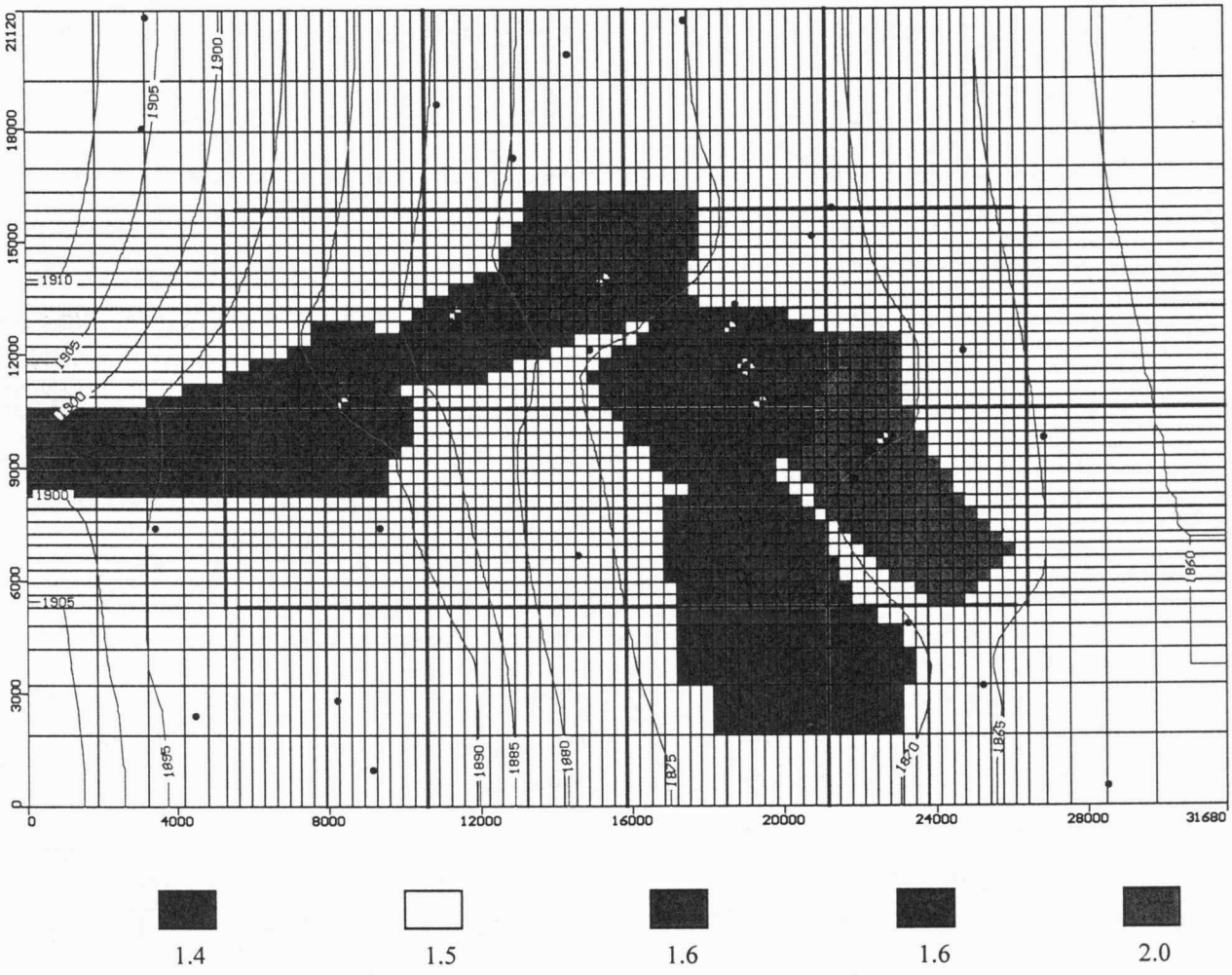

Figure 37 Distribution of specific storage in layer 2 of the transient lobe model. Specific storage is indicated as x 10^{-6} ft^{-1}. The specific storage of layer 1 is a uniform 1.5 x 10^{-6} ft^{-1}. Shown also is the simulated potentiometric surface map with a contour interval of 5 ft.

x 10^{-6} ft^{-1}. To the south of D-2 the lobe was split into two specific storage zones. After calibration the specific storage values of the northern and southern sections were 1.0 x 10^{-6} ft^{-1} and 1.4 x 10^{-6} ft^{-1}, respectively.

The following is a comparison of the lobe and fringe model simulation results for the 1992 and 1997 pumping tests from fringe and lobe transient models after calibration. Using the 1997 D-6 pumping test data from MD-6 as a calibration goal, there was no change in the simulated drawdowns between the fringe and the lobe transient models (Figure 38A).. Simulation of the 1992 D-5 pumping test shows a slightly better match with the drawdowns at MD-5 up to about 0.3 days (Figure 38B). Beyond this point the model begins to seriously overpredict drawdown at late time in the test after about 0.6 days. Similar results are obtained with the simulation of the 1992 pumping test of D-1 when observing drawdown at MD-1 (Figure 38C). There is a slight improvement of fit between the "observed" and the simulated drawdowns for the early part of the test, but at later time after about 1.5 days the drawdown from pumping is over predicted. In the D-3 pumping test the lobe conceptual model is slightly better at simulating the "observed" drawdown at MD-2&3 and at D-2 (Figure 39A and B) than the fringe conceptual model. The lobe model still underpredicts drawdown for most of the test and eventually overpredicts it near the end of the test, but it is significantly better at simulating the drawdown from the D-2 pumping test at MD-2&3 than the fringe model (Figure 39C and D). The simulated drawdowns also seem to more closely follow the "observed" from this test at D-3, even though they are somewhat underestimated at early time and overestimated at late time in the test. Figure 40 indicates that the lobe model better simulates the "observed" drawdown at MD-4 from the 1992 D-4 pumping test than does the fringe model.

The steady-state flow simulation using the lobe conceptual model has a RMS error of 0.47 ft, which is only slightly higher than the error in the fringe conceptual model. The plot of the "observed" vs. simulated hydraulic heads for the steady-state lobe and fringe models shows that the lobe model better simulates the observed hydraulic-head gradient in wellfield (Figure 41). Note that the slope of the best-fit line is 1.0 for the lobe model in this plot with very little change in the r^2 value from the fringe model. The best-fit line has a slope that is statistically significant ($p = 0.0001$) and the 95% confidence interval on the slope includes a slope of 1. In contrast, the lower slope of the best-fit line through the simulated steady-state hydraulic heads in the fringe model is less than 1.0 even if the 95% confidence interval is included. Overall, the flow through this model is very nearly the same as in the fringe model at 3,297 ft^3/day.

Summary and evaluation of the calibration results

Three transient, conceptual, ground-water flow models were calibrated using the 1992 and 1997 pumping test results presented and analyzed in Volume 1 of this report. The three

Figure 38

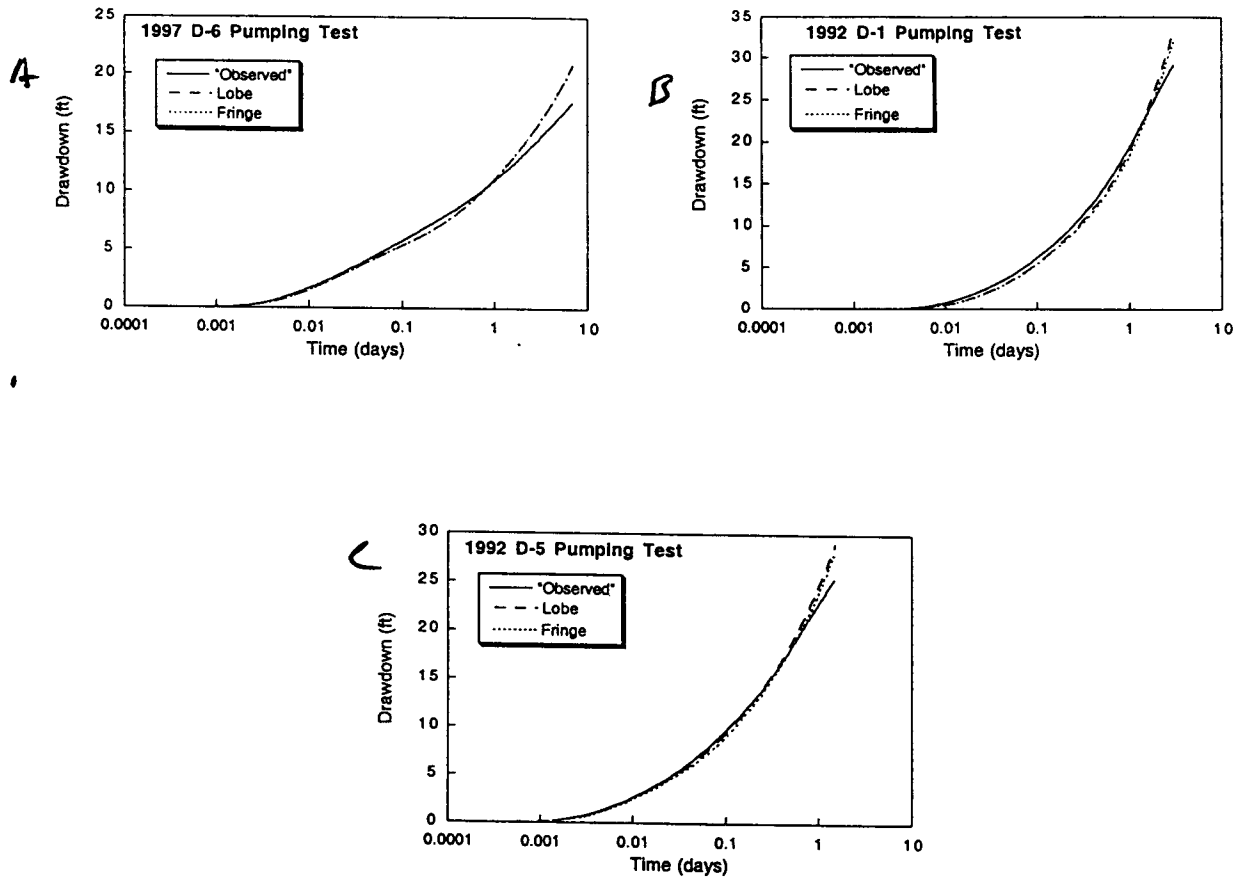

Figure 38. Simulated and "observed" drawdowns from the fringe and lobe models at the at the near observation wells in the D-6 (A), D-1 (B), and D-5 (C) pumping tests.

Figure 39

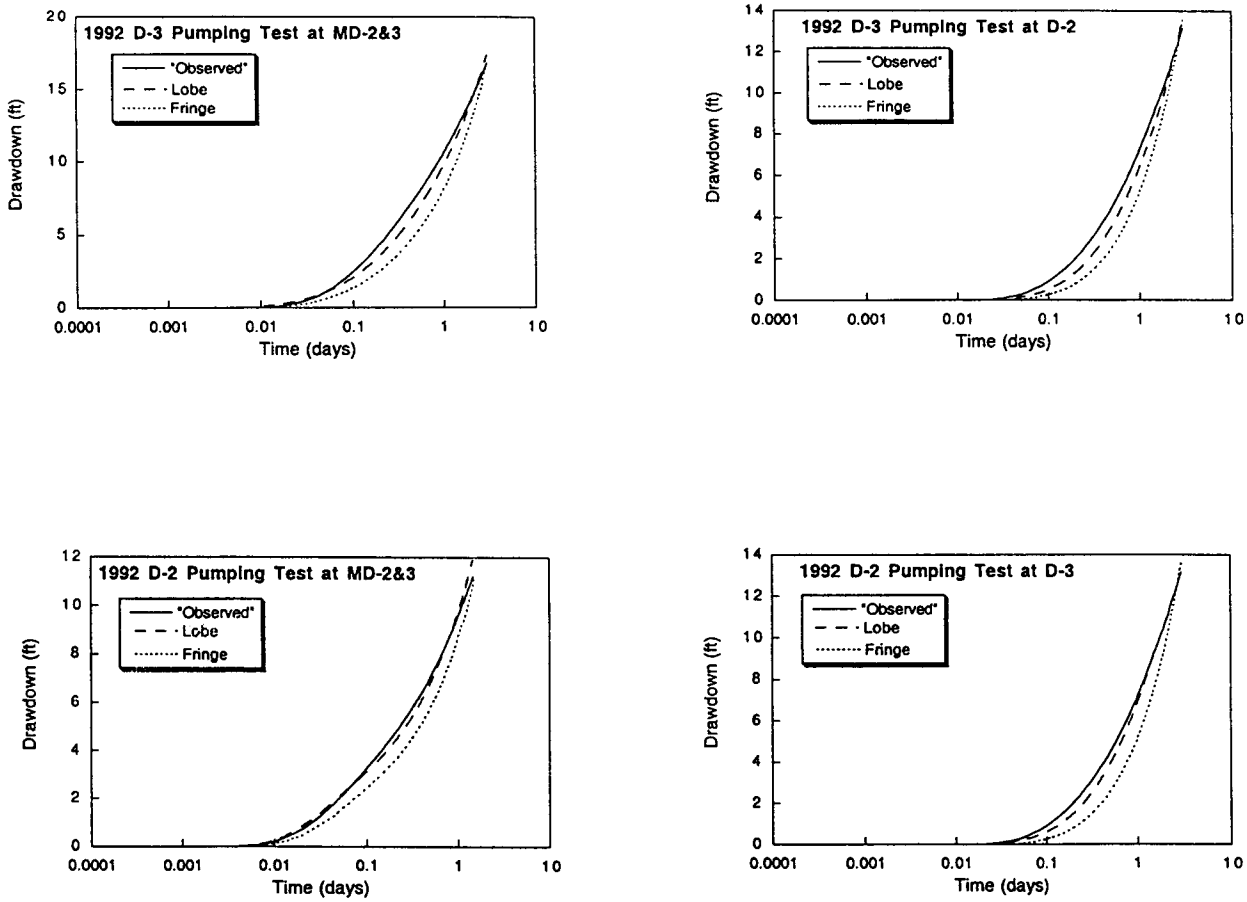

Figure 39. Simulated and "observed" drawdowns from the fringe and lobe models at MD-2&3 (A) and D-2 (B) from the D-3 pumping test and MD-2&3 (C) and D-3 (D) from the D-2 pumping test.

Figure 40

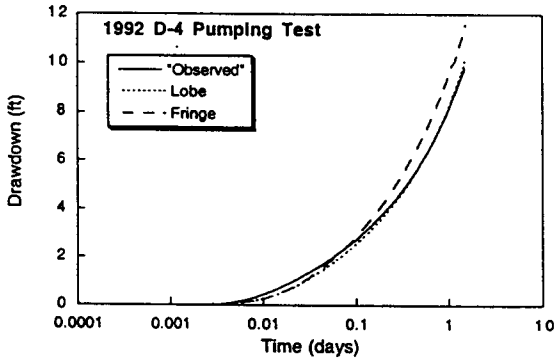

Figure 40. Simulated and "observed" drawdowns from the fringe and lobe models at MD-4 from the D-4 pumping test.

Figure 41

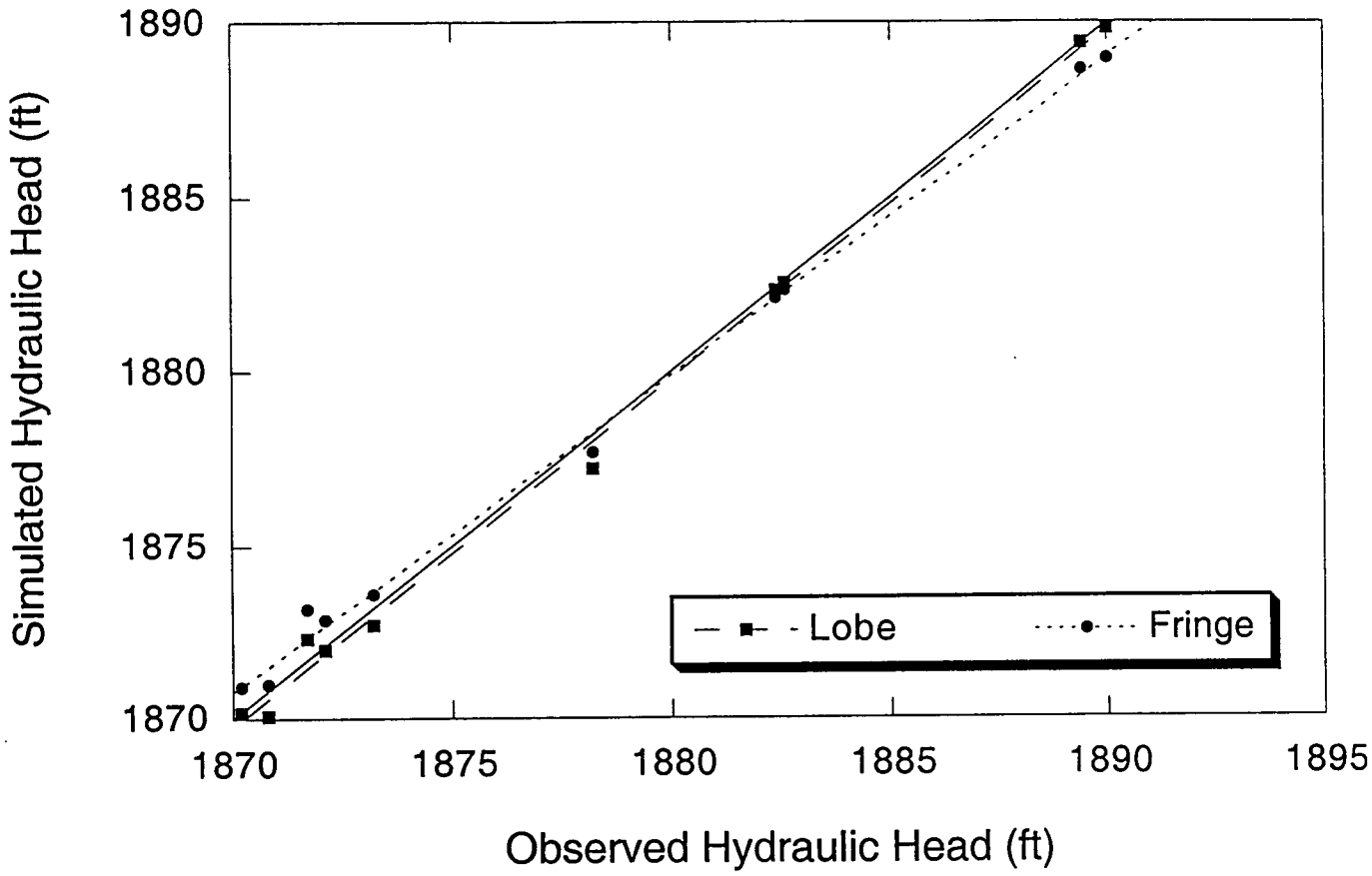

Figure 41. Plot of observed and simulated hydraulic heads from the steady-state, fringe and lobe conceptual models. The dashed lines are the best fit lines from linear regression and the solid line represents a perfect fit of the simulated to the observed.

transient models differ significantly in their ability to simulate the observed drawdowns from the pumping tests. The most realistic of these, the fringe and the lobe models, are able to simulate the drawdown histories reasonably well for at least the early part of each of the pumping tests. The sandstone aquifer model drastically underestimates the observed drawdown from some of the tests, while in others it is able to match only the early parts of each test. In both the fringe and the lobe models, the "observed" drawdowns are overestimated in the later parts of each set of tests used in calibration.

One possible explanation for the lack of fit between the observed and simulated drawdowns in the later part of the tests is that neither model is able to account for other sources of water to the sandstone aquifer in Subunit 2 of the Dakota Formation during pumping. The additional water source could be leakage from the surrounding mudstone aquitard, the underlying Subunit 3 sandstones in the central and western parts of the wellfield, the confining unit above the upper Dakota aquifer or a combination of these sources depending on which well is being pumped. The sandstone isolith map of Subunit 3 (Figure 6) suggests the presence of a separate significant sandstone aquifer displaced slightly to the north of the sandstone aquifer in Subunit 2. If the hydraulic connection between the Subunit 2 and Subunit 3 sandstones is poor, leakage across a fringe zone or a thin mudstone might be sufficient to reduce drawdown in the pumping wells at late time. The addition of significant leakage from the overlying Upper Cretaceous aquitard to the aquifer where it is being impacted by pumping is unlikely because of its estimated low vertical hydraulic conductivity (Macfarlane, 1993).

To investigate the hypothesis that the mudstone may be a significant additional source of water to the wells during pumping, the lobe model was modified by arbitrarily increasing the hydraulic conductivity of the mudstone by a factor of 300, which corresponds to about three orders of magnitude less than the hydraulic conductivity of the sandstone aquifer in the wellfield. The new hydraulic conductivities for the western and eastern zones in the mudstone for each layer were 0.027 and 0.06 ft/day, respectively. Recalibration of the steady-state model caused a reduction in the width of the sandstone aquifer at the western end of the model by 990 ft to a new width of 1,320 ft with no change in the assumed sandstone aquifer hydraulic conductivity upgradient of the wellfield (Figure 42). Downgradient of the wellfield the sandstone aquifer hydraulic conductivity was reduced from 15.7 ft/day to 14 ft/day. No other changes were made to the cell-by-cell hydraulic conductivity distribution in the rest of the model and no changes were made to the cell-by-cell specific storage distribution to generate this new model. This newer steady-state model has a slightly lower RMS error (0.36 ft) than the error in the lobe model and the steady-state flux is slightly higher in this model (3,700 ft^3/day) than in the lobe model.

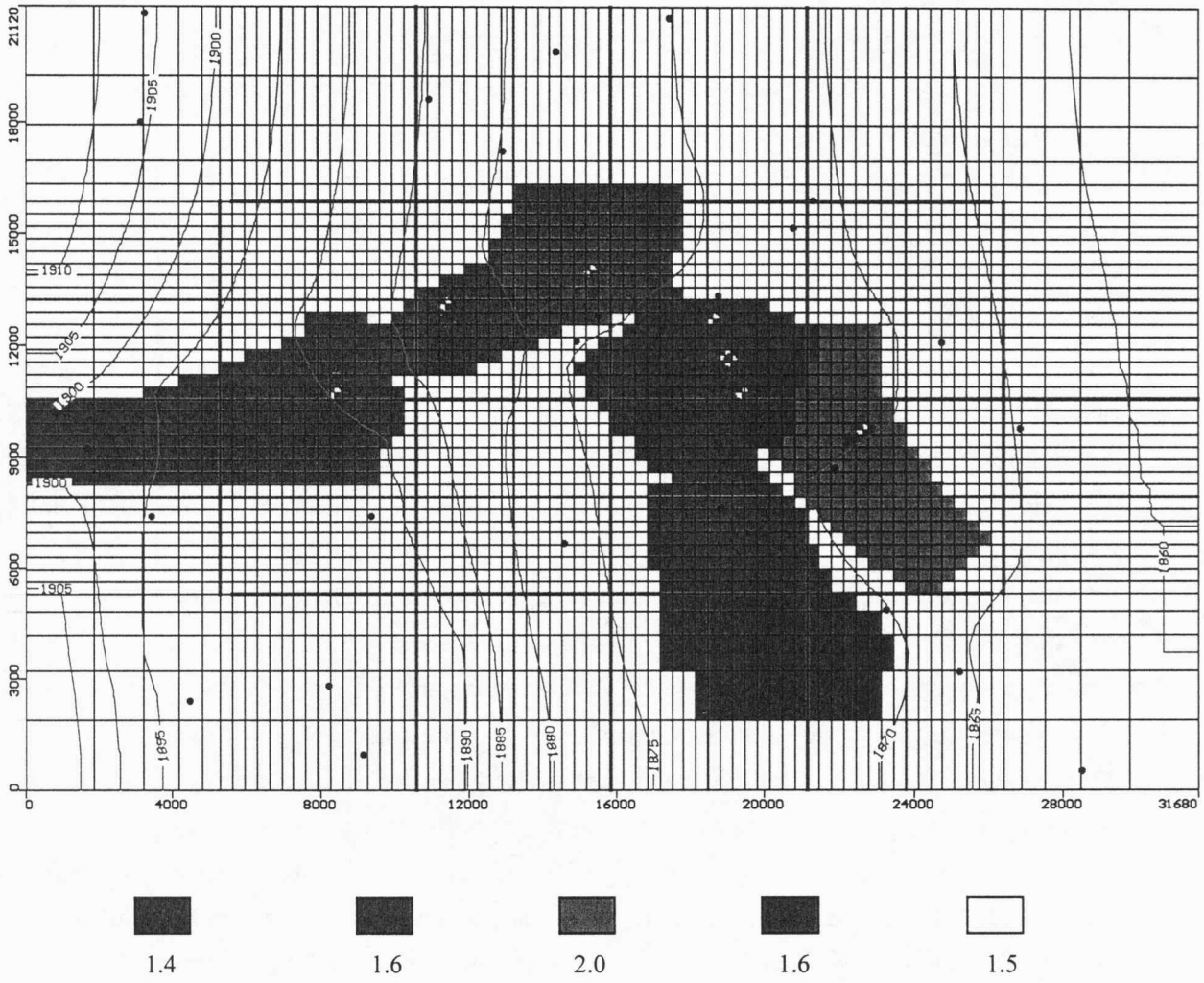

Figure 42. Specific storage of layer 2 in the lobe model. Specific storage in the figure is given as x 10^{-6} ft^{-1}. Layer 1 specific storage is a uniform 1.5 x 10^{-6} ft^{-1}. In the potentiometric surface map, the hydraulic head contour interval is 5 ft.

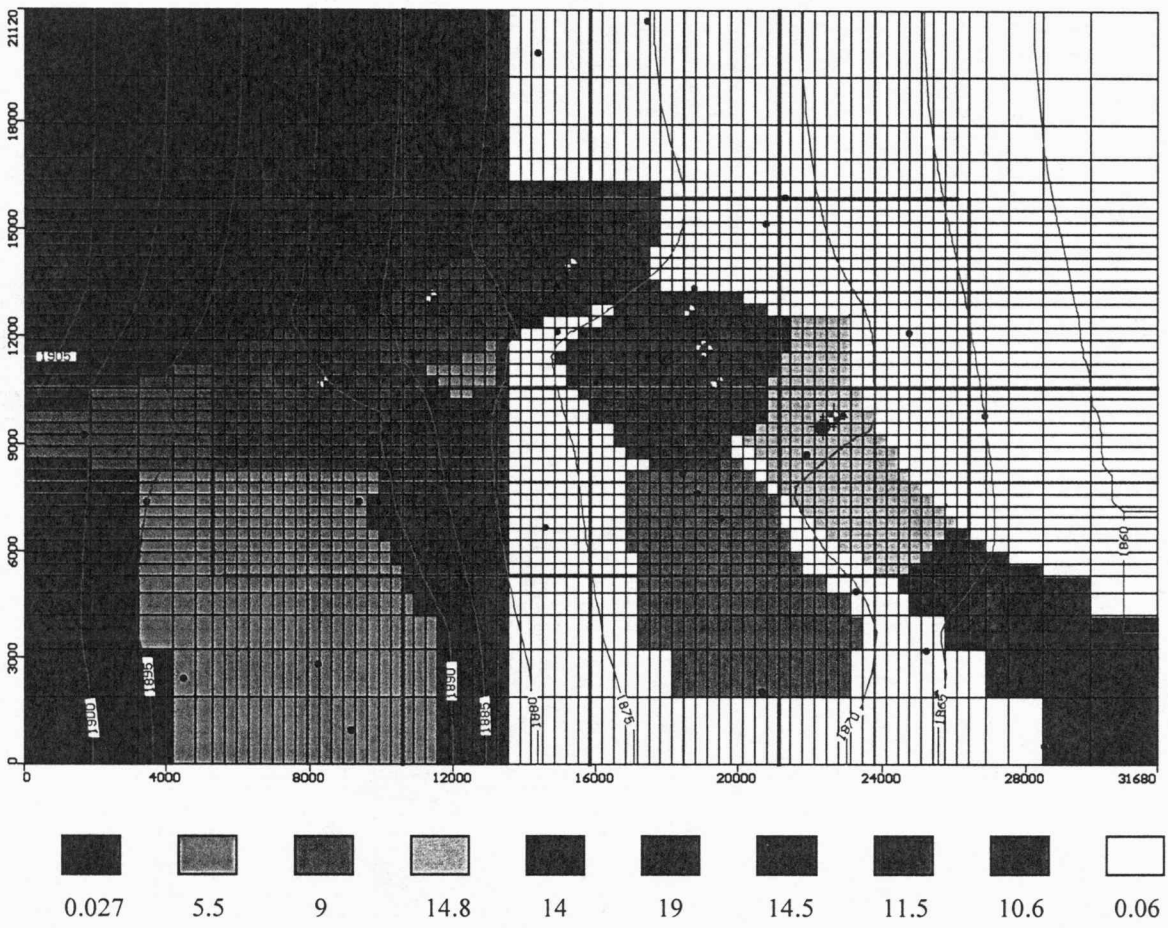

Figure 42 Continued. Hydraulic conductivity and hydraulic head distribution of layer 2 in the modified lobe model. Hydraulic conductivity is in ft/day. The hydraulic head contour interval on the potentiometric surface map is 5 ft.

Figure 43

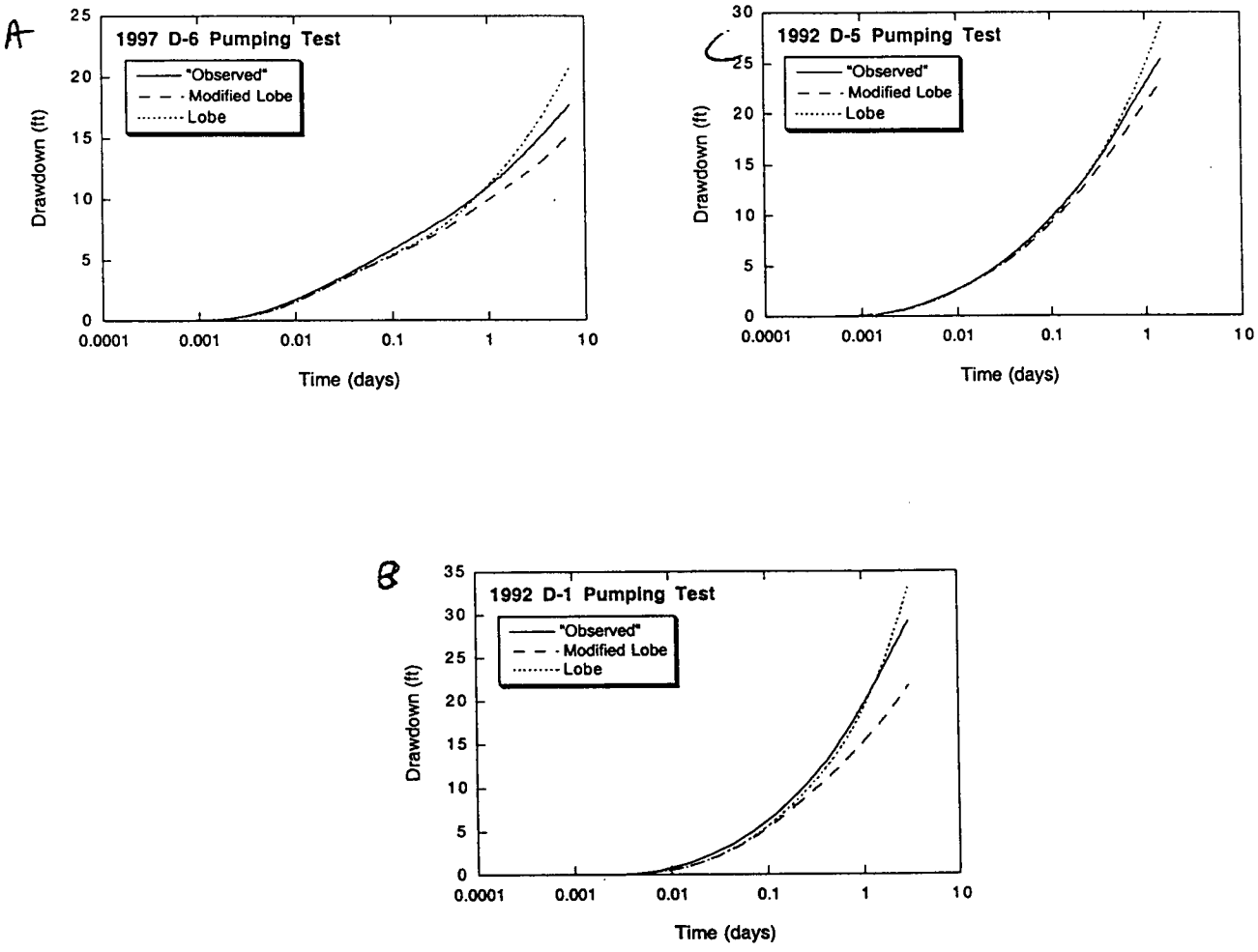

Figure 43. Simulated and "observed" drawdowns from the lobe and modified lobe models at the at the near observation wells in the D-6 (A), D-1 (B), and D-5 (C) pumping tests.

Figure 44

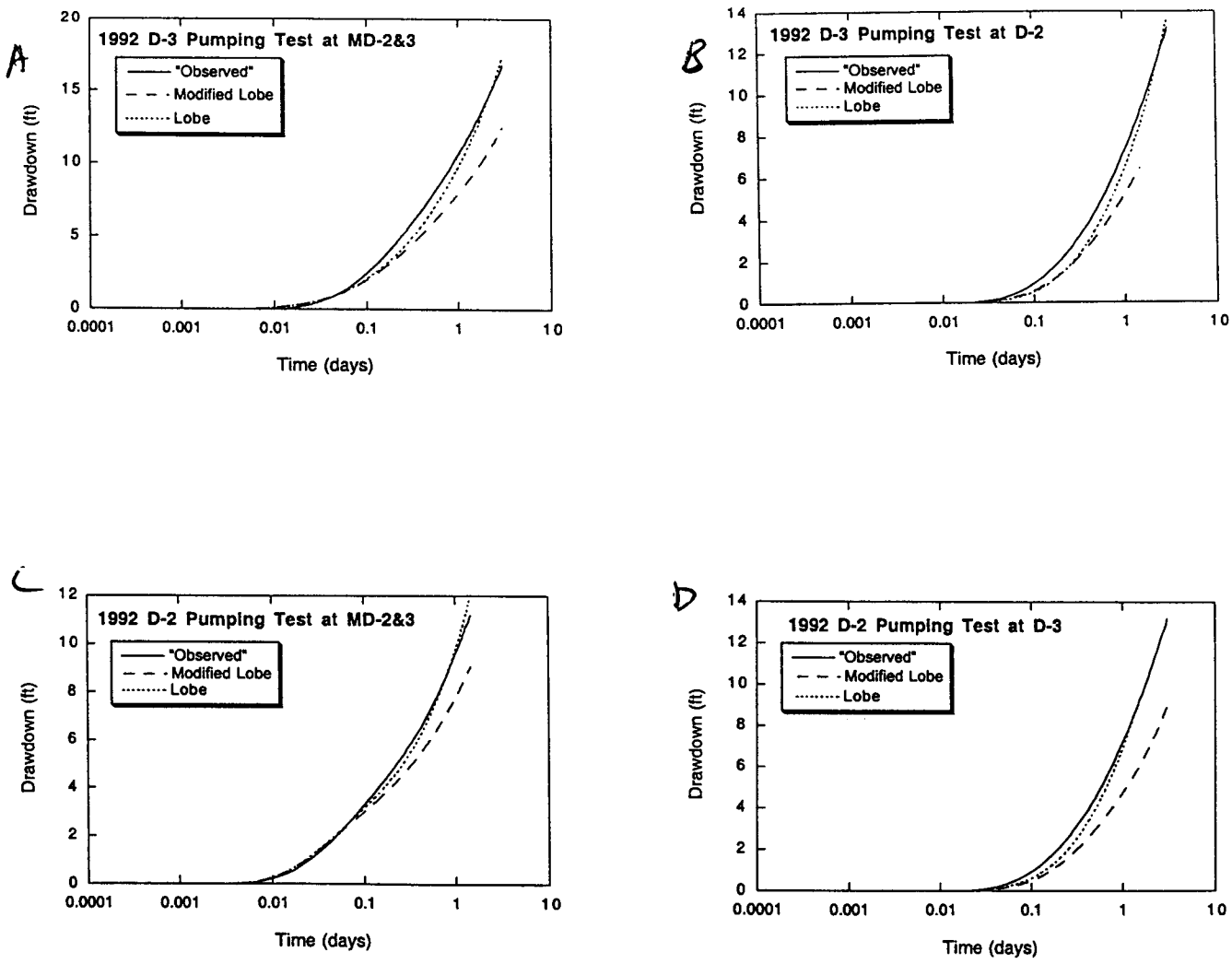

Figure 44. Simulated and "observed" drawdowns from the lobe and modified lobe models at MD-2&3 (A) and D-2 (B) from the D-3 pumping test and MD-2&3 (C) and D-3 (D) from the D-2 pumping test.

Figure 45

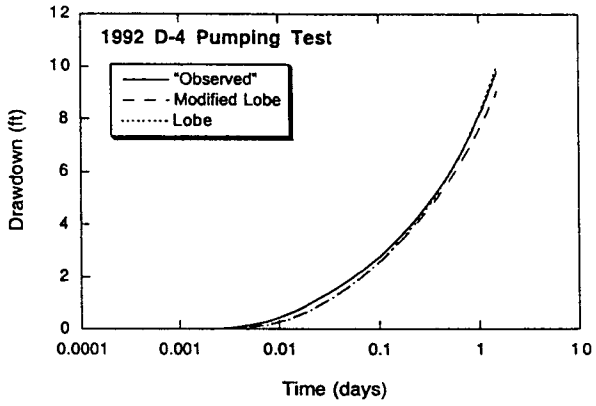

Figure 45. Simulated and "observed" drawdowns from the lobe and modified lobe models at MD-4 from the D-4 pumping test.

Figures 43-45 present the simulated drawdowns from the modified lobe model in comparison to the simulated drawdowns from the lobe model and the "observed" drawdowns generated from SUPRPUMP (Bohling et al., 1990). In all cases, the simulated drawdowns from the modified lobe model are slightly to much less than the simulated drawdowns from either the lobe model or the "observed" drawdowns from each test. The lack of fit begins early in the simulated test results. The drawdown reduction due to the increased mudstone hydraulic conductivity is less in MD-6, MD-5, and MD-4 than in MD-1, MD-2&3, D-2 and D-3 in the central part of the wellfield. A visual comparison of the shapes of the simulated and "observed" drawdown curves suggests that the simulated curves seem to straighten out at later times during the D-6, D-5, and D-4 pumping tests at MD-6, MD-5, and MD-4. The apparent straightening of the simulated drawdown curves seems to mimic the shape of the "observed". Overall, the results from this simulation suggest that a more permeable aquitard could be an additional source of water for at least some of the pumping wells. However, the range of drawdown reductions across the wellfield also suggests that the mudstone hydraulic conductivity could be more variable than was previously thought in this investigation.

Another possibility to explain the lack of fit at late time in these tests is that the assumed aquifer/aquitard properties may not be correct. This would apply not only to the assumed aquifer properties of the sandstones upgradient and downgradient of the wellfield but also to the hydraulic conductivity used to calculate the conductance in the general head boundary conditions. This is particularly problematic because there are no data to guide the estimation of the hydraulic conductivity used to estimate the conductance parameter, C, in the general head-boundary condition. Adjustments to any of these parameters could result in a significant increase in the flow of water to the wellfield during pumping.

Sources of error affecting transient model calibration

Several sources of error undoubtedly affected the calibration process because of the assumptions made in model construction. It was assumed that all of the aquifer heterogeneity could be represented by a model grid with the finest map-view dimensions of 330 ft by 330 ft using the available limited well log and pumping-test results. In most cases, the well log information is not sufficient to characterize the internal structure of the amalgamated fluvial sandstone complexes or the lateral and vertical aquifer extent. Cursory examination of the gamma-ray logs of the pumping and nearby observation wells at many of the wellsites reveals that the sandstone aquifer framework consists of a sequence of amalgamated channel sandstone bodies. Individual sequences of sandstones can be traced between the pumping and observation wells at each wellsite and often between nearby wellsites. The bounding surfaces of these individual sequences are clearly recognizable as kicks on the gamma-ray logs of boreholes

drilled within the wellfield. This local heterogeneity influences the results of pumping tests as indicated above in the case of the D-2 and D-3 tests. The limited test-hole drilling and pump testing performed in the wellfield precludes inclusion of significant local aquifer heterogeneity in the model.

In the development of the hydrogeologic and the numerical models, the aquifer extent in map view was approximated using the sand-fraction distribution map and the results of the pumping tests. None of the test-hole drilling done by the city was directed to defining aquifer extent. Thus for the most part, it has been assumed that the aquifer extent as determined from the pumping tests is correct because it is consistent with what we believe the sand fraction distribution to be. In Volume 1 of this report, it was noted that the analysis of the D-3 pumping test was complicated, in part by what was believed to be the very close proximity of the production well to the aquifer boundary. Test drilling had not been done to locate the sandstone aquifer/mudstone aquitard boundary to the north. Problems were encountered in analyzing the drawdown data from this test that necessitated simultaneous estimation of the boundary location and the local hydrologic properties. This was accomplished by minimizing the error between the observed and SUPRPUMP (Bohling et al., 1990)-generated drawdowns. As a result, there is additional uncertainty in the flow-boundary location and the local hydrologic properties from this test. As another limitation, the complexity of the mudstone aquitard-sandstone aquifer boundary is simplified in the models. This boundary is treated as a vertical boundary within each model which does not take into account the local irregularity of the boundary which may have a significant effect on drawdown during pumping.

The lack of information on the hydrologic properties of the aquitard and the aquifer outside of the wellfield led to the necessity to assume what appear to be reasonable values for these properties. The lack of drawdown data from the pumping tests or long-term water-level records from monitoring wells outside of the wellfield hampered evaluation of these choices and the calibration of the transient model for these properties. With regard to model calibration, the assumed low hydraulic conductivity coupled with the low specific storage of the mudstone may have prevented significant leakage of water from the mudstone during pumping. This may cause the poor fit of the simulated to the observed drawdowns in the later segments several of the pumping tests.

Chapter 6: Verification of the Transient, Lobe Conceptual Model

Model verification

Model verification is a way to establish greater confidence in the simulation results from a model by using a set of calibrated parameter values and stresses to reproduce a second set of field data (Anderson and Woessner, 1992). Spitz and Moreno (1996) indicate that this procedure is a shortcut to gaining greater confidence in model predictions in the absence of uncertainty analyses. They state further that in the absence of verification, a model is untested beyond the exact conditions used in the calibration, and the use of the model to make other than general predictions is questionable.

At this stage of the project, neither the lobe nor the fringe conceptual transient model appears to be adequate to the task of fully simulating the hydrogeology because the models do not correctly simulate the later drawdown histories from each of the pumping tests. The numerical models generated in this project are based on extremely limited geologic and hydrologic data from the entire model region. In particular, the hydrologic data come almost entirely from the central region of the model grids representing the immediate wellfield area. The absence of data from outside the wellfield introduces considerable uncertainty in the model calibration process. This inability to perform adequately stems from either unknown additional sources of water that are not simulated or incorrect model parameters. Model verification is used here to demonstrate that the model in its present form is not a suitable tool to be used by the city to address its planning and management needs.

Water production history

Since pumping began in early April, 1993, the wellfield has been in nearly continuous operation punctuated occasionally by periods of shutdown. By early June, 1999, a total of approximately 162.6 million gal (21.7 million ft^3) of water had been produced from the production wells in the field. As noted in Volume 1 of this report, the records of daily pumpage provided by the city indicate three distinct periods of pumping: April-July, 1993; February, 1994-July, 1997; and January, 1998-June, 1999. The first pumping period lasted a total of 92 days, the second 1,252 days and the third 519 days. Between the first and second periods of pumping the wellfield was shutdown for 229 days and between the second and third periods, wellfield shutdown lasted for 153 days (Figure 46).

In the first period of pumping the majority of the wells were pumped on any given day. Only D-3 was shutdown for longer than two days (Table 3). Early in the first pumping period the wellfield water production exceeded 500,000 gal/day (Figure 46), but declined later in the

Figure 46

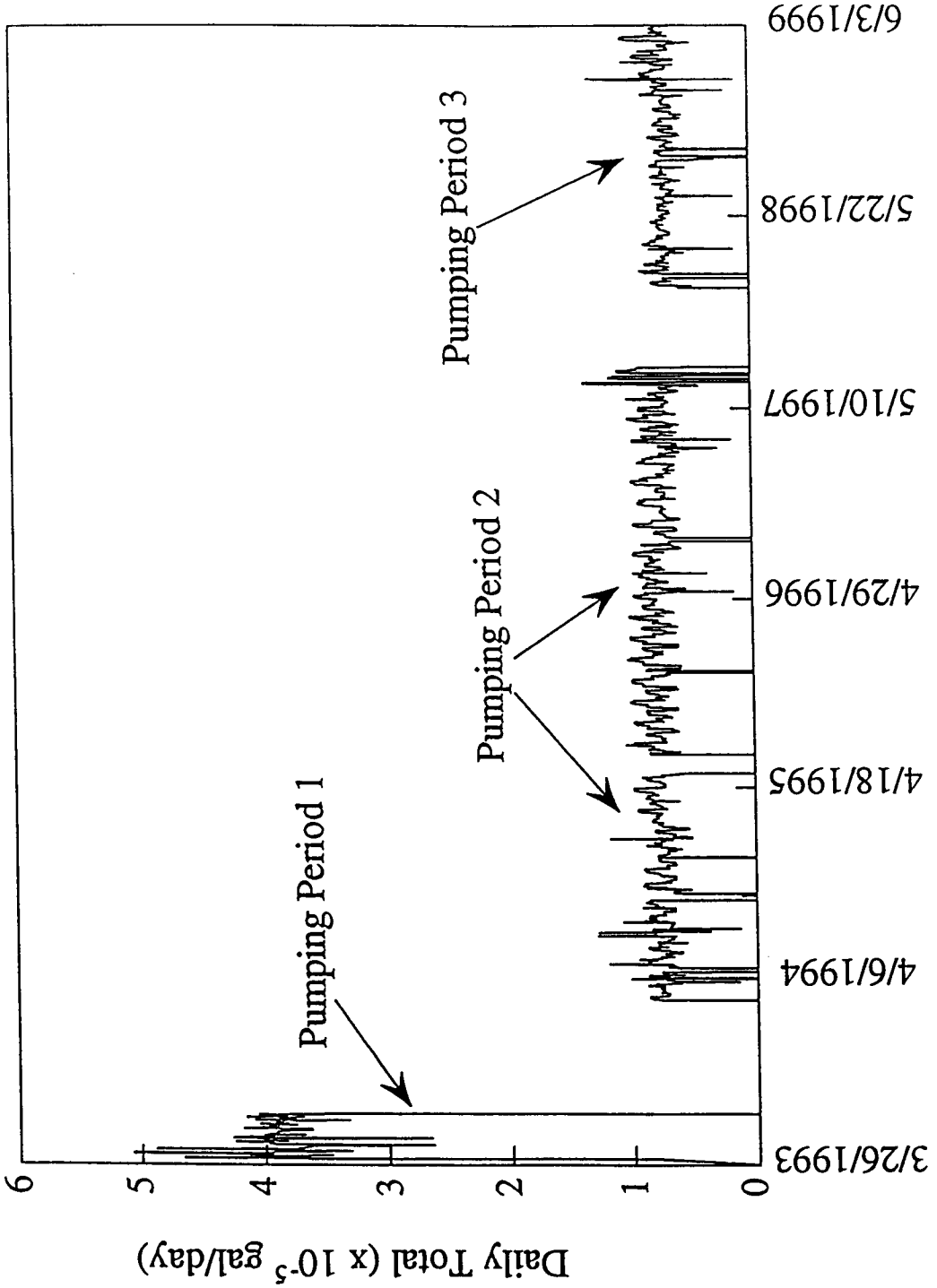

Figure 46. Daily total ground-water withdrawals from the Hays wellfield in the upper Dakota aquifer. The wellfield production history can be subdivided into three pumping periods separated by periods of wellfield shutdown.

period and stabilized at slightly less than 400,000 gal/day. Total daily pumpage from the wellfield ranged from a low of 81,000 to a maximum of 507,164 gal and the total mean daily

Table 3. Production history from the Hays Dakota wellfield for the period April 7-July 7, 1993.

Well	Number of Days Pumping	Min. Daily Pumpage (gal)	Max. Daily Pumpage (gal)	Mean Daily Pumpage (gal)	Total for the Period (gal)
D-1	90	7,599	149,697	64,595	5,813,524
D-2	90	3,897	126,202	62,897	5,660,696
D-3	89	5,901	106,597	64,701	5,758,390
D-4	90	897	201,600	70,400	6,336,041
D-5	90	299	104,196	59,136	5,322,227
D-6	90	5,901	117,697	72,277	6,504,965
				Grand Total	35,395,843

pumpage was 384,740 gal or approximately 267 gal/min (35.7 ft^3/min). The total withdrawal from the aquifer for this period was 35,395,843 gal (108.6 acre ft)

In the second pumping period from February, 1994-July, 1997, only one well was pumped at a time and production was rotated between wells every 5-7 days. When the field was in operation during this period, D-1 was pumped approximately 22.1%, D-2 15.6%, D-3 13.4%, D-4 19.6%, D-5 20.3%, and D-6 20.9% of the time (Table 4). Total daily pumpage ranged from a low of 4,200 gal to a maximum of 135,300 gal when the pumps were operating, and the mean daily withdrawal from the aquifer was 77,519 gal (Figure 46). The total volume pumped from the field during this period was 91,251,774 gal (280 acre-ft) or an average pumping rate of 50.61 gal/min (6.77 ft^3/min).

The third interval of pumping began after a 4 month well recovery period following the 1997 pumping tests, beginning on January 1, 1998, and continuing up to the writing of Volume 1 (June 3, 1999). As in the second pumping period, individual wells were pumped on a 5-7 day rotating basis and only one well was pumped at a time. When the field was producing water, D-1 was pumping approximately 20.4%, D-2 20.8%, D-3 16.2%, D-4 21.2%, D-5 21.4%, and D-6 21.4% of the time (Table 5). The maximum and minimum daily withdrawals were 130,800 gal and 7,200 gal, respectively, and the mean withdrawal rate was 70,424 gal/day or an average pumping rate of 48.91 gal/min. The total pumpage from the field for this period was 35,845,705

gal (110 acre-ft). The total daily withdrawals from the field varied little with time in this period as indicated by the data in Figure 46.

Table 4. Production history from the Hays Dakota wellfield for the period February 22,1994-July 31, 1997.

Well	Number of Days Pumping	Min. Daily Pumpage (gal)	Max. Daily Pumpage (gal)	Mean Daily Pumpage (gal)	Total for the Period (gal)
D-1	277	200	108,300	62,389	17,281,806
D-2	195	100	91,300	65,669	12,805,498
D-3	168	100	90,200	64,833	10,891,999
D-4	246	200	111,998	74,764	18,392,040
D-5	254	100	128,199	62,883	15,972,304
D-6	262	100	135,300	60,718	15,908,127
				Grand Total	91,251,774

Table 5. Production history from the Hays Dakota wellfield for the period January 1, 1998-June 3, 1999.

Well	Number of Days Pumping	Min. Daily Pumpage (gal)	Max. Daily Pumpage (gal)	Mean Daily Pumpage (gal)	Total for the Period (gal)
D-1	106	100	130,800	57,611	6,106,802
D-2	108	100	88,200	50,995	5,507,505
D-3	84	200	79,433	57,589	4,837,498
D-4	110	100	103,200	59,024	6,492,699
D-5	111	100	79,100	58,433	6,486,102
D-6	111	100	86,667	57,794	6,415,099
				Grand Total	35,845,705

The model verification process

Model verification was carried out on the calibrated, transient, conceptual lobe model. The input data set to this model consisted of the pumping schedule and rate history of the wellfield taken from the water production history supplied by the city. Since the pumping periods were tallied as days in the data supplied by the city, each time step in this transient model run was one day in length. Also, daily withdrawal rates for each well were determined from the total amount of water withdrawn during pumping and the number of days the well was producing water during a given pumping period. Following the model run, the simulated daily drawdowns (drawdown during pumping and residual drawdown during recovery periods) for the 5 yr pumping period at the monitoring wells were plotted and compared qualitatively to the observed drawdown data set from the same period.

The model verification drawdown data set

Figures 47-51 present the observed drawdown histories for the monitoring wells (MD-6, MD-5, MD-1, MD-2&3, and MD-4) in the wellfield. The observed drawdowns are calculated data from water-level measurements made in the field. The observed drawdowns do provide a benchmark that can be used to assess the history-matching ability of the lobe model.

Results and evaluation of the 5 yr simulation

Figures 47-51 also present the simulated drawdowns at the monitoring wells from pumping of the production wells over the 5 yr period. Overall, the simulated drawdowns are much higher than the observed drawdowns from pumping at all of the observation wells. In the first pumping period with the highest production rates, the simulated drawdown is 50 ft more than was observed at MD-6 and MD-5; almost 50 ft more than was observed at MD-1; and nearly 40 ft greater than was observed at MD-2&3 and MD-4. In the second and third pumping periods with much lower production rates, the simulated drawdowns are approximately 20 ft greater than was observed in MD-6 and MD-5 and between 10 to 20 ft greater than was observed in MD-1, MD-2&3, and MD-4.

Figures 52-54 show the drawdown pattern in the model region at three different times during its nearly 1,600 days of production history. Figure 52 shows the simulated drawdown in the wellfield at the end of the 89th day of production history near the end of the high production rate period. Drawdowns exceeding 50 ft occur in an area that extends to the mudstone/sandstone aquifer and mudstone/fringe boundaries. The 5 ft drawdown contour extends beyond the edge of the model indicating that the cone of depression has reached the edge of the model. Likewise, during the lower production rate periods (700 days and 1,500 days after the beginning of water production), drawdowns exceeding 10 ft occur in an area that extends to the edge of the

Figure 47

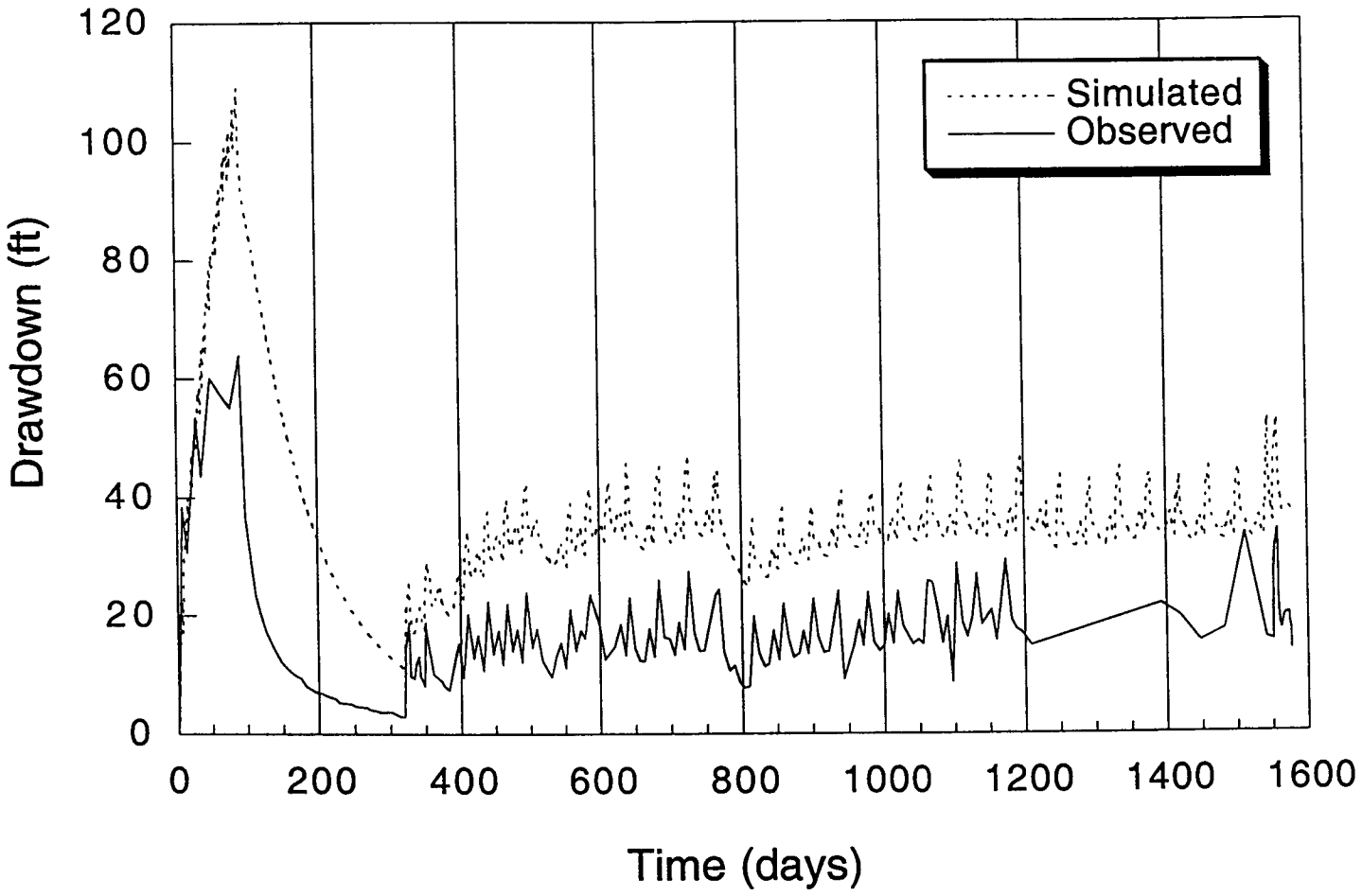

Figure 47. Simulated and observed drawdowns during the nearly 5 yr pumping period within the wellfield at MD-6.

Figure 48

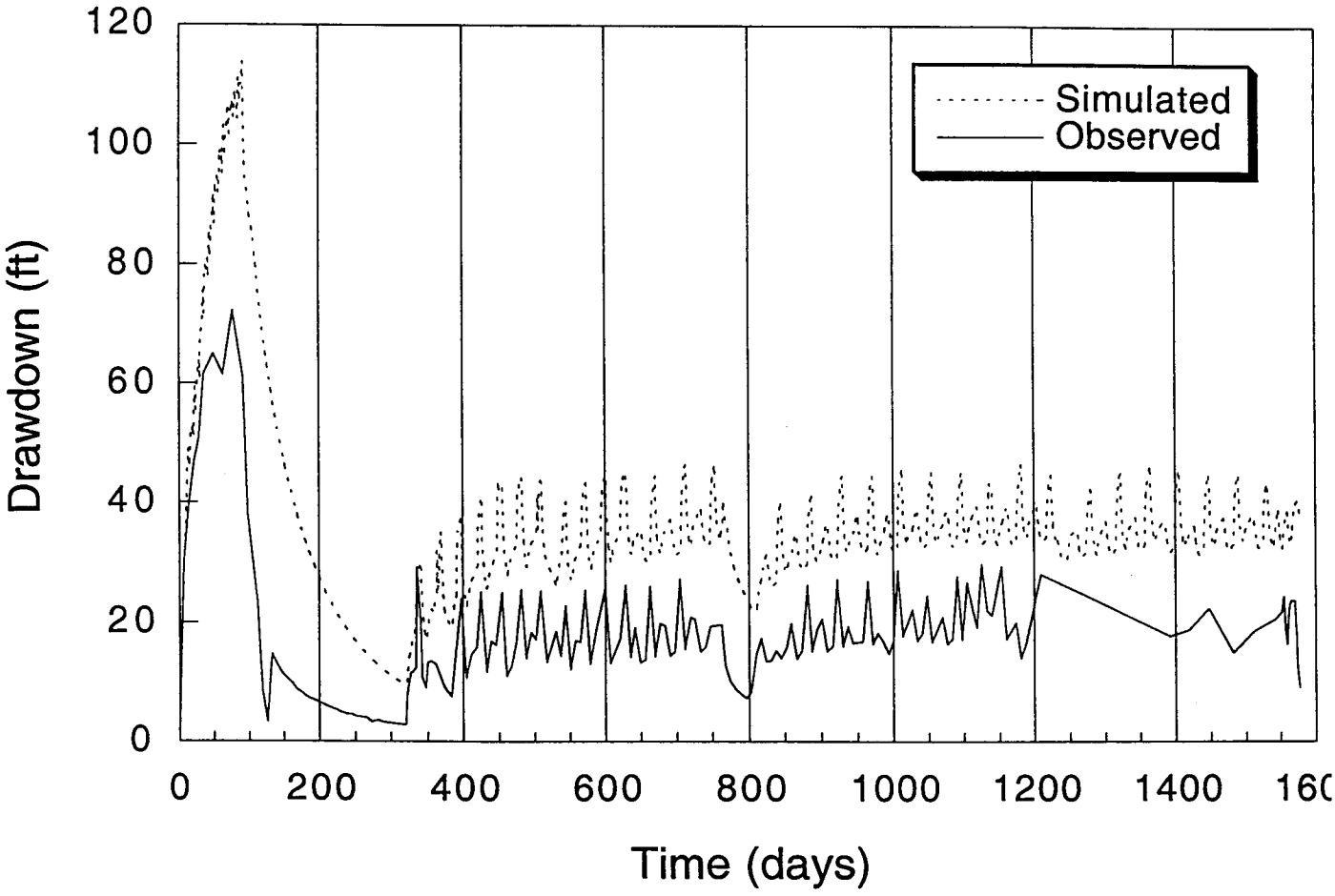

Figure 48. Simulated and observed drawdowns during the nearly 5 yr pumping period within the wellfield at MD-5.

Figure 49

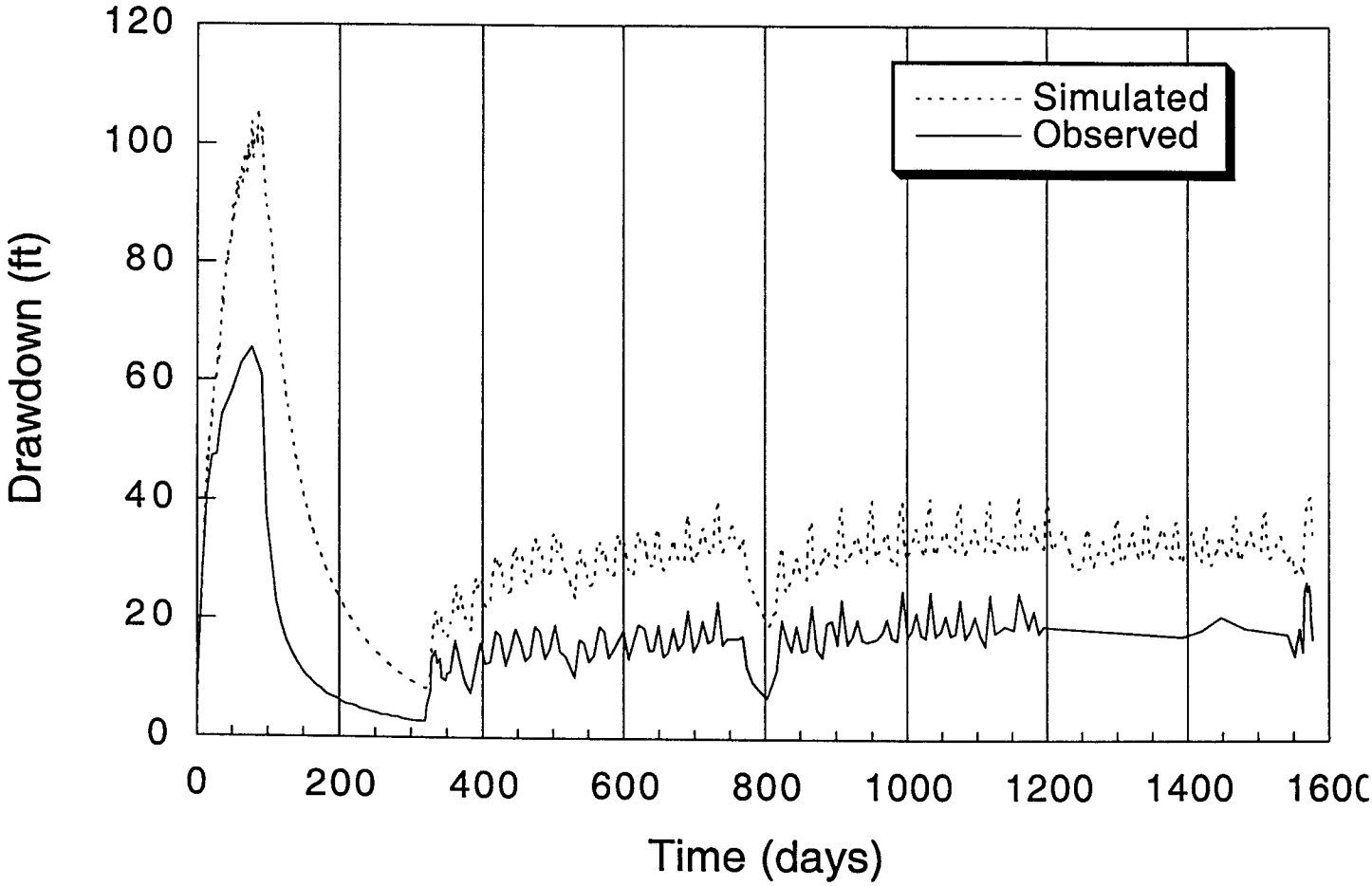

Figure 49. Simulated and observed drawdowns during the nearly 5 yr pumping period within the wellfield at MD-1.

Figure 50

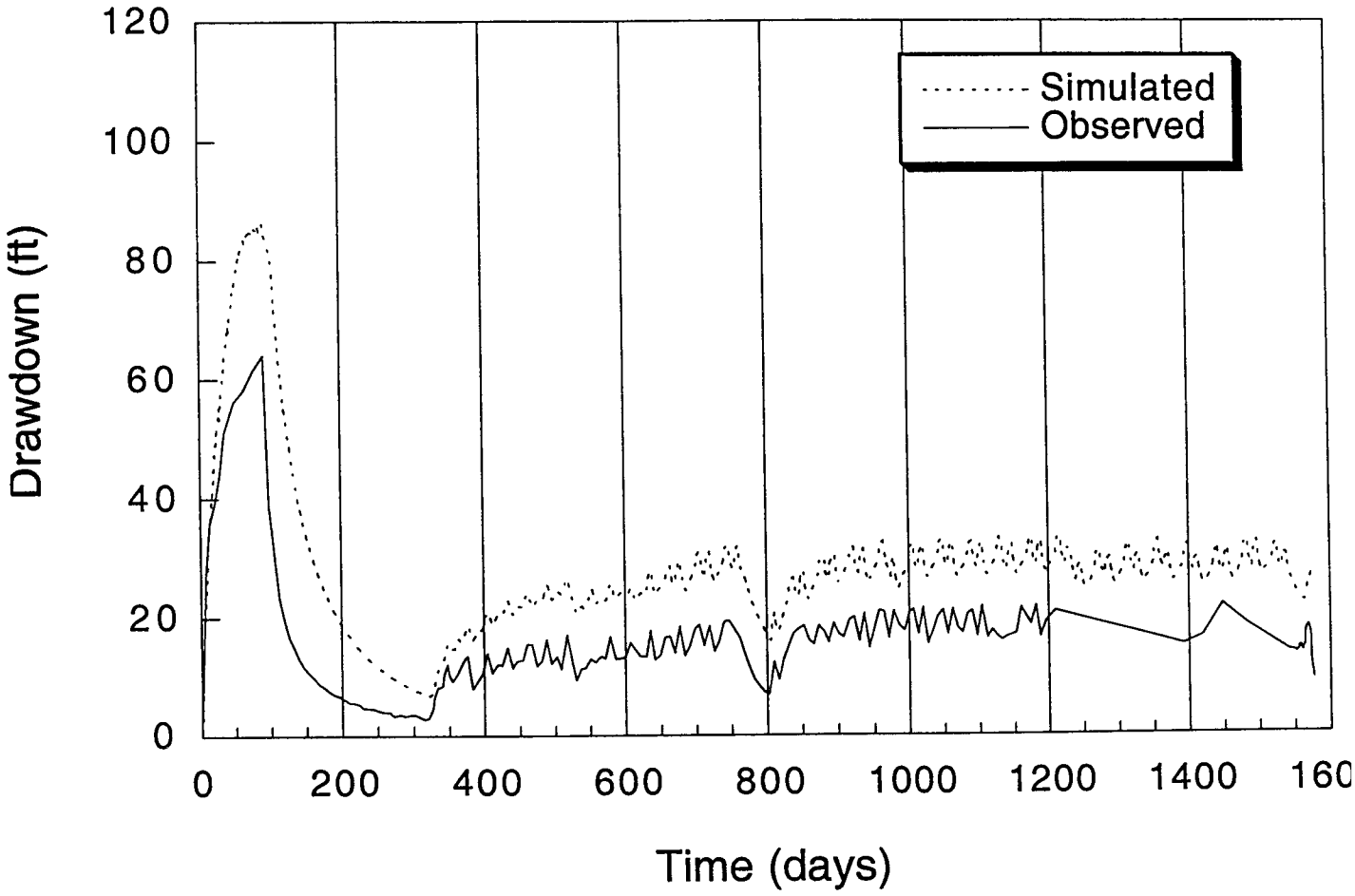

Figure 50. Simulated and observed drawdowns during the nearly 5 yr pumping period within the wellfield at MD-2&3.

Figure 51

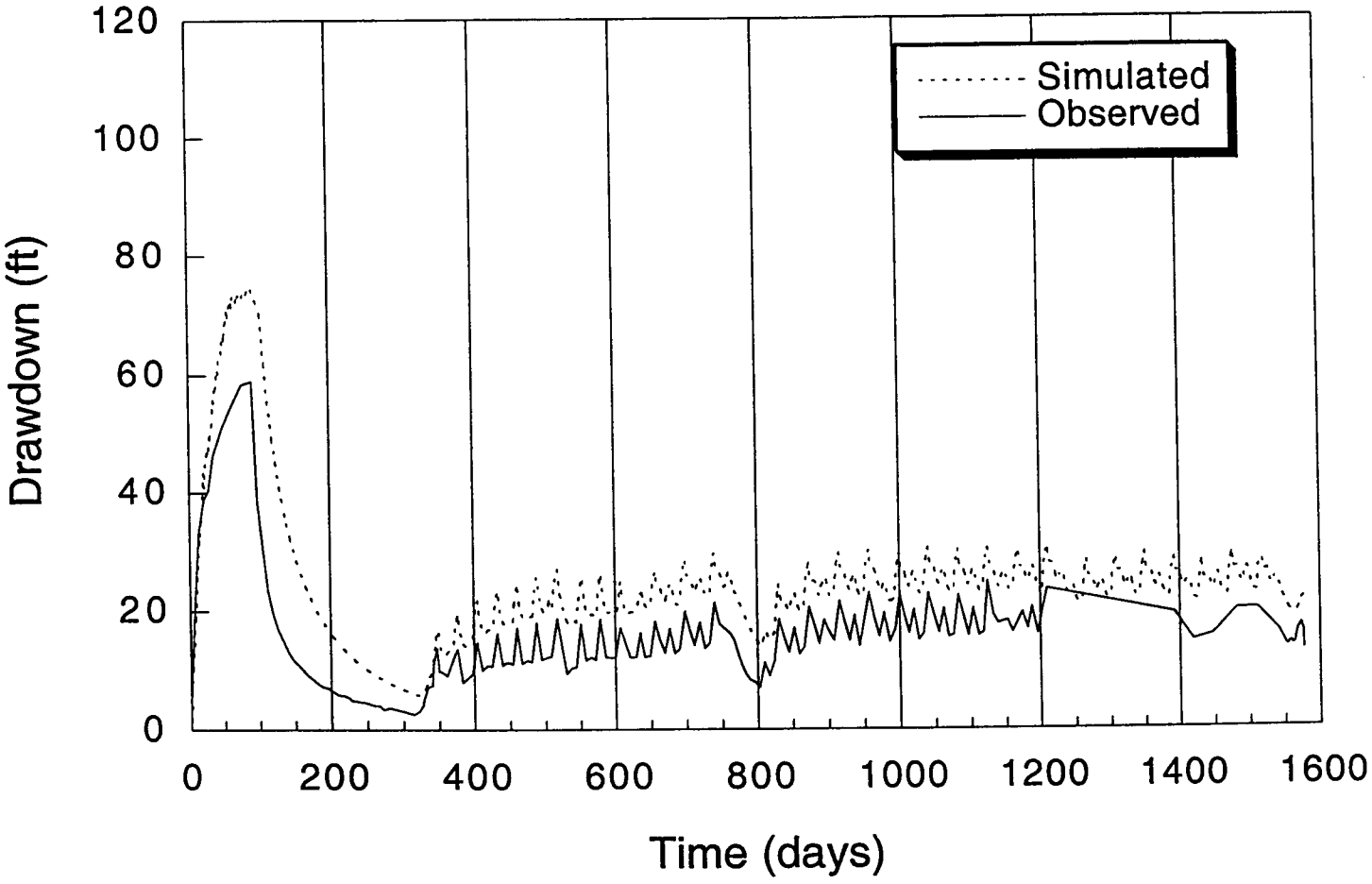

Figure 51. Simulated and observed drawdowns during the nearly 5 yr pumping period within the wellfield at MD-4.

Figure 52

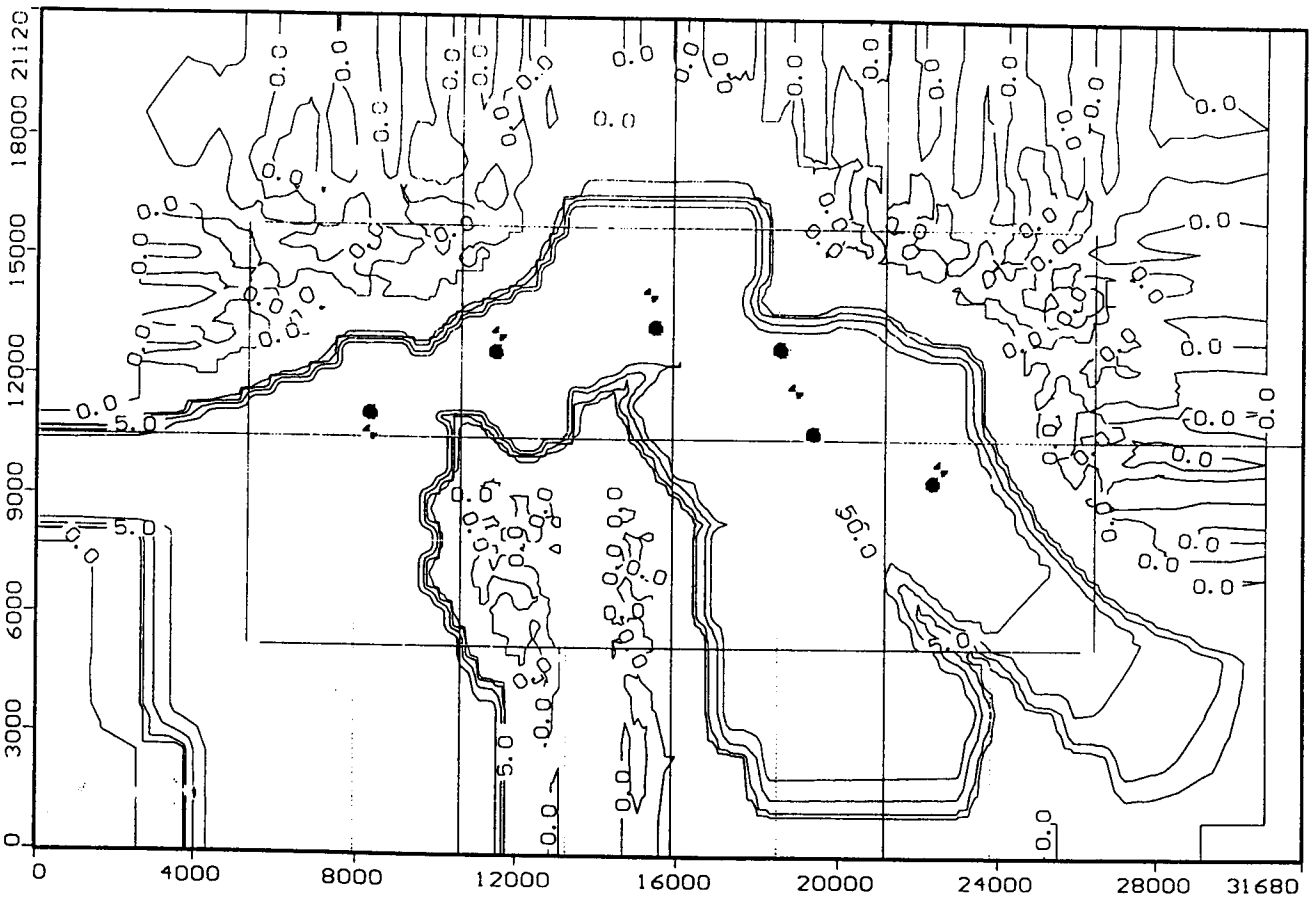

Figure 52. Simulated pattern of drawdown after the 89th day of wellfield operation.

Figure 53

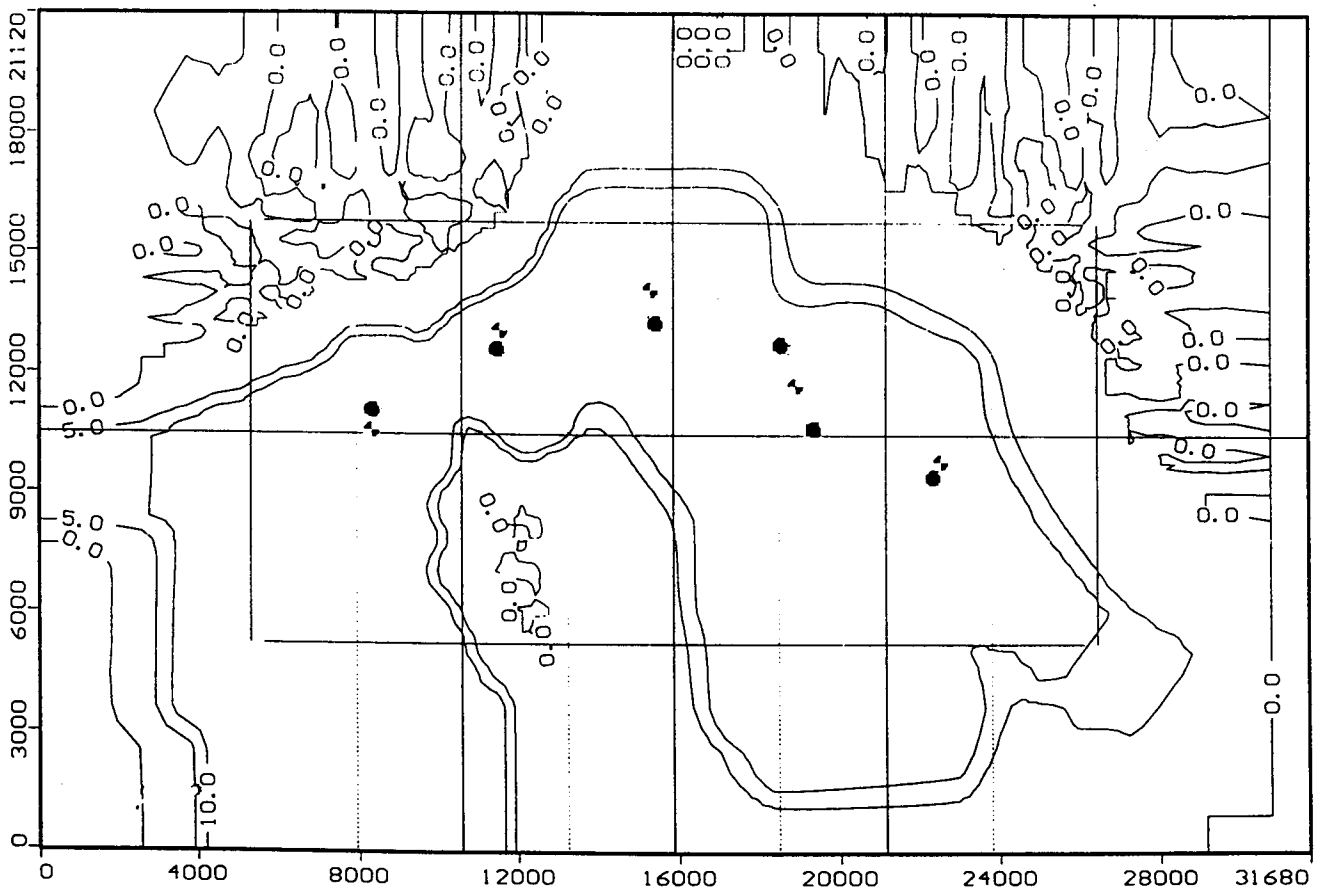

Figure 53. Simulated pattern of drawdown after the 700th day of wellfield operation.

Figure 54

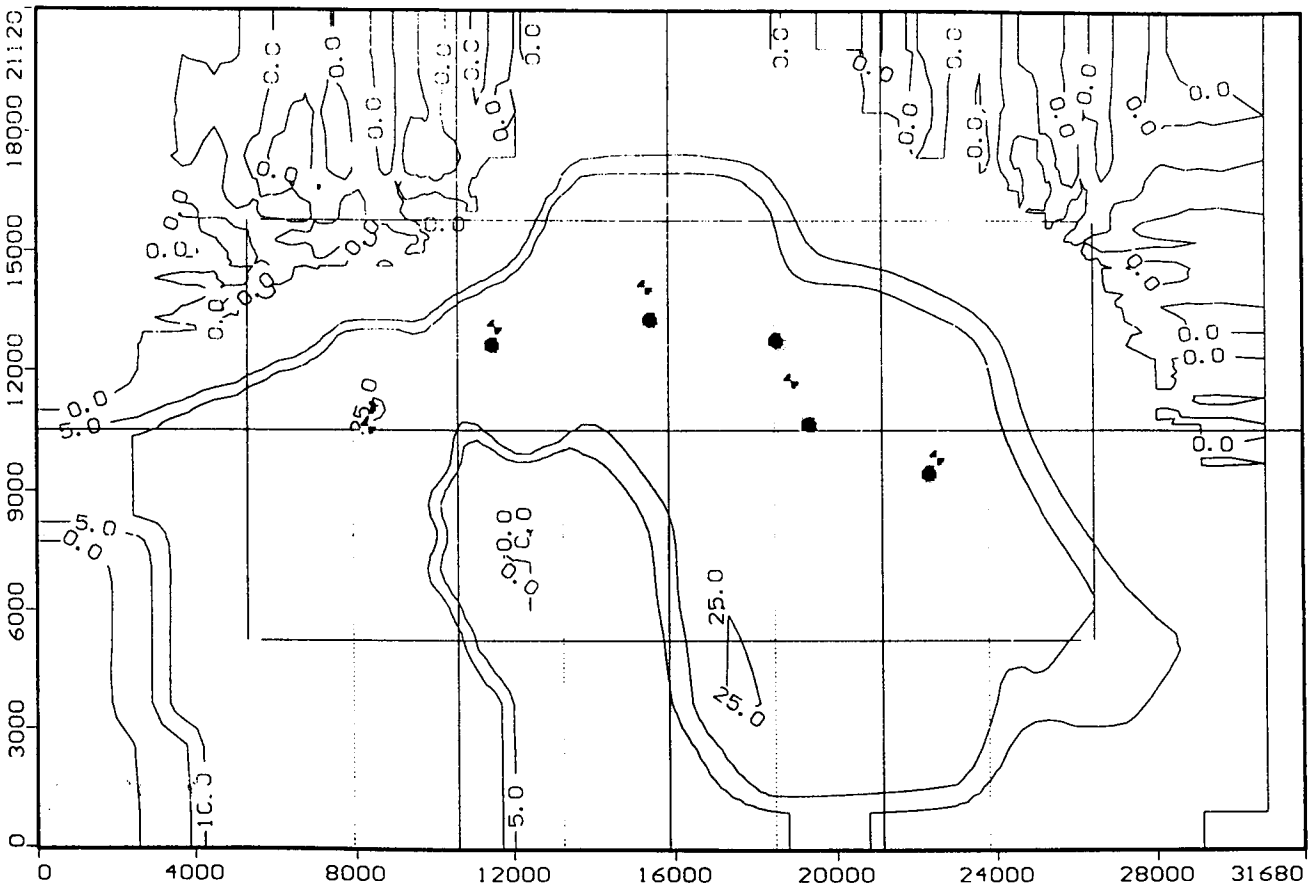

Figure 54. Simulated pattern of drawdown after the 1500th day of wellfield operation.

permeable deposits (Figures 53 and 54). Additionally, at the west end of the model the cells representing the channel sandstone aquifer show drawdowns that exceed 5 ft. This indicates that even under low pumping regimes, the cone of depression from long term pumping extends at least to the west edge of the model.

As in the previous chapter, the much higher than observed drawing down of the potentiometric surface throughout the wellfield during the pumping period suggests that not enough water is getting to the wellfield to sustain the potentiometric surface at the observed levels during pumping. One explanation for this failing of the model is that the calibrated set of parameters may not accurately represent the hydrologic properties of the aquifer or the aquitard or significant aspects of the local hydrogeology are not being simulated by the model (Anderson and Woessner, 1992). Consequently, the calibrated model would not accurately represent the flow system under the imposed hydrologic stresses of the 5 yr pumping.

It is clear that the current conceptual transient model can not be used to provide an assessment of the city's management/planning options with regard to the upper Dakota aquifer. The size of the modeled area needs to be increased to avoid the possibility that the cone of depression might impinge on the model boundaries and be influenced by them (Anderson and Woessner, 1992). It is possible that by accounting for additional sources of water the need to enlarge the model area may be unnecessary because of the overall reduction in drawdown and possibly the size of the coalesced cone of depression at the lower rates of pumping. However, in a future model that would be used to evaluate the consequences of increased production rates for longer periods of time, a model of a much larger area of the aquifer coupled with a different model grid design would be needed to eliminate the possibility of the model boundaries having an impact on the simulated drawdowns.

Chapter 7: Recommendations for Future Work

On the basis of the data collection, analysis, and preliminary modeling of the upper Dakota aquifer we make the following recommendations. The data analysis in the Volume 1 report and the numerical modeling to date indicate that more data are needed before an assessment can be made of the impact of future pumping on the aquifer and surrounding users. This additional information will be particularly important if the city wishes to increase its annual water appropriation from this source. The most recent modeling effort clearly demonstrates the need for (1) hydrologic properties data on the sandstones outside of the wellfield as well as the mudstones, (2) improved assessment of the hydraulic connection between Subunit 2 and Subunit 3 sandstone bodies, and (3) drawdown data from monitoring wells outside of the wellfield under a variety of pumping conditions. All of this information is needed to produce more realistic conceptual hydrogeologic and predictive numerical models.

Test drilling is needed to further define (1) the aquifer-mudstone boundary and the nature of that transition and (2) the characteristics of the interbedded sandstone and mudstone that characterizes the fringe zones incorporated in the numerical models of the wellfield vicinity. Currently, the well control used to define sandstone aquifer extent near the wellfield is poor. In the models we have assembled, a relatively large subregion of what we think is fringe is located southwest of wellsite 6. In this large fringe zone, both the extent and the sandstone fraction are largely unknown from the existing subsurface geology information. It is recommended that three transects of test holes should be drilled to further define the stratigraphic relations between the mudstone, the fringe and the sandstone bodies in Subunits 2 and 3 of the Dakota Formation. The proposed transect locations and test hole drilling sites within each transect are indicated on Figure 55.

Additional monitoring wells should be constructed at locations outside of the wellfield to collect additional water-level and water-chemistry data over time as the production wells are pumped by the city. This new data will allow an evaluation of the response of the aquifer to pumping outside of the wellfield. In the current models, there are no data from areas outside of the wellfield with which to improve the conceptual hydrogeologic or the numerical models. With the acquisition of this information, it may be possible to select the best hydrogeologic model of the aquifer and produce a better numerical model of the wellfield that would reproduce the existing and future data sets from the monitoring network.

A minimum of 5 new monitoring sites should be constructed (Figure 55). One monitoring well should be located near each of the following three locations: N1/2, N1/2, Sec 21, T. 14 S., R. 19 W.; SW corner, Sec. 27, T. 14 S., R. 18 W.; and in the center of the south line, Sec. 1, T. 14 S., R. 19 W. These wells should be screened through the entire thickness of the sandstone in

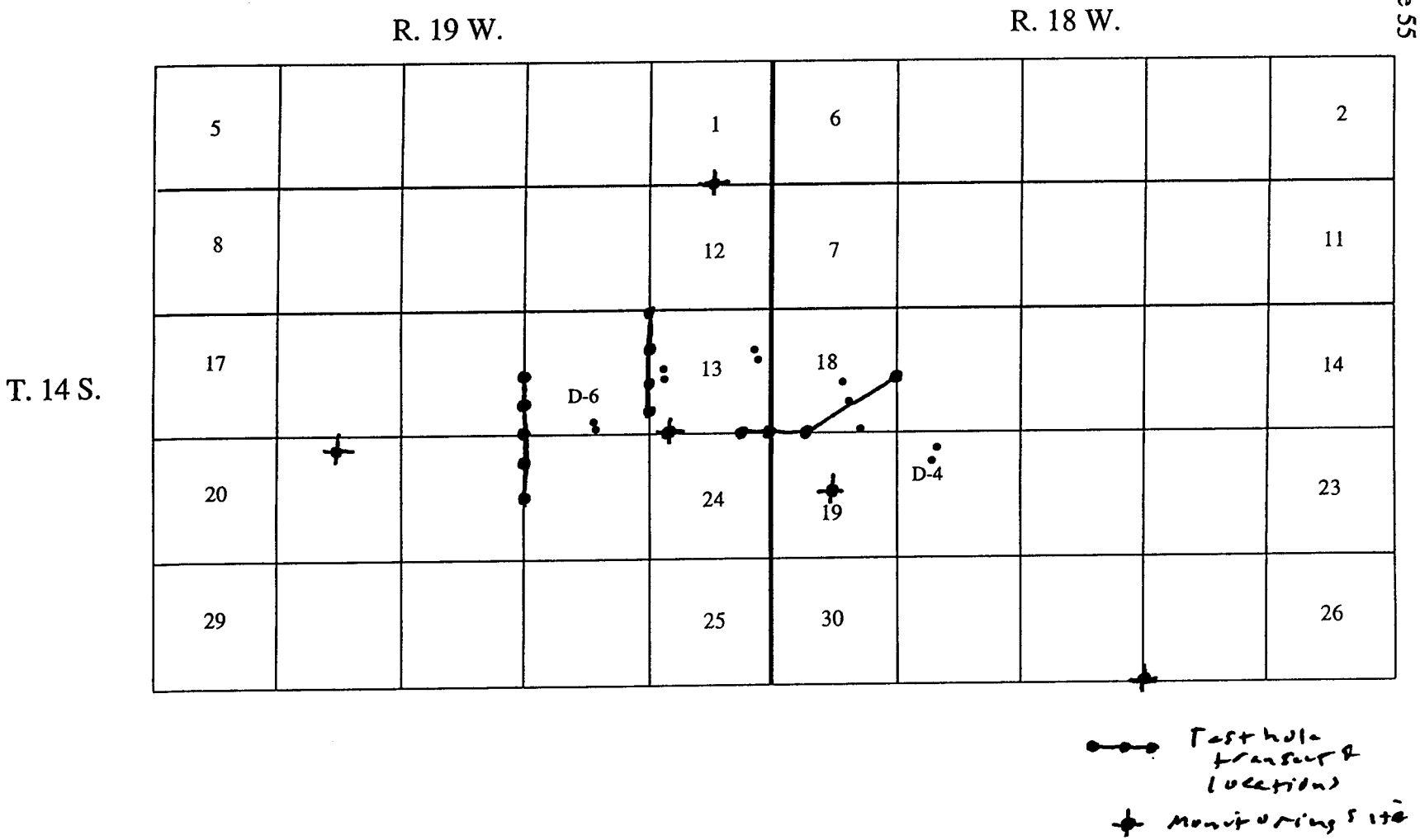

Figure 55. Proposed test-hole drilling transect locations in and around the wellfield and the monitoring well site locations.

Subunit 2 of the Dakota Formation. The fourth and fifth monitoring wells should be located in the SE corner SW, SW, SW, Sec. 13, T. 14 S., R. 19 W. and near the center of Sec. 19, T. 14 S., R. 18 W. These wells should be screened through the entire thickness of sandstone in Subunit 3 of the Dakota Formation. The proposed monitoring wells in Sec 21, T. 14 S., R. 19 W.; Sec. 27, T. 14 S., R. 18 W.; and in Sec. 1, T. 14 S., R. 19 W. are located approximately 2 miles away from the wellfield and will be used to assess the far field response of the aquifer to pumping. The proposed monitoring well in Sec. 13, T. 14 S., R. 19 W. will be used to assess the importance of leakage from fringe deposits in Subunits 2 or 3 to the overlying sandstone aquifer in Subunit 2. The proposed monitoring well in Sec 19, T. 14 S., R. 18 W. would provide drawdown data from what appears to be hydraulically connected sandstones in Subunit 3 of the Dakota Formation.

After the drilling of the test holes and prior to installation of each monitoring well, API-calibrated gamma-ray, SP, and induction log suites should be run in each borehole to collect additional borehole geophysical log data, estimate water quality, and in the case of the monitoring wells, determine well-screen and gravel-pack intervals. Considerable care will need to be exercised in the installation and development of each well. Prior to installation, the borehole will need to be thoroughly circulated to remove the accumulated fines from the drilling. Also, the driller should be cautioned to drill with clear water without use of synthetic polymers. The use of polymers will only make later well development more difficult. Additionally, if slug tests are used to estimate local hydraulic conductivity, well skin effects due to the polymers may bias the results of these tests. Prior to and at the end of well development, water levels should be recorded referenced to the top of the casing. Water samples should be collected following well development.

The water levels in these new observation wells should be monitored continuously using pressure transducers and data-logging equipment to record the effects of pumping in the well field over a period of at least one year. In addition, the city will need to purchase a recording barometer to keep track of atmospheric-pressure fluctuations over time. This will be particularly important for interpreting the water-level fluctuations in the more distant wells in the monitoring network.

City personnel should continue monitoring water levels in the pumping and observation wells and collecting water samples for analysis. It should be noted that even though the city has continued to monitor water levels over time, the frequency of monitoring is now much less than what it was back when the well field was first installed. Weekly water-level measurements from the pumping and observation wells in the field should adequately provide the data needed for further model calibration should the city decide to collect additional data to support an increase in its annual appropriation. The water quality samples will provide useful information on mixing

of water masses and may signal important changes in the system over time. As a result, it will be important for the city to contract analytical services with a laboratory that can produce results with the appropriate level of accuracy and reproducibility.

This new water-level and water-chemistry data set should be analyzed to reevaluate and reformulate the existing conceptual hydrogeologic model of the upper Dakota aquifer. This will involve an analysis of the water-level response in these wells to prolonged pumping from the field, perhaps at a number of different levels of production. Most importantly, the data from these wells should provide the needed information to assess leakage effects and vertical hydraulic connection between sandstone aquifers in Subunits 2 and 3 of the Dakota Formation.

The revised conceptual hydrogeologic model will be used as a basis for assessing the conceptual numerical model simulations to date and to assemble a new, ground-water flow model to simulate the drawdown history and to evaluate the potential effects of different pumping scenarios in the wellfield on the surrounding aquifer.

Chapter 8: Summary

Analyses of the field data from the 1997 pumping tests, the data presented to us by the city of Hays, and the subsurface data from the Data Library at the Kansas Geological Survey, were completed by near the end of June, 1999. The results from that work were summarized in a draft final report which was reviewed internally and presented to the city as Volume 1: Hydrogeologic Setting.

In Volume 1, concerns were raised about the lack of data with which to characterize the hydrogeology of the upper Dakota aquifer in the wellfield vicinity considering the nature of the questions to be addressed by this investigation. The well-log coverage and the pumping tests are only generally adequate for determining aquifer extent and properties within the well field; however, outside of the well field the extant geophysical log data-base is also only marginally adequate and the sandstone hydrologic properties are unknown. Furthermore, of the total thickness of the Dakota Formation only about 30% is sandstone. The rest of the formation is made up of a mudstone whose hydrologic properties are unknown. The lack of hydrologic properties data for the mudstone is particularly troubling because the mudstone may be a significant source of water (recharge or leakage) to the well field during pumping. The pre-pumping water-level data for the Dakota aquifer are concentrated within the well field and the rest of the data base consists of a few poorly documented historic water levels from wells located several miles or more away from the well field. The resulting potentiometric surface map only very generally portrays the west to east movement of ground water across the study area and does not reveal any of the complexity imposed by aquifer heterogeneity on the local ground-water flow pattern. Also, there is a pronounced lack of data on water-level fluctuations in distant monitoring wells located outside of the well field during the 1993-1999 pumping period. This makes it impossible to determine the effects of pumping stress on the local ground-water flow system outside of the immediate wellfield area and to directly address issues of impairment with any reliability.

Nevertheless, development of computer models began using Visual MODFLOW to simulate the effects of pumping on the Dakota aquifer in the wellfield vicinity. Because of the lack of hydrogeologic and hydraulic-head data, the numerical ground-water flow model developed for this project is more of a conceptual than a predictive model. A conceptual model is constructed primarily to provide an understanding of the aquifer system and can only be used very generally to address the two of the project goals if it could be sufficiently calibrated.

Increasingly complex conceptual, 3-dimensional, pre-development (steady-state) numerical models of the upper Dakota aquifer flow system were formulated in this phase of the project. The goal was to simulate the hydraulic head distribution in the wellfield and the

hydraulic gradient of the regional potentiometric surface prior to the beginning of pumping. All of the models used reasonable estimates of hydrologic properties values for the mudstones and a simple distribution of hydrologic properties values for the sandstone aquifer in the well field based on the 1992 and 1997 pumping test results. Outside of the wellfield vicinity we assumed hydrologic properties values of the sandstones that were the geometric mean of the values from these tests.

The early numerical models simulated regional flow through simple, effective hydraulic conductivity aquifers calibrated to the regional potentiometric surface. From these simple models, a sandstone aquifer was added to simulate the local flow regime as it is influenced by aquifer heterogeneity. Two more complex, steady-state, conceptual models, the fringe and the lobe, were then developed based on the hydrogeologic model.

The transient, fringe and lobe conceptual models best reproduce the drawdowns from the 1992 and 1997 pumping tests. The fringe model includes the main sandstone aquifer in Subunit 2 and zones of fringe. The fringe zone represents areas where significant accumulations of less permeable, interbedded sandstone and mudstone occur in the Dakota Formation. The lobe model has the same features as the fringe model except that it contains a sandstone aquifer from Subunit 3 of the Dakota Formation that hydraulically connects to the sandstone aquifer in Subunit 2 south of D-2. The latter model was developed to improve on the simulation of drawdown in the D-2 and D-3 pumping tests. Both models were calibrated to produce acceptable matches to the early drawdowns from the pumping tests. However, both calibrated models overpredict drawdown at later times during the pumping tests. Attempts to improve these focussed on increasing mudstone hydraulic conductivity. The increased mudstone hydraulic conductivity significantly reduced overall drawdown in some of the tests, but not in others. This confirms the interpretation of the pumping test results presented in Volume 1 that leakage from the mudstone aquitard may be an important source of recharge to the production wells in the field. However, it is just as likely that hydraulic connection to underlying sandstones in Subunit 3 may be another significant source. Additional hydrologic and geologic data are needed to evaluate all of these potential sources of recharge to the wellfield.

To further evaluate its performance, the lobe model was used to simulate the drawdown history at the observation wells in the field over a nearly 5 yr period. This model was chosen because it incorporates significantly more of the hydrogeologic complexity of the aquifer system than exists in the other models developed in this project. The results show a consistent discrepancy between simulated and observed drawdowns over the five years of wellfield history. Predicted drawdowns are as much as 50 ft higher than observed, in the western observation wells, MD-6 and MD-5 during the high water production period at the start of the 5 yr. period. Lower pumping levels reduced this discrepancy down to approximately 20-30 ft in most of the

wells. The coalesced cone of depression from this extended nearly 5 yr period of wellfield operation extends to the edges of the model and beyond.

It is clear that this model cannot be used to quantitatively assess the effects of long term pumping because of its inability to simulate the observed drawdowns from the later parts of the pumping tests and to more closely match the record of drawdown during longer periods of pumping. An improved simulation would reduce the composite drawdown at the model edges and a total redesign of the model could be avoided. However, to be conservative if future modeling is to be done on this project, a larger region needs to be included to insure that the effects of pumping do not propagate to the edges of the model.

Recommendations

On the basis of our work to date, we make the following recommendations to the city:

(1) Test drilling is needed to further define (a) the aquifer-mudstone boundary and the nature of that transition and (b) the characteristics of the interbedded sandstone and mudstone that characterizes the fringe zones incorporated in the numerical models of the wellfield vicinity. Currently, the well control used to define sandstone aquifer extent and the characteristics of the fringe zone near the wellfield is poor.

(2) A minimum of 5 new monitoring wells should be constructed in and around the wellfield vicinity. One monitoring well should be located near each of the following three locations: N1/2, N1/2, Sec 21, T. 14 S., R. 19 W.; SW corner Sec. 27, T. 14 S., R. 18 W.; and in the center of the south line Sec. 1, T. 14 S., R. 19 W. Each well should be screened through the entire thickness of the sandstone in Subunit 2 of the Dakota Formation. The fourth and fifth monitoring wells should be located in the SE corner SW, SW, SW, Sec. 13, T. 14 S., R. 19 W. and near the center of Sec. 19, T. 14 S., R. 18 W. These wells should be screened through the entire thickness of sandstone in Subunit 3 of the Dakota Formation. The proposed monitoring wells in Sec 21, T. 14 S., R. 19 W.; Sec. 27, T. 14 S., R. 18 W.; and in Sec. 1, T. 14 S., R. 19 W. are located approximately 2 miles away from the wellfield and will be used to assess the far field response of the aquifer to pumping. The proposed monitoring well in Sec. 13, T. 14 S., R. 19 W. will be used to assess the importance of leakage from fringe deposits in Subunit 3 of the Dakota Formation to the overlying sandstone aquifer in Subunit 2. The proposed monitoring well in Sec 19, T. 14 S., R. 18 W. would provide drawdown data from what appears to be hydraulically connected sandstones in Subunit 3 of the Dakota Formation. The water levels in these new observation wells should be monitored continuously using pressure transducers and data-logging equipment to provide a continuous record of the effects of pumping in the well field over a period of at least one year. In addition, the city will need to

purchase a recording barometer to keep track of atmospheric-pressure fluctuations and their influence on water levels during the monitoring period.

(3) City personnel should continue monitoring water levels in the pumping and observation wells and collecting water samples for analysis. Weekly water-level measurements from the pumping and observation wells in the field should adequately provide the data needed for further model calibration should the city decide to collect additional data to support an increase in its annual appropriation of water. The water quality sample analyses will provide useful information on mixing of water masses and may signal important changes in the system over time. As a result, it will be important for the city to contract analytical services with a laboratory that can produce results with the appropriate level of accuracy and reproducibility.

(4) This new water-level and water-chemistry data set should be analyzed to reevaluate and reformulate the existing hydrogeologic model of the upper Dakota aquifer. The revised hydrogeologic model will be used as a basis for evaluating the conceptual numerical model simulations to date and to assemble a new, ground-water flow model to simulate the drawdown history and to evaluate the potential effects of different pumping scenarios in the wellfield on the surrounding aquifer.

REFERENCES CITED

Anderson, M.P., and Woessner, W.W., Applied groundwater modeling simulation of flow and transport: San Diego, Academic Press, 381 p.

Belitz, K., and Bredehoeft, J. D., 1988, Hydrodynamics of the Denver basin: explanation of fluid subnormal pressures: American Association of Petroleum Geologists Bulletin, 72(11), pp. 1334–1359.

Bohling, G.C., McElwee, C.D., Butler, J.J., Jr., and Liu, W., 1990, User's guide to well test design and analysis with SUPRPUMP version 1.0: Kansas Geological Survey. Computer Program Series #90-3, 95 p.

Bridge, J.S., and Mackey, S.D., 1993, A theoretical study of fluvial sandstone dimensions: *in* Bryant, I.D., and Flint, S.S., (eds.), The Geological Modeling of Hydrocarbon Reservoirs and Outcrop Analogues: International Association of Sedimentologists Special Publication 15, pp. 3-20.

Butler, J.J., 1998, Type-curve analysis of July 1997 pumping tests in the Dakota well field of the city of Hays, Ellis County, Kansas: Kansas Geological Survey Open-File Report 98-15c, 55 p.

Dagan , G., 1979, Models of groundwater flow in statistically homogeneous porous formations: Water Resources Research, 15(1), pp. 47–63.

Desbarats, A.J., 1987, Numerical estimation of effective permeability in sand-shale formations: Water Resources Research, 23(2), pp. 273–286.

Domenico, P.A., and Schwartz, F.W., 1990, Physical and chemical hydrogeology: New York, NY, John Wiley and Sons, 824 p.

Fielding, C.R., and Crane, R.C., 1987, An application of statistical modeling to the prediction of hydrocarbon recovery factors in fluvial reservoir sequences: *in* Etheridge, F.G., Flores, R.M., and Harvey, M.D., eds., Recent Developments in Fluvial Sedimentology, SEPM Special Publication 39, pp. 321–327.

Fogg, G.E., 1986, Groundwater flow and sand body interconnectedness in a thick multiple-aquifer system: Water Resources Research, v. 22, p. 679–694.

Fogg, G.E., 1990, Architecture and interconnectedness of geologic media–role of low-permeability facies in flow and transport: *in* Neuman, S.P., and Nevetniaks, I., (eds.) Hydrogeology of Low-Permeability Environments: Special Symposium of the 28th International Geological Congress, Washington, D.C., pp. 19-40.

Fortner Research LLC, 1996, Transform 2D: Fortner Research LLC, Sterling, VA., 280 p.

Franks, P. C., Coleman, G. L., Plummer, N., and Hamblin, W. K., 1959, Cross-stratification, Dakota Sandstone (Cretaceous) Ottawa County, Kansas, Kansas Geological Survey Bulletin 134, pt. 6, p. 224-238.

Franks, P.C., 1979, Paralic to fluvial record of an Early Crtetaceous marine transgression–Longford Member, Kiowa Formation, north–central Kansas: Kansas Geological Survey Bulletin 219, 55 p.

Freeze, R.A., and Cherry, J.A., 1979, Ground Water: Englewood Cliffs, N.J., Prentice Hall Inc., 604 p.

Galloway, W.E., and Sharp, J.M., Jr., 1998a, Characterizing aquifer heterogeneity within terrigenous clastic depositional systems: *in* Fraser, G.S., and Davis, J.M., (eds.), Hydrogeologic Models of Sedimentary Aquifers, SEPM Concepts in Hydrogeology and Environmental Geology No. 1, Society for Sedimentary Geology, pp. 85–90.

Galloway, W.E., and Sharp, J.M., Jr., 1998b, Hydogeology and characterization of fluvial aquifer systems: *in* Fraser, G.S., and Davis, J.M., (eds.), Hydrogeologic Models of Sedimentary Aquifers, SEPM Concepts in Hydrogeology and Environmental Geology No. 1, Society for Sedimentary Geology, pp. 91–106.

Hamilton, V.J., 1989, Stratigraphic sequences and hydrostratigraphic units in Lower Cretaceous strata in Kansas: MS thesis, Colorado School of Mines, Golden, CO, 165 p.

Hamilton, V.J., 1994, Sequence stratigraphy of Cretaceous Albian and Cenomanian strata in Kansas, *in* Shurr, G. W., Ludvigsen, G. A., and Hammond, R. H., eds., Perspectives on the Eastern Margin of the Cretaceous Western Interior Basin: Geological Society of America Special Paper 287, p. 79-96.

Harbaugh, A.W., 1990, A computer program for calculating subregional water budgets using results from the U.S. Geological Survey modular three-dimensional finite-difference ground-water flow model: U.S. Geological Survey, 46 p.

Helgeson, J.O., Leonard, R.B., and Wolf, R.J., in press, Aquifer systems underlying Kansas, Nebraska, and parts of Arkansas, Colorado, Missouri, New Mexico, Oklahoma, South Dakota, Texas, and Wyoming--hydrology of the Great Plains aquifer system in Nebraska, Colorado, Kansas, and adjacent areas: U.S. Geological Survey Professional Paper 1414-E, 161 p.

Holbrook, J., Ray, T., Cui, Y., and Raghunath, M.D., 1995, Stochastic modeling of the Dakota Sandstone in central Kansas using architectural element analysis: unpublished, Kansas Geological Survey, 44 p.

Jones, A, Doyle, J., Jacobsen, T., and Kjønsvik, D., 1995, Which subseismic hetergeneities influence waterflood performance–a case study of a low net-to-gross fluvial reservoir: *in* de Hann, H.J., (ed.), New Developments in Improved Oil Recovery, Geological Society of London Special Publication 84, pp. 5-18.

Karl, H.A., 1976, Depositional history of Dakota Formation (Cretaceous) sandstones, southeastern Nebraska: Journal of Sedimentary Petrology, 46 (1), pp. 124–131

Macfarlane, P.A., Townsend, M.A., Whitemore, D.O., Doveton, J.H., and Staton, M., 1988, Hydrogeology and water chemistry of the Great Plains (Dakota, Kiowa, and Cheyenne) and Cedar Hills aquifers in central Kansas - end of contract report: Kansas Geological Survey Open-File Report 88-39, 184 p.

Macfarlane, P.A., Doveton, J.H., Feldman, H.R., Butler, J.J., Jr., Combes, J.M., and Collins, D.R., 1994, Aquifer/aquitard units of the Dakota aquifer system in Kansas: methods of delineation and sedimentary architecture effects on ground-water flow and flow properties: Journal of Sedimentary Research, B64(4), p. 464–480.

Wade, A., 1992, Ground-water flow systems and the water-resources potential of the Dakota aquifer in a two-county area in north–central Kansas: Unpublished MS, University of Kansas, Lawrence, 158 p.

Wang, H.F., and Anderson, M.P., 1982, Introduction to ground-water modeling finite difference and finite element methods: San Francisco, W. H. Freeman and Co., 237 p.

Waterloo Hydrogeologic, 1994, Visual MODFLOW user's manual: Waterloo Hydrogeologic, Inc., Waterloo, Ontario, Canada, 311 p.

Zeller, D.E. (ed), 1968, The stratigraphic succession in Kansas: Kansas Geological Survey Bulletin 189, 81 p.